11:23:15 OCA PAD AMENDMENT - PROJECT HEADER INFORMATION 03/13/95

Active

Project #: E-16-X36 Cost share #: E-16-378 Rev #: 1
Center # : 10/24-6-R8140-0A0 Center shr #: 10/22-1-F8140-0A0 OCA file #:
Work type : RES
Contract#: NAG 2-900 Mod #: SUPPLEMENT 1 Document : GRANT
Prime #: Contract entity: GTRC

Subprojects ? : N CFDA: 43.002
Main project #: PE #:

Project unit: AERO ENGR Unit code: 02.010.110
Project director(s):
SCHRAGE D P AERO ENGR (404)894-6257

Sponsor/division names: NASA / AMES RESEARCH CTR, CA
Sponsor/division codes: 105 / 006

Award period: 940101 to 951231 (performance) 960331 (reports)

Sponsor amount	New this change	Total to date
Contract value	75,000.00	150,000.00
Funded	75,000.00	150,000.00
Cost sharing amount		2,000.00

Does subcontracting plan apply ?: N

Title: EVALUATION OF HIGH SPEED CIVIL TRANSPORT (HSCT) METRIC USING THE TAGUCHI...

PROJECT ADMINISTRATION DATA

OCA contact: Anita D. Rowland 894-4820

Sponsor technical contact

THOMAS L. GALLOWAY
(415)604-6181

NASA AMES RESEARCH CENTER
SYSTEMS ANALYSIS OFFICE, 237-11
MOFFETT FIELD, CA 94035-1000

Sponsor issuing office

BARBARA HASTINGS
(415)604-5802

SAME
UNIVERSITY AFFAIRS BRANCH, ASC:241-1

Security class (U,C,S,TS) : U ONR resident rep. is ACO (Y/N): N
Defense priority rating : supplemental sheet
Equipment title vests with: Sponsor GIT X
REF. NASA GRANT PROVISIONS, 1260.408, "EQUIPMENT AND OTHER PROPERTY"
Administrative comments -
SUPPLEMENT 1 AWARDS AN ADDITIONAL YEAR AND FUNDS ($75000)

SR 2 7/6

GEORGIA INSTITUTE OF TECHNOLOGY
OFFICE OF CONTRACT ADMINISTRATION

U

NOTICE OF PROJECT CLOSEOUT

Closeout Notice Date 04/10/96

Project No. E-16-X36_____ Center No. 10/24-6-R8140-0A0_

Project Director SCHRAGE D P_____ School/Lab AERO ENGR_____

Sponsor NASA/AMES RESEARCH CTR, CA_____

Contract/Grant No. NAG 2-900_____ Contract Entity GTRC

Prime Contract No. _____

Title EVALUATION OF HIGH SPEED CIVIL TRANSPORT (HSCT) METRIC USING THE TAGUCHI.

Effective Completion Date 951231 (Performance) 960331 (Reports)

Closeout Actions Required:	Y/N	Date Submitted
Final Invoice or Copy of Final Invoice	Y	_____
Final Report of Inventions and/or Subcontracts	Y	_____
Government Property Inventory & Related Certificate	Y	_____
Classified Material Certificate	N	_____
Release and Assignment	N	_____
Other _____	N	_____

Comments_____
NOTE USE SPONSOR FORM FOR PATENT._____

Subproject Under Main Project No. _____

Continues Project No. _____

Distribution Required:

Project Director	Y
Administrative Network Representative	Y
GTRI Accounting/Grants and Contracts	Y
Procurement/Supply Services	Y
Research Property Managment	Y
Research Security Services	N
Reports Coordinator (OCA)	Y
GTRC	Y
Project File	Y
Other _____	N
_____	N

NOTE: Final Patent Questionnaire sent to PDPI.

E-16-X36
#1

Final Report to

Mr. Tom Galloway
Acting Branch Chief
Systems Analysis Branch
NASA Ames

for Contract NAG-2-900

Evaluation of High Speed Civil Transport (HSCT) Metrics Using the Taguchi Robust Design Approach

(A combined Aerodynamics/Propulsion Optimization Study)

Principle Investigators:

Dr. Daniel P. Schrage
Professor and Co-Director (ASDL)

Dr. Dimitri N. Mavris
Assistant Professor & Associate Director (ASDL)

March 31, 1996

Aerospace Systems Design Laboratory (ASDL)
School of Aerospace Engineering
Georgia Institute of Technology
Atlanta, GA 30332-0150

Executive Summary

This report documents the efforts of the Georgia Tech Aerospace Systems Design Laboratory (ASDL) in completing a design methodology demonstration under the sponsorship of NASA Ames Systems Analysis Branch (NAG- 2-900).

Research at the Aerospace Systems Design Laboratory (ASDL) at Georgia Tech's School of Aerospace Engineering has been evolving over the past three years in constructing a comprehensive methodology for the integration of aircraft design, manufacturing, and economics. NASA's High Speed Civil Transport (HSCT) concept has been selected as a pilot project for this study because of its potential global transportation payoffs and impact on U.S. competitiveness in the world economy. The methodology is based on a Concurrent Engineering/ Integrated Product and Process Development (IPPD) approach, and, in this case, is specifically applied to the design of an HSCT. The procedure employs the use of a Design of Experiments approach to facilitate the development of Response Surface Equations (RSEs) which capture the essence of sophisticated, computationally intense disciplinary analyses tools and replace them by simple second order polynomial equations. Since this aircraft must be economically competitive with current subsonic transports, emphasis has been given throughout this study on understanding and assessing economic viability. The determination of this objective is based on the required average yield per Revenue Passenger Mile ($/RPM), a metric that captures the concerns of all interested parties. This final report will describe the overall approach from concept formulation to concept feasibility and the identification and assessment of all possible means of achieving economic viability. A major theme will be the evolution from point design solutions to distributions of solutions through the consideration of uncertainty ("noise").

An example application using the HSCT will be described in detail including the use of DOE/RSM in multiple forms throughout the design process. This example, the result of the method being implemented by a student design team over a two-course series, will show how aerodynamic and propulsion analyses are integrated into the synthesis code FLOPS through RSEs in order to improve the code's accuracy and applicability. The resulting sizing process will be used in an optimization, where the objective function, average yield per Revenue Passenger Mile ($/RPM), is constrained by noise, approach speed, and field length restrictions.

Finally, different means of improving the economic viability of this hypothetical HSCT are examined, and methods to assess their relative impact are presented in terms of risk and benefit. A goal is to enable the designer to detect not only the optimal condition for a specific design, but also the sensitivity of this design to changes in design parameters.

Acknowledgments

The authors would like to thank Mr. Tom Galloway for his help and support of this research in his role as Technical Monitor. Also, a portion of this work was completed by ASDL's 1995 Student Design Team. That work was performed by the student team members in a two course sequence under the advisement and coordination of Dr. Dimitri Mavris and Dr. Daniel Schrage. The following individuals comprised the 1995 Design Team: Juergen Baecher, Oliver Bandte, Daniel DeLaurentis, Kemper Lewis, Jason Pratt, Jose Sicilia, Craig Soboleski. Others who contributed to the team's efforts included: Florian Bachmaier, Andreas Hahn, Jae Moon Lee, Peter Rohl, Jimmy Tai, and Bill Marx.

Table of Contents

Table of Contents (cont.)

List of Figures

List of Figures (cont.)

List of Tables

Introduction

Over the past several years, the aerospace industry (airlines and manufacturers alike) has felt the impact of the combined effect of increasing aircraft systems costs and budget restrictions and is reacting through a series of initiatives to help minimize their overall system Life Cycle Costs (LCC)[1]. Under these circumstances, the need for a comprehensive method for the identification, assessment, and mitigation of critical technologies needed to ensure concept feasibility *and* economic viability of new aircraft is apparent. It is also evident that new technology benefit studies must be accompanied by a corresponding risk assessment to avoid overly optimistic conclusions. Furthermore, the evolution of Multidisciplinary Design Optimization (MDO) as a new discipline and the increased emphasis from government and industry to design for quality and affordability are enabling designers and decision makers to become aware of the benefits that could be achieved through an Integrated Process and Process Development (IPPD)/Concurrent Engineering (CE) approach. IPPD specifically brings together design and manufacturing considerations, while CE considers concurrently, as the word implies, contributions from all the pertinent disciplines[2].

Designing aircraft in an IPPD/CE framework could be viewed as designing with a focus on affordability, which implies an understanding of how the various discipline, mission, design, and economic variables affect the feasibility ("can it be built") and viability ("should it be built") of an aircraft. Economic viability is usually measured through such metrics as total or direct operating cost per trip, aircraft acquisition cost, or required yield per revenue passenger mile ($/RPM). If only one metric is to be tracked and optimized, then, for commercial transport studies, $/RPM may be the most useful as the Overall Evaluation Criterion (OEC)[3,5]. The emphasis in determining viability is on robustness, not simply point design optimization.

This report presents the steps for the implementation of one such proposed methodology, with a focus on the means of improving economic viability through relaxation of customer requirements, relaxation of design constraints, or infusion of new technology. If the latter option is selected, a risk-to-benefit rating can be used along with such tools as relevance trees and the technology/schedule risk ranking tables to assist the evaluator with the decision process. Section 1 will present the method formulation, Section 2 will illustrate in detail the implementation of the whole approach on the HSCT, while Section 3 closes the report with some conclusions. Appendix A, which covers the basics of the DOE/RSM method, should be read before Section 2 as it provides the foundation for understanding the subsequent use of the techniques.

1. Methodology Formulation

1.1 Robust Design with Technology Assessment

The Georgia Tech methodology can be described as a Concurrent Engineering approach to aircraft design applied in an IPPD environment. Concurrent Engineering is commonly defined as a systematic approach to the integrated, concurrent design of products. Hence, this multi-disciplinary approach considers simultaneously all pertinent disciplines involved in a given design. If applied in the conceptual design phase it allows the designer to confront potential challenges and conflicting requirements in the early design stages when the system is still flexible enough to be altered[3]. Furthermore, the concurrent consideration of manufacturing and product development forms the foundation of an IPPD. An approach like this might increase the initial costs and time needed for the early design stages, but produces significant cost savings in the long run and leads to a more efficient design. The Robust Design environment envisioned by ASDL is depicted in Figure 1.

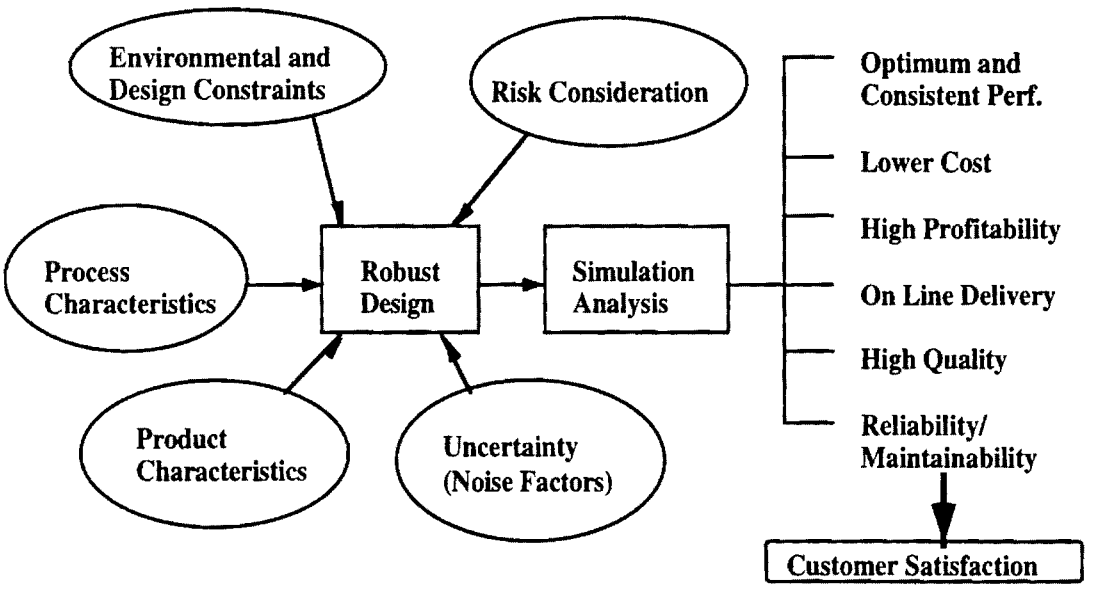

Figure 1: CE/IPPD Robust Design Environment

In the traditional design process the designer employs a synthesis code to integrate information related to a similar type vehicle and to size the vehicle for a set of imposed design requirements and constraints. The design variables (product characteristics) are then varied within the pre-specified range of interest to yield an optimum configuration. In this case, optimization could be with respect to maximizing performance or minimizing empty or gross weight. The latter implying minimization of Life Cycle Cost of the aircraft.

On the other hand the proposed CE/IPPD Robust Design environment represents a more comprehensive approach to design and exhibits the following characteristics:

- It is based on a truly multidisciplinary synthesis tool, which can be tailored to the specific applications.
- Design variables are analyzed in an environment that considers or accounts for both product and process design variables.
- The analysis is subjected not only to design but also manufacturing and environmental constraints.
- It accounts not only for the benefits of new technologies but also for the risk associated with them. This way the effect and consideration of new technologies is modeled realistically, accounting for the penalty in increased RDT&E cost for the additional effort.
- It replaces the notion of "point design" for solutions that account for disciplinary, technological, economic, etc. variability. In a realistic representation some variables in the design process can not be set to a specific (optimized) value, because they are uncontrollable. These variables are commonly called "noise" factors[6], and cause a variability in the response dependent on their own distributions.
- In this new methodology designing for affordability does not mean any longer simple minimization of gross or empty weight. Instead it assesses and quantifies economic viability of an aircraft by modeling and accounting for manufacturer and airline business practices also.
- It links the economic viability assessment to the aircraft design via a synthesis code.
- Finally, the designer can examine and understand the design space around the optimum. This enables him to appraise how robust is the obtained solution.

The proposed methodology is attempting to achieve these objectives through the process illustrated in Figure 2. Following Figure 2, the procedure is broken down to eight design phases or steps which will implemented on an HSCT example in Section 2.

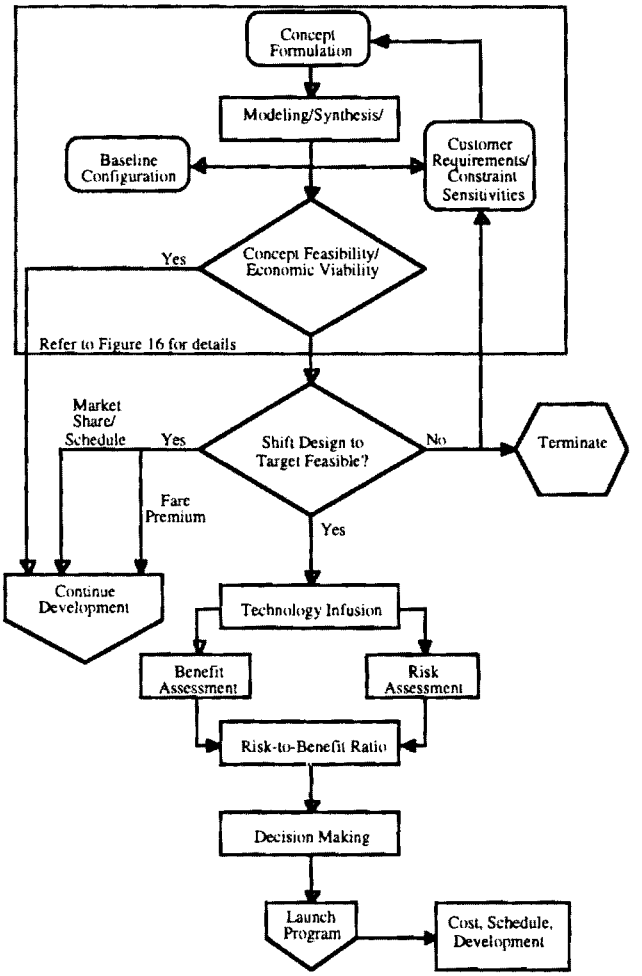

Figure 2: Critical Technology Assessment Methodology

Eight Step Approach:

Step 1 : *Concept Formulation.* During this phase the design team is formed and the voice of the customer is translated into design and economic requirements through a series of brainstorming sessions. In addition, a mission profile is determined and all relevant design and environmental constraints are identified.

Step 2 : *Concept Modeling/Synthesis/Sizing.* For revolutionary (or non-traditional) aircraft, the current conceptual design process and its associated analysis tools often break down. This situation requires the use of more complex tools which were usually associated with preliminary design stages. These tools are used in a new conceptual sizing procedure via the use of Response Surface Equations (RSEs). Given the requirements and constraints from the previous step, a parametric study for each one of the disciplines involved is performed to create vehicle specific RSEs for all needed responses. The RSEs are written in polynomial form as a function of the most significant contributing factors (which are themselves determined through a screening test and

Pareto Analysis)[6]. The outcomes of these analyses are then considered concurrently and integrated in a synthesis code to yield a sized vehicle. This vehicle is next referred to as the baseline for the economic viability evaluation (i.e. a vehicle that satisfies all requirements and is capable of flying the mission profile).

Step 3 : *Economic Viability Evaluation.* The baseline vehicle can now undergo an economic evaluation to determine whether the concept is economically viable. For commercial transports, viability may be measured in terms of the required average yield per Revenue Passenger Mile ($/RPM). The steps above are illustrated in the dashed box in Figure 2 and more explicitly in the expanded flowchart presented in Figure 16.

Step 4 : *Identification of means to improve the design's economic viability.* If the resulting feasible design is not economically viable, then viability may be achieved through customer requirement and/or design constraint alteration/relaxation, yield management, market share, technology infusion, or if everything else fails through a fare premium. It is also during this phase that the relative contribution of each one of the proposed alternatives to the response is quantified.

Step 5 : *Technology Benefit Assessment.* If technology infusion has been selected to enhance the economic viability, relative benefit gains associated with each alternative design improvement must then be assessed. Therefore, all possible new critical technologies must be identified and their effect on the evaluation criterion must be quantified. A relevance tree decomposition scheme may be utilized to assist this process.

Step 6 : *Technology Risk Assessment.* The technological and schedule risk associated with each of the design improvements proposed must next be examined. In order to measure or assess the risk, a readiness level and a corresponding confidence have to be determined for all alternative materials, processes, technologies, or methods. The readiness levels can be assigned to the various alternatives throughout the relevance trees so as to determine paths/options which may lead to reduction in risk.

Step 7 : *Evaluation, Decision Making, and Resource Allocation.* Each new critical technology is examined next from a combined risk to benefit viewpoint. This evaluation is subjected to funding/ budget and time constraints. Once the most appealing projects/ technologies are selected, the evaluator must verify that these projects can be completed by the scheduled date. Utilizing an activity network restrained by budget and schedule, the sequence of events/tasks that need to be performed can be determined. Because of constraints imposed by budget allocation and schedule deadlines this process will be iterative.

Step 8 : *Project/overall program tracking.* Provided that a critical technology development effort is going to be pursued, the program manager will have to conduct a series of periodic evaluations to determine if the program is on schedule. This process can be assisted through the identification of critical paths, show stoppers or potential problems ahead of time and carefully plan around them.

With this general framework in mind, Section 2 describes in detail the implementation of this eight step process to design of robust systems. But first, the IPPD method, up to now only mentioned in concept, is developed next before the actual implementation phase.

1.2 The IPPD Method

An IPPD procedure begins when the voice of the customer is translated into a series of design (range, payload, speed, technology level, etc.) and economic (airline return on investment (ROI-A), desired load factor, target $/RPM, etc.) requirements. IPPD is focused around a concurrent treatment of both product and process characteristics early in the design process, where the cost of modifications is relatively inexpensive. The framework for implementing this IPPD effort, in the broadest view, is depicted in Figure 3[14]. The use of all four of the techniques shown in the figure will be illustrated and explained throughout this report. The Computer-Integrated Environment, for this pilot study, was implemented using UNIX shell scripts, though in the future more advanced computing structures will be available.

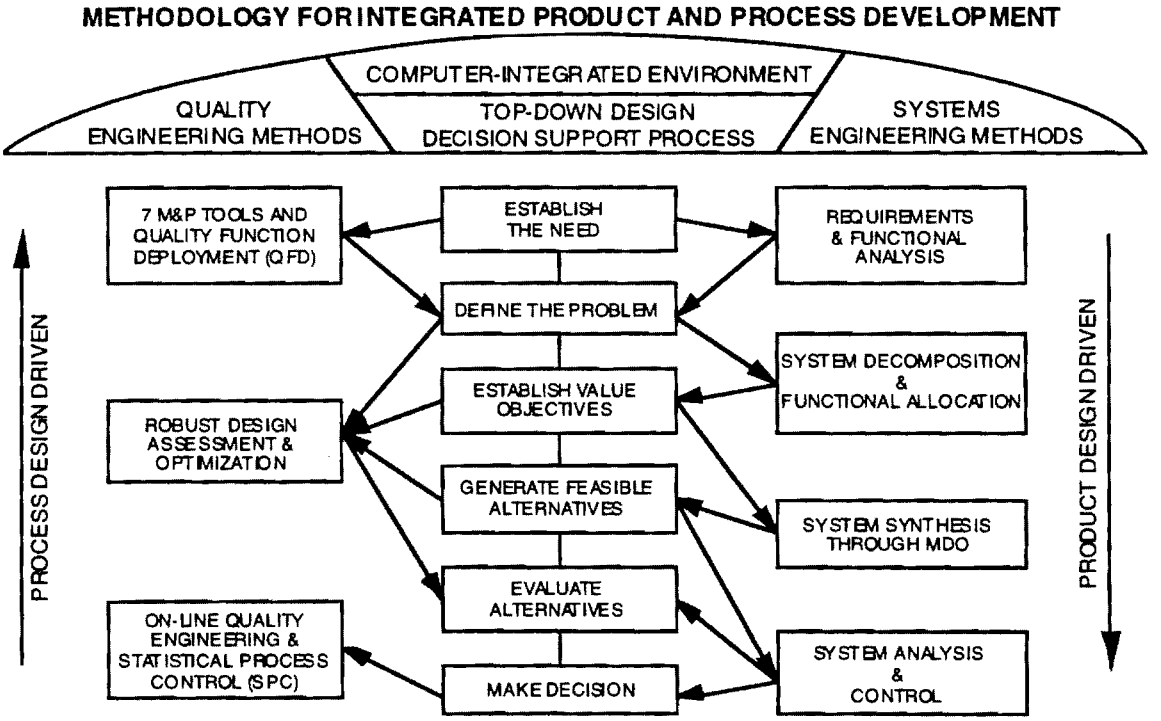

Figure 3: The IPPD Framework

Given this framework, the Georgia Tech IPPD methodology can best be viewed in more detail as a recomposition process, employed once the various parts of the problem have been broken down and analyzed. In order to do this recomposition in an intelligent way, *Product* and *Process* design variables and constraints must be considered simultaneously. Product

characteristics are those that pertain directly to the subject of product design, such as geometry, materials, propulsion systems, etc. Process characteristics, on the other hand, refer to those items related to how the product is designed, produced, and sustained over its lifetime.

A rational approach to executing the integration process, with the $/RPM as its Overall Evaluation Criterion, takes the form of a "Funnel", as illustrated in Figure 4.

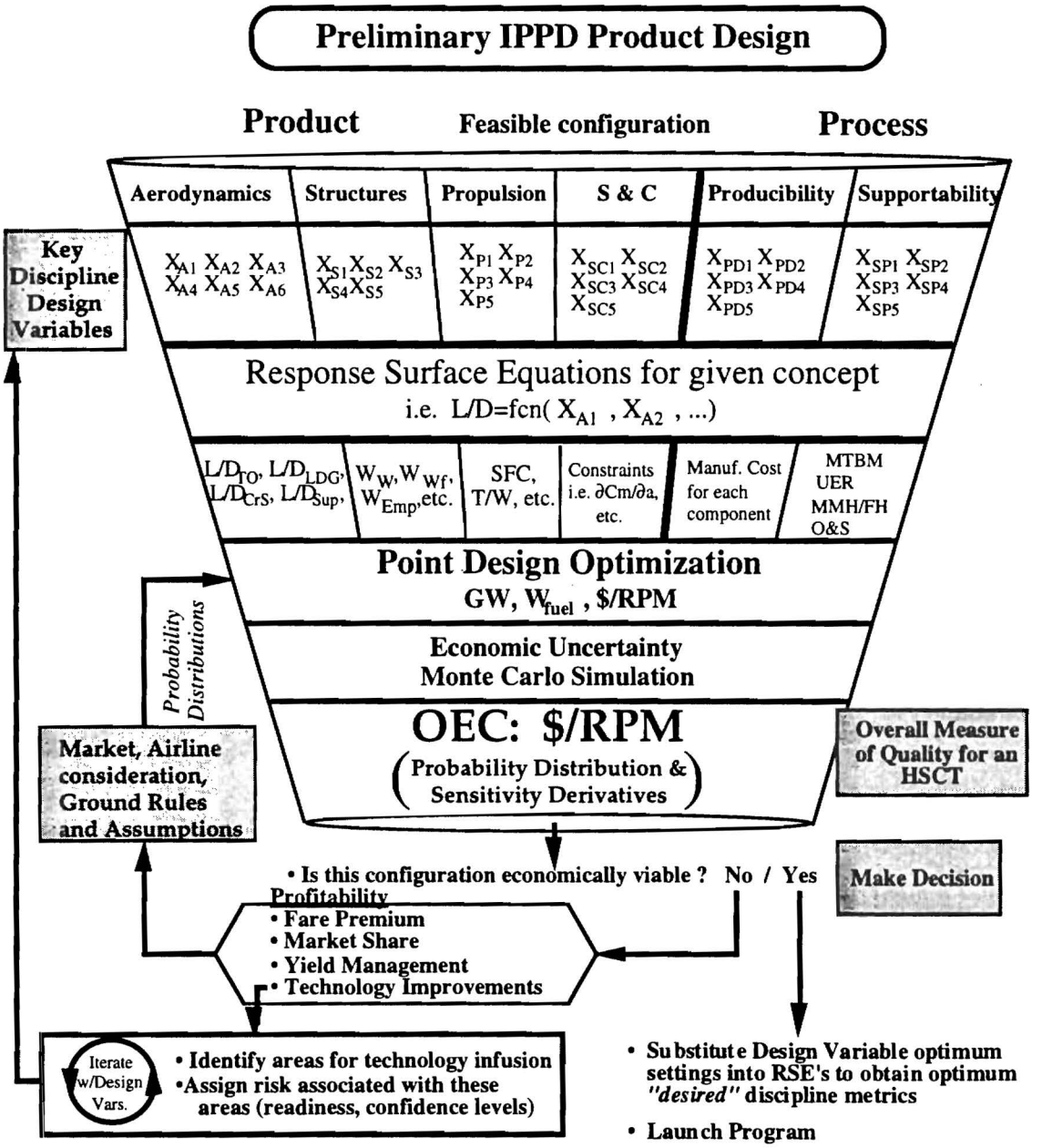

Figure 4: Implementing IPPD: Systematic Recomposition

In essence, the Funnel represents a concurrent recomposition process in which all of the various disciplinary interactions, ideally, are accounted for during "synthesis", or recomposition.

In reality, as this is a developing methodology, smaller parts are tackled first in order to discover the strengths and weaknesses of the method. For this study, the aerodynamic and propulsion disciplines were examined in detail, with structures considerations being limited to weights. A stability & control analysis method is outlined but not implemented. The first level in the funnel represents fundamental design variables in each category. These are the parameters available to the engineer in formulating configurations. The next step, the introduction of RSM, is the newest innovation in the approach, and its importance lies in two facts. First, it allows the formation of response model equations which can be used to replace complex simulation codes needed to arrive at a point design optimum. Second, as is illustrated at the bottom of the figure, once an economically viable alternative is synthesized, these RSE's can be used to obtain the *optimum discipline metrics* such as L/D or SFC. After the equations are formed, this discipline level information is used to perform system synthesis (with appropriate constraints) through the use of a sizing code (in this case FLOPS). This synthesis is Step 2 of the overall approach described above. What is thus obtained are the various design variable settings which correspond to the point design optimum (i.e. one aircraft configuration) and a corresponding $/RPM value. Uncertainty enters the problem at this stage by introducing economic factors which the designer cannot control, such as market and airline considerations. It is the result of this step which becomes the overall objective, a distribution of $/RPM, subsequently used to determine if viability has been achieved or if a design iteration (see bottom, right of figure) is necessary (Step 3). The introduction of risk and benefit (Steps 4-8) then follows in turn.

As the design methodology described above has been evolving from year to year, design teams from Georgia Tech have been attempting to implement it for the HSCT. Each year, new methods and techniques developed through research conducted in ASDL are incorporated into a plan for implementation by the student teams. Last year's team made significant contributions by introducing Taguchi Parameter Design Methods. In the "Future Work" section of their final report, the team recommended the incorporation of Response Surface Methodology into the design process. The RSM approach has been in use for some time in a variety of capacities, with some recent work being done at NASA Langley's Vehicle Analysis Branch on Single-Stage-to-Orbit vehicles [15]. So then, the use of RSM became a key development goal in this study.

A summary of new advances developed for year two of this study include the following:

- Application of Robust Design Methods via Design of Experiments and RSM
- Aerodynamic / Propulsion Integration
- Modification of FLOPS to include Response Equations for Subsonic and Supersonic Drag
- Constrained Optimization using Response Equations
- Means for evaluating a design based on risk / benefit

2. Methodology Implementation

2.1 Concept Formulation (Step 1)

2.1.1 The High Speed Civil Transport - Defining the Problem

The first, and probably most important, step in any engineering design task is the proper definition of the problem. Once a need has been recognized, the proper definition of the problem will help to make the solution of that problem more efficient. Problem definition is based on identifying the true needs of the customer and formulating them into a set of goals for the problem solution. The necessary components of a problem definition include: need statement, goals, constraints and trade-offs, and criteria for evaluating the design. In order to identify and understand the problem in a systematic manner, the seven management and planning tools and quality function deployment (QFD) methods were employed.

The seven management and planning tools are a formal approach to the decomposition of a complex or seemingly overwhelming task. These tools utilize brainstorming and organizational techniques (i.e. affinity diagrams, tree diagrams, interrelationship digraphs, etc.) to generate information related to the task in order to expose the obvious as well as the hidden concepts[16]. From the results obtained during this exercise, the items are identified which explain the needs in terms of the voice of the customer(s). It is important to maintain an emphasis on satisfying the needs that the solution is intended to meet. To accomplish this consideration and to identify the important product and process characteristics involved with the problem the QFD is used. Figure 5 shows the cascade of QFDs used in carrying the voice of the customer through problem definition to the generation of a feasible design and the courses at GT in which they are formulated.

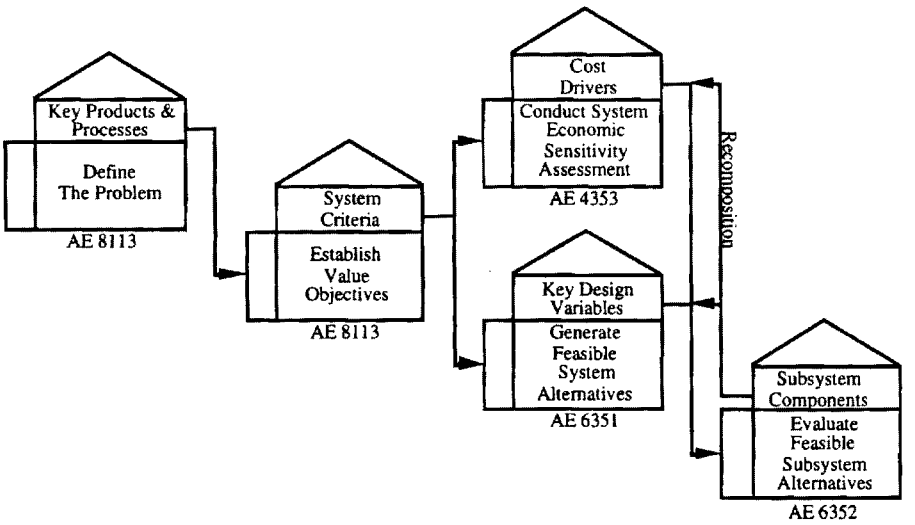

Figure 5: Cascade of QFD Matrices Used for Design Problem Decomposition

The detailed results of the brainstorming and decomposition exercises are contained in the respective reports for AE 8113 and AE 6351 listed in References. Shown below are the QFDs obtained from the procedures described above. From these QFDs the items which are identified with the largest relative importance become the focus of the solution effort for the defined problem and customer needs.

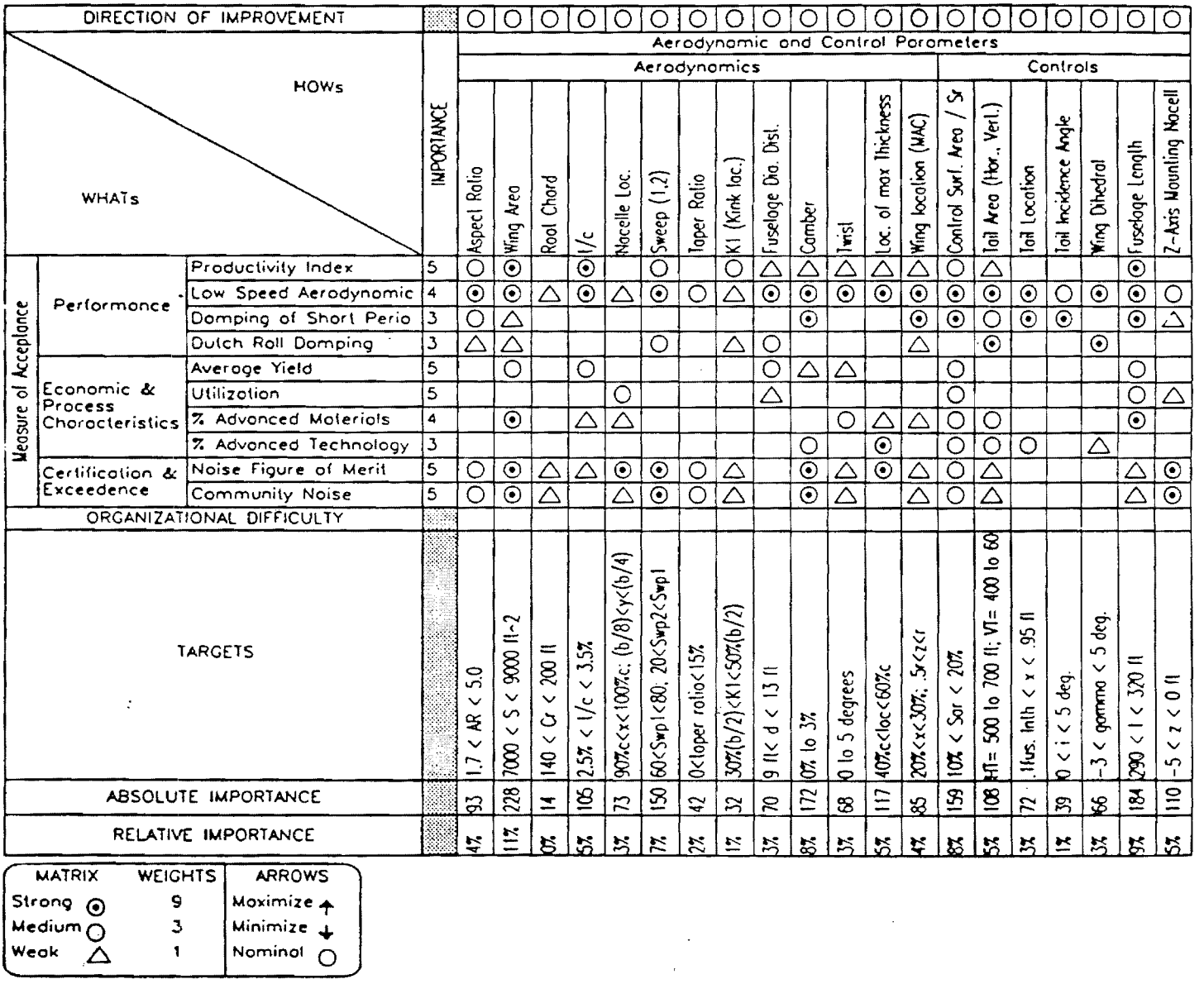

Figure 6: Aerodynamics and Stability and Controls QFD

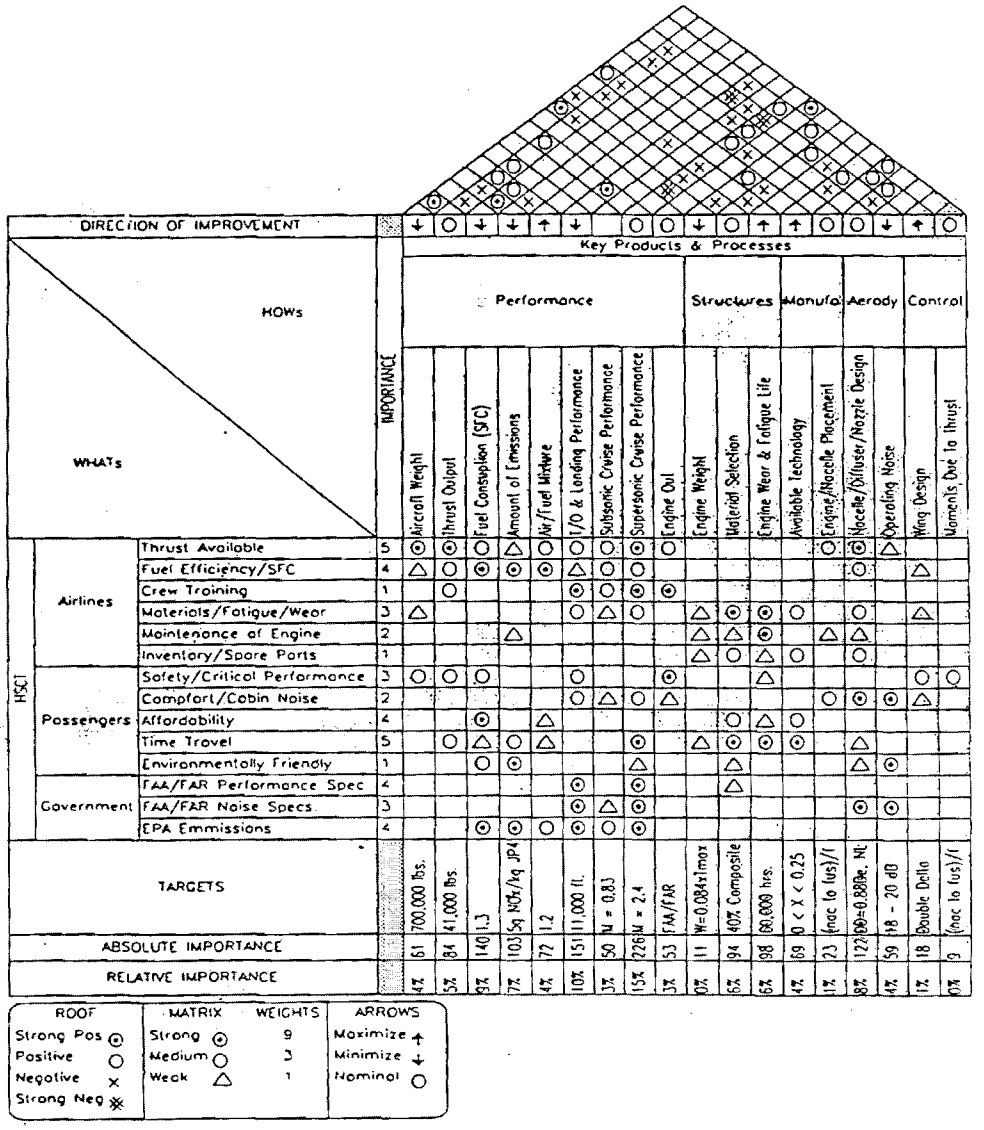

Figure 7: Propulsion QFD

After performing the problem decomposition, enabling a better understanding of the customers' needs and the steps required to meet them, a formal and well planned problem definition can be formulated. The problem definition for the HSCT is as follows:

- **Need statement:** The need for a supersonic commercial transport, or High Speed Civil Transport, in the early 21st century has been identified by market analysis and forecasts. The HSCT is envisioned to be an aircraft capable of flying supersonically and carrying 250-300 passengers to destinations ranging from 5,000 to 6,500 nautical miles.
- **Goals (aims and objectives):** In order to meet this need for a HSCT, there are several goals and objectives which must be realized. The primary objective is the justification for the production of a HSCT by proving with reasonable certainty the economic viability of such a system. From this primary objective there exists a cascade of system objectives. The systems which are considered in this research are the aerodynamic and propulsion systems.

The goals for these areas are drag polars, take-off noise, vehicle empty weight, fuel consumption, thrust output, and engine weight.

- **Constraints and trade-offs:** The technological challenges involved with the HSCT program can be represented as constraints to the design. The constraints this research will address are: stability and control and the environmental constraints involving FAA and EPA regulations concerning noise and NO_x emissions.
- **Criteria for evaluating the design:** The criteria for evaluating the design is directly related to the goal of economic viability which is captured by the overall evaluation criteria (OEC), the aforementioned dollars per revenue passenger mile ($/RPM). This OEC will also be discussed in more detail in the following section.

2.1.2 Establishing the Objective

The objective for this study is to generate an economically feasible design for the HSCT. This feasibility is determined by the metric $/RPM. The goal for the HSCT $/RPM value is that of the principle competition for the same travel routes, the current long range subsonic fleet, which includes such aircraft as the Boeing 777, Airbus 340, and MD 11. If the $/RPM distribution for the an HSCT configuration can be shown to be at a level which is competitive with these aircraft, then that configuration will be deemed economically viable and further development may continue. This objective was chosen due to the decisive role of economics in the fate of any commercial system. From this primary objective, individual system and component objectives which contribute to the realization of the $/RPM objective can be identified and pursued. The propulsion system contribution to economic viability will come about from reduced system weight and minimum fuel consumption. The contributions of the aerodynamics toward economic viability come from reductions in drag and improved lift.

2.1.3 Generating a Baseline Configuration

The baseline configuration used for this study is similar to the NASA Langley 24e. The baseline aircraft is an area-ruled, tail-less, fuselage (maximum diameter of 12 ft.) with a double delta planform and four below the wing nacelles housing mixed flow turbofan (MFTF) power plants. The values for some of the important baseline design parameters are given below in Table 2.1. The baseline for the propulsion system will be a mixed flow turbofan engine. A justification for this powerplant selection will be given later in this section along with values for the important design variables which define the baseline propulsion cycle.

Table 2.1: Description of the NASA Langley 24e and GT Baseline HSCTs

Parameter	24e	GT
Range	6500 nm	5000 nm
Payload	30,000 lb.	67,200 lb.
Fuselage length	300 ft.	280 ft.
Span	77.5 ft.	24e
Sweep 1	74 deg.	24e
Sweep 2	45 deg.	24e
S_{ref}	9,100 ft^2	24e
M	2.4	24e
Cruise Altitude	~63,000 ft.	optimized
Sustained Load	2.5 g	2.5 g

The mission definition for this aircraft is seen in Figure 8. The likely restriction of subsonic flight over land forces the need for modeling a split subsonic / supersonic mission. This subsonic restriction is due to the fact that sonic booms over land are currently not allowed. The baseline aircraft, engine, and mission described will be used in the sizing/synthesis phase of this research. The study of deviations from this baseline will be used to gain a better understanding of the system response to various design variables and the design space. From the knowledge gained, an improved solution to the problem will be obtained.

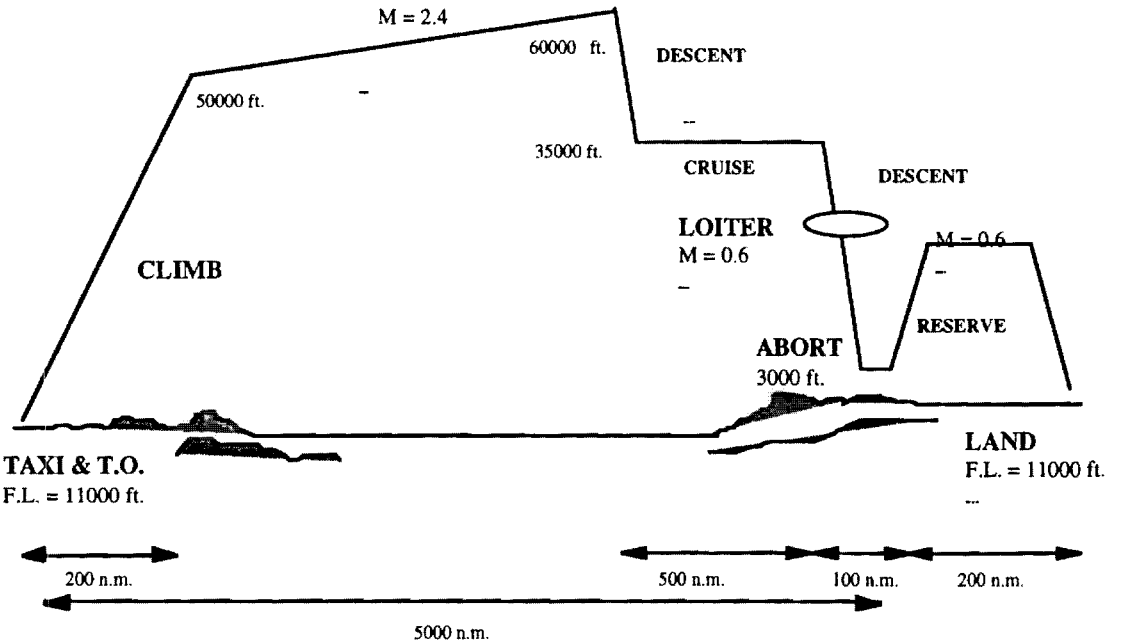

Figure 8: HSCT Mission Profile

2.1.4 Baseline Requirements and Study Assumptions

2.1.4.1 Aerodynamics

Choosing a planform shape for a supersonic transport is a task that to this day is still a long and tedious one. The apparent need for efficient performance at both sub- and supersonic cruise conditions exhibit immediately the presence of a tradeoff process. Studies by Boeing and Lockheed during the 1970's for the SuperSonic Transport (SST) program looked extensively at this issue. Basically what emerged was that low aspect ratio, highly swept wings have low drag at $M > 1$, since the cranked leading edge serves to provide for subsonic type flow normal to the wing leading edge. Unfortunately, such planforms are poor in subsonic cruise. Another option studied was the variable sweep wing, which, as the name implies, has the advantage of adapting to the flight condition. However, complications involving reduced fuel volume and weight and complexity penalties resulted in this concept never being seriously considered. The so-called double delta emerged as a compromise. Here the outboard panel helps retain some subsonic performance while keeping acceptable supersonic cruise efficiency[17]. The study carried out presently employs a Design of Experiments technique which models and examines planforms ranging from the pure delta (arrow) to the double delta.

The trades involved in planform selection are complicated by the presence of design and performance constraints which are directly related to the wing. The limit on approach speed, for example, is for the most part a function of wing loading. Similarly, fuel volume constraints impact the wing size since most of the fuel is carried in tanks located inside the wing structure. Both of these constraints become sizing points and both tend to increase the wing in size. Of course, increased wing area brings with it higher induced and skin friction drag.

Outside of the challenge of designing a supersonic aircraft which is aerodynamically efficient at both supersonic and subsonic cruise, terminal performance at takeoff and landing also presents a challenge. Increasing the low speed aerodynamic performance of the aircraft will reap benefits for noise control through reduced thrust and more modest climb rates. The HSCT will need its maximum C_L at takeoff, and the use of high lift devices will play a major role in making that maximum as high as possible. In terms of active high lift devices, those being considered include leading edge, trailing edge, and slotted flaps as well as in- and outboard flaperons (surfaces acting both as ailerons and flaps). In subsonic flight, an increase in camber results in increased lift. At supersonic speeds, however, camber does not increase lift, only angle of attack does. Fortunately, it is in the low speed regime where the C_{Lmax} is required, making the various flaps effective for increasing lift[18]. Passive systems for high lift being considered include pneumatic aerodynamic control devices. If proven effective, the incorporation of one or both of these passive

techniques could bring tremendous weight reductions in the HSCT high lift system. Of course, consideration of such technologies is out of the scope of this report.

The Lockheed Corporation did a study of an arrow wing SST configuration in the 1970's which included various high lift devices. Their configuration consisted of some interesting characteristics. There were no leading edge flaps between the root and outer break (where a vertical fin is located). Outboard from the break are Krueger Flaps (slats) for increasing the transonic L/D. However, these were found to not appreciably increase low speed lift. The wing trailing edge was divided into 4 plain flap panels. Panels 1 - 3 were conventional flaps with maximum deflection of 20 degrees for C_{Lmax} on takeoff. A plain spoiler was located ahead of panel 1 and used as speed brake. Roll control was provided by ailerons (panels 2 and 3), slot-deflectors (in front of panels 2 and 4) and Inverted slot-deflectors (in front of panel 3). The study found that a C_{Lmax} of about 1 was achieved at full flap deflection and at an angle of attack of 20 degrees.

Based on this and other references, a configuration of flap settings was selected for the baseline aircraft in this study and the takeoff and landing polars were generated using the code AERO2S. This exercise is discussed in Section 4.

2.1.4.2 Structures

Although not a main focus of this study, the structural issues related to the HSCT are not insignificant and an awareness of what can be modeled in the synthesis code is essential. The structural design of the High Speed Civil Transport must guarantee the integrity of the fuselage, empennage, wing, and landing gear for the aircraft's entire flight envelope. Design restrictions such as the double delta wing planform force the designer to compromise between strength, weight, and ease of manufacturing of the structure. The aerodynamic heating expected on the structure's surface implies the use of new materials that resist high temperatures; the expansion of the skin panels due to the aerodynamic heating is a great concern for the HSCT program, especially at the wing-fuselage junctures. Likewise, the structural layout of the wing, particularly at the kink location, represents a challenge not only from the structural integrity point of view, but from the manufacturing point of view as well. The geometry and materials used in the design of the wing structure are limited by aeroelastic flutter constraints, and the size and location of the control surfaces are set mainly by the aircraft's stability and control needs. Furthermore, the integration between the wing and the engine nacelle must be considered in as much as the engine weight could induce high shear and bending at that particular location.

Finally, the HSCT structural design must strive to achieve low supportability cost. The location and number of access panels throughout the entire structure must enable the maintenance crews to access, inspect, and fix any component or part in a relatively short time. Thus,

performance constraints are no longer the only design drivers. However, performance constraints implicitly include the different "discipline" induced design constraints. Figure 9 shows a typical HSCT structural flight envelope diagram. The static envelope is defined by the critical "st-x" points while the more restrictive flutter case, indicated by "fl-x" points, reduces the HSCT envelope.

HSCT Flight Envelope

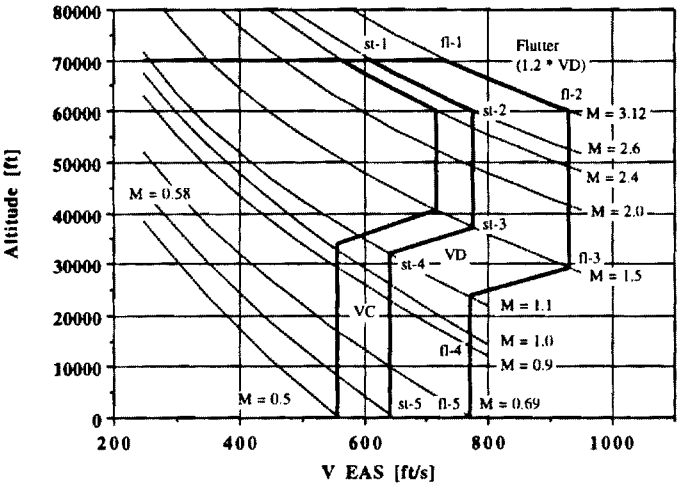

Design Load Cases

	M	Alt [ft]	g	VEAS [ft/s]
st-1	2.60	70000	2.5	610.89
st-2	2.60	60000	2.5	714.65
st-3	1.50	37000	2.5	714.65
st-4	1.10	31800	2.5	490.20
st-5	0.58	0	2.5	490.20
fl-1	3.12	70000	1.0	733.07
fl-2	3.12	60000	1.0	930.55
fl-3	1.50	29200	1.0	930.55
fl-4	0.90	14000	1.0	770.69
fl-5	0.69	0	1.0	770.69

Ref: Peter Rohl, 1995

Figure 9: Structural Envelope for the HSCT

The aircraft synthesis code FLOPS introduces structural capabilities into the analysis through the specification of the ultimate load factor. The design variable ULF (ultimate load factor) was set to 3.5 in the program's input namelist $WTIN. The HSCT's structural flight envelope shows the speeds that must not be exceeded in order to prevent any type of structural failure.

Aeroelastic constraints are usually expressed in the form of divergence speeds or flutter boundaries. The divergence speed is defined as the airspeed at which deformation of the structure occurs. Thus, what starts as a simple twisting or bending of the wing could end up in the failure of the structure. By the same token, the flutter boundary is defined as the flight condition at which the oscillation of the structure (wing, panel, etc.) becomes simple harmonic. The oscillation of the structure produces structural fatigue and, ultimately, structural failure. It is also important to understand the time and amplitude coupling that take places once flutter occurs. Furthermore, the decrease in control surface effectiveness can develop into a reversal condition in which the pilot loses total control of the aircraft. The torsional divergence of the wing, the control surface reversal effect, and surface flutter can all be prevented by increasing the mass and strength of the structure in an appropriate manner. Furthermore, panel flutter is prevented by decreasing the dimensions, increasing the thickness of the wing's skin panels, or adding more structural damping by coating the surface of the structure with special materials. In order to increase the aeroelastic flutter

boundary (increase the speed at which flutter first occurs), the number of spars, ribs, and fasteners could be increased. Coating certain parts of the wing with a special material or resin is also an option. All of these actions will, of course, increase the total weight of the structure. Furthermore, the use of special fasteners which use composites add complexity to the design and are more difficult to manufacture. Thus, the design and selection of materials for the different wing components becomes a key compromise in the structural integrity of the HSCT.

The geometry of the HSCT's double-delta wing also imposes complications. The location of the "kink", where the sweep angle changes, is a design parameter which plays an important role in the subsonic-supersonic performance of the aircraft. Furthermore, the variation of camber along the span (i.e., wing twist) also has very important consequences on the aerodynamic performance of the HSCT. The wing's root must be able to support all the aerodynamic, aeroelastic, and inertial loads. These loads are intensified due to forces near the tip of the wing (outboard part). The location and size of the flaps and ailerons also play an important role in the strength-weight design compromise of the wing. Thus, both the spacing and number of the spars, ribs, stiffeners, fasteners, stringers, struts, caps and panels must guarantee structural integrity and low cost. The reduction of structural weight will reduce the acquisition cost of the aircraft. However, increasing the weight by increasing the structural damping of the materials, making a stronger structural design, and adding more access panels will reduce the operations and support cost of the aircraft. Materials properties such as yield strength, creep strength, tensile strength, compressive strength, modulus of elasticity, and torsional stiffness must be accounted for in the fuselage, empennage, and wing structural design. The wing truss design must be able to withstand the structural stresses, strains, bending moments, torque, and fatigue generated by all of the aircraft's flight conditions. By the same token, material properties such as thermal coefficient of expansion, thermal conductivity, thermal shock resistance, and melting point must enable the structure to withstand the aerodynamic heating and thermal gradients induced by supersonic flight. Both metallic materials and composites are being considered for the HSCT's structural design. Metallic structures have the advantage of being easy to manufacture, but their weight is a concern to designers, especially when critical parts of the structure have to be reinforced. Certain composites, on the other hand, have superior strength characteristics, though they are often difficult to manufacture. Thus, a trade-off must be made in order to reach the most cost effective design configuration.

The landing gear size and weight is another important design consideration in the development of the HSCT. The HSCT's gross takeoff weight requires a sturdy landing gear. This sub-system must be able to withstand and absorb significant loads upon impact with the runway; thus, by necessity, landing gears are usually constructed from steel.

2.1.4.3 Propulsion

As previously discussed, one objective of this study is to perform the aero/propulsion integration for the HSCT. Current developments involving engine design as well as engine selection for the HSCT will therefore be discussed in this section. Also included are some basic definitions and assumptions made during the propulsion portion of the effort.

In order for the HSCT to accomplish the aggressive split mission discussed earlier, it will need an engine cycle that can deliver the necessary thrust while simultaneously satisfying several demanding environmental constraints, such as noise and NO_X emissions. Translating the emissions constraints into engineering terms means that in order to reduce the NO_X emissions, new combustion techniques, such as rich burn - quick quench - lean burn, must be considered. For the noise constraints, the jet velocity of the nozzle must be slowed down while ensuring that the engine produces the same thrust. The resulting engine performance after satisfying these constraints will dictate the feasibility of the engine design. The selection of materials and manufacturing processes also influences the feasibility of the engine design as well the performance and the economic viability of the concept.

The development cost for a new engine has always been a major concern for the engine manufacturers, especially the cost of a completely new core. Therefore, careful attention must be paid to the design of the engine components so that development costs do not become exorbitantly high, placing the future of the program at risk. Other desirable qualities for the HSCT propulsion system are ease of maintainability and supportability, as well as low operating cost. From the performance point of view, the engine must endure extremely high temperatures, stressful centrifugal forces, high shaft rpm's, long operating time at near maximum output, and fatigue life close to 60,000 hours. The high component reliability and low system supportability envisioned for this engine suggest that the materials used in the design must be relatively easy to manufacture, while the engine parts must be easy to assemble and maintain. These strict requirements and constraints imply that primarily mature technology should be employed with the introduction of some high risk technologies in only areas where it is required.

Impact of Engine Design on the OEC

There are three different engine concepts which have been recently been considered for the HSCT. Each engine has advantages and disadvantages related to its performance, noise levels, and NO_X emission levels. However, before a sensible selection can be made, the aircraft/engine design requirements must be studied and understood. Thus, decomposition of the problem becomes a necessary step in understanding the implications of design constraints. Like in any other design, compromises must be made in order to satisfy the performance requirements as well as associated constraints.

Performance requirements of the HSCT engine are dictated by the type of mission that the aircraft is to fly. For example, the engine cycle must produce enough thrust (F_N) in order for the aircraft to accomplish the climb to a supersonic cruise altitude of 60,000 feet. Furthermore, the engine cycle must be designed so as to achieve a reasonable supersonic specific fuel consumption to minimize fuel cost. In order to increase the fuel efficiency, the combustion temperature (T3) must be raised (assuming an acceptable combustion scheme) to higher temperatures, and this implies higher Turbine Inlet Temperatures (TIT). Raising TIT's from the present average limit temperature of 1800 °F (2260 °R) to a temperature near 2800 °F (3260 °R) increases the engine's specific horsepower and reduces specific fuel consumption. However, increasing the TIT runs the risk of turbine blade melt down. Thus, the engine design must incorporate a blade cooling system which has an adverse effect on the engine performance because the core airflow is bled to provide the cooling. New technology, however, can be infused to improve materials in order to withstand the severe thermal conditions, but this also has its associated consequences in the OEC since new technology means higher risk and higher development cost [19].

The emission of nitrogen oxides as combustion by-products is another concern in the selection and design of the HSCT propulsion system which impacts the Overall Evaluation Criteria. A major environmental concern results from the HSCT cruise altitude, which may pose a potential for damage to the ozone layer due to NO_X emissions. A stringent constraint has been imposed on the NO_X emissions, requiring that they not exceed 5 grams of NO_X per kilogram of JP-4 burned. NO_X is a by-product of the combustion process; therefore, the most effective way to control this emission is through the combustion process. Current combustor technology utilizes a stoichiometric burning process to achieve high combustion efficiency. However, this process also contributes to the high levels of NOx by-product. Therefore, if the NOx is to be controlled through non-stoichiometric burning, then some new, higher risk technology must be introduced which will most likely increase the development cost of the engine, significantly driving the $/RPM value even higher. Due to the lack of modeling tools, however, NOx emissions are not considered in this research.

Finally, the noise constraints dictated by FAR 36 Stage III requirements also have an effect on the OEC. The main contributor to takeoff noise is the high jet velocity exiting the nozzle. Thus, a significant noise reduction can be achieved by reducing the exhaust velocity while maintaining the same thrust. Equation 2.1 below shows that the only way to maintain the same thrust (F_N) while lowering the exhaust jet velocity is by increasing the mass flow rate. This method of reducing jet velocity and increasing mass flow rate to maintain the same thrust is the principle behind the design of an ejector nozzle. The flight condition at which noise is the biggest concern is take-off; therefore, at this mission point the up-stream nozzle doors are opened to allow extra mass flow to mix with the high energy core flow in the nozzle before it is ejected. However,

the fact that this nozzle is in the experimental stages of design and that its weight is hard to predict makes its use in this methodology development study unwarranted. It is, though, a key to future efforts to deal with takeoff noise for the HSCT.

$$F_N = \dot{m}_a \cdot V_{jet} \tag{2.1}$$

Engine Type Selection

The three candidate engines considered as alternatives to power the HSCT are the Turbine Bypass Engine (TBE), the Fan-in-bLADE (FLADE) engine, and the Mixed Flow TurboFan (MFTF) engine. Each of these candidate engine cycles are briefly described in the following paragraphs.

The TBE is a single spool turbojet engine with an oversized compressor. This engine concept takes advantage of the simplicity of the turbojet cycle, and it uses a bypass valve to maintain constant turbine correct airflow throughout the flight envelope which eliminates the need of throttling. By bypassing some of the compressor discharge air around the combustor and turbine instead of throttling, the TBE is able to achieve higher (as compared to turbojet) cycle pressures and temperatures and still maintain total airflow. Furthermore, this bypassed air helps the cycle maintain high airflow during part power operations which reduces spillage and boattail drag. One of the biggest drawbacks for the TBE is its inherent high jet velocity which contributes to its high noise level, a disadvantage that requires the use of noise suppression devices or complex nozzle designs[20,21].

The Fan-in-bLADE engine (FLADE) is a derivative of the variable stream control engine concept. The variable stream control engine is a twin spool turbo-fan with a variable bypass ratio. In this concept, the primary duct exhaust stream and the fan duct exhaust stream are controlled independently via two burners and two exhaust throat areas. The FLADE incorporates an additional fan duct (i.e. separate bypass duct) in order to increase the engine's airflow which increases thrust during takeoff. This same concept is used to provide extra thrust during transonic/supersonic acceleration and supersonic cruise. Due to the extra airflow from the fan duct, the FLADE has a lower exhaust jet velocities (as compared to the TBE) and a moderate noise footprint. Another advantage of the FLADE is its good subsonic SFC characteristics. But, the overwhelming disadvantage of this engine cycle is its cycle complexity[20,21].

The last candidate considered is the mixed flow turbofan (MFTF) engine which is a twin spool, low bypass ratio turbofan engine. In the MFTF, nominal amount of fan airflow bypasses the compressor, the combustor, and the high and low pressure turbine. This bypassed air is then mixed with the high energy gas of the core in the mixer right before the flow is exhausted through

the nozzle. Due to the mixing of the bypassed and the core air, the MFTF inherently has a low jet velocity, which translates to low jet noise, and good subsonic SFC[20,21].

A prime objective of the implementation portion of this research was to investigate the impact of the propulsion and aerodynamic design variables on the overall evaluation criterion ($/RPM) and to find an optimum setting for these variables to minimize the $/RPM. Before this task can be accomplished, one of the engine cycles discussed above must be selected. The TBE was rejected because it had an unacceptable level of jet noise and because it is not as efficient as the MFTF or the FLADE. The FLADE, on the other hand, was also rejected because its cycle complexity made it difficult to model and because of the lack of a historical database on this engine. Finally, the MFTF engine was chosen because it had an efficient and simple cycle which could be easily modeled and studied and because it is an off-the-shelf technology which reduces both development and manufacturing cost. Even with the weight penalty associated with a complex nozzle system to reduce jet noise further, the MFTF was still the winner compared to the other two alternatives. However, a much lighter nozzle with less complicated mechanisms must be developed in order to this engine cycle to be truly appropriate for the HSCT. Now that an engine cycle has been decided upon, the MFTF cycle is then modeled in ENGGEN, an internal engine cycle analysis code that resides in FLOPS. Figure 10 shows a block diagram of the MFTF engine cycle that was used in the modeling process.

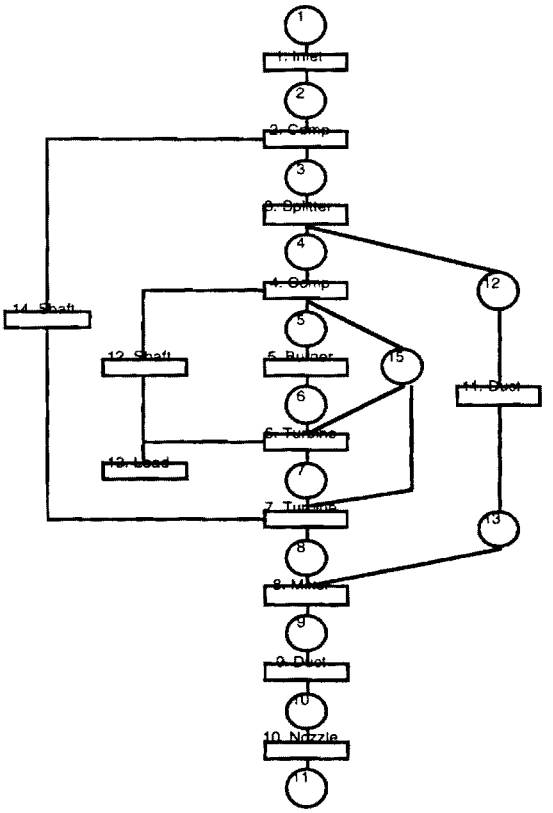

Figure 10: MFTF Engine Layout Showing Flow Stations and Components

As shown in the layout, the MFTF is modeled with an inlet, a fan or low speed compressor, a splitter, a second compressor (high speed), a burner, a high pressure turbine, a low pressure turbine, a mixer, and a nozzle. The compressor and the high pressure turbine are driven by the same shaft. Likewise, the fan and the low pressure turbine are spooled together. Part of the fan flow is bypassed around the core of the engine, and it rejoins the core flow at the mixer behind the low pressure turbine.

Engine Variable Selection: An Example Recomposition

With the engine modeled in ENGGEN, the key propulsion design variable selection process can now be carried out, as illustrated in Figure 11.

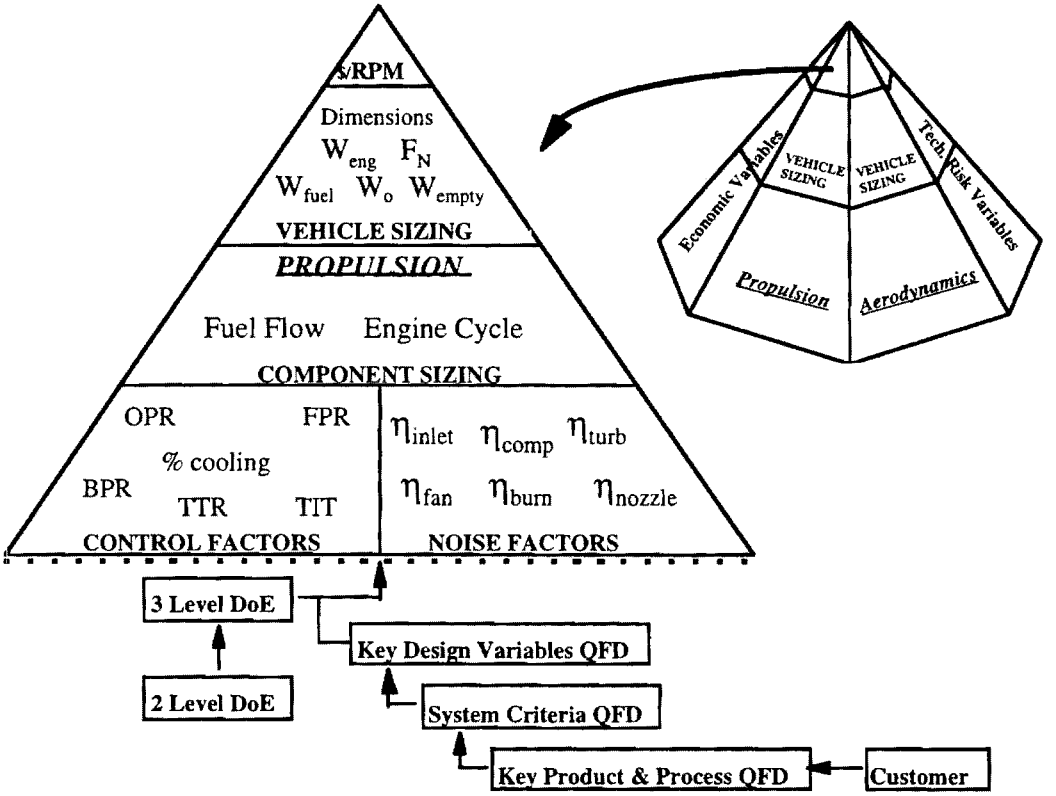

Figure 11: MFTF Design Variable Decomposition-Recomposition Structure

As seen in the figure above, starting from the customer requirements, the design effort is concentrated on understanding the problem through decomposition. The deployment of QFDs and the conducting of a 3 level DOE result in the control factors and the noise factors. The control factors are those parameters which the designer is free to manipulate to shape the design. The noise factors are viewed as parameters of which the designer has no control over. Here, the

different component efficiencies reflect the influence of the noise factors. For example, manufacturing imperfections of the engine components induce a loss in performance, and the resulting efficiencies try to capture the performance losses. Moving up in the pyramid, it is illustrated that the design variables affect the component sizing variables. In the case of the engine, SFC, F_N, weight, and dimensions are all determined by the selection of the cycle variables and the vehicle mission requirements. Next, the pyramid depicts how component sizing variables can affect the vehicle sizing variables. The weight of the engine and its SFC influence the aircraft's empty weight, fuel weight, and, ultimately, its gross weight. Finally, the influence of the vehicle sizing variables on the $/RPM is depicted at the top of the pyramid. The other sides or faces of the pyramid are occupied by other design disciplines, economic uncertainty variables, and technology risk variables. Other disciplines such as aerodynamics, structures, or stability and controls can be decomposed in a way similar to that of propulsion. For the analysis to be describe in the remaining portion of this section (synthesis and sizing), only the propulsion control variables will be considered. This is described in Section 2.2.3.

2.1.4.4 Stability and Control

A part of the process of designing a civil transport is ensuring that the airplane passes the certification procedure successfully. The designer has significant control over the aircraft performance by selection of the vehicle's geometric and configuration characteristics. But to meet the certification requirements as spelled out by the Federal Aviation Administration (FAA) in FAR Parts 25 and 36, compliance with certain flying qualities criteria is required. The purpose of these requirements is to ensure that the airplane's flying qualities do not place any limitations on the vehicle's flying safety or its ability to perform an intended mission. As such, flying qualities are related to the static and dynamic stability of the airplane as well as to the control power.

Static longitudinal stability ensures that the airplane will tend to fly at a constant speed and angle of attack as long as the controls are not moved. The requirement on dynamic stability is typically expressed in terms of the damping ratio and the frequency of a natural mode. The level of static stability, if it exists at all, is a major factor in determining such things as ride qualities, maneuver envelopes, and handling characteristic requirements. Several studies have begun to define these requirements for an HSCT type vehicle[22,23]. Chances are that, for a variety of reasons, this HSCT aircraft will employ Relaxed Static Stability (RSS). RSS is defined as the reduction or elimination of inherent static stability for the purposes of improved performance. Examples of modern aircraft which have employed RSS include the F-16 Falcon and the B-1 Lancer. The accompanying requirement, though, is that a Stability Augmentation System (SAS) is required.

Whether augmentation is employed or not, a control authority assessment must be made. The level of authority is determined by examining both augmentation duties and trim requirements. Certain flight conditions, such as low speed flight in the presence of gusts, serve as the "sizing" conditions in terms of control power. Of course, excessive authority should be avoided as it results in increased weight and drag. Control authority (or control power), in essence, represents the ability of the control surfaces to produce a range of steady equilibrium or maneuvering states under commanded deflections. So then the level of authority is determined by the surface size (force) and its location in relation to the CG (moment arm). For example, the total pitching moment for the aircraft is the sum of its zero lift pitching moment, moment due to angle of attack, and its pitching moment due to an elevator deflection as given in Equation 2.2. It is this last term, $Cm_{\delta e}$, which represents the elevator control power.

$$C_m = C_{m_o} + C_{m_\alpha}\alpha + C_{m_{\delta e}}\delta e \qquad (2.2)$$

Various new technologies may be available for the HSCT which would enhance its aerodynamic performance while maintaining adequate control power. Once such concept is the Active Flexible Wing (AFW). The AFW attempts to use wing flexibility as an advantage by using smaller control surfaces in combination with the power of the air stream to twist the wing as appropriate for the desired maneuver. Examples of the use of AFW technology to increase control power have been demonstrated[24].

In the case of static stability, a classical measure is the *static margin*. The static margin is given by

$$\frac{(X_{np} - X_{cg})}{\bar{c}} \qquad (2.3)$$

where X_{np} defines the position of the neutral point (or center of lift) and X_{cg} is the position of the center of gravity. Thus, if the center of gravity is rear of the center of lift, the static margin is negative and the aircraft is staticly unstable in pitch. This case corresponds to the case when the Cm_α curve has a negative slope. So for a negative slope of Cm_α, a *positive* static margin is necessary. It will be seen that Cm_α can be used as a design constraint in the optimization task to be described in section 4 below. For dynamic stability, some possible measures include the convergence characteristics of the natural modes (of the linearized dynamics), the period (for the complex case) and time-to-double / time-to-half of the modes.

As a first step towards tackling these S&C issues, it must first be determined how the stability requirements can be addressed. In the broadest sense, this can be done as follows:

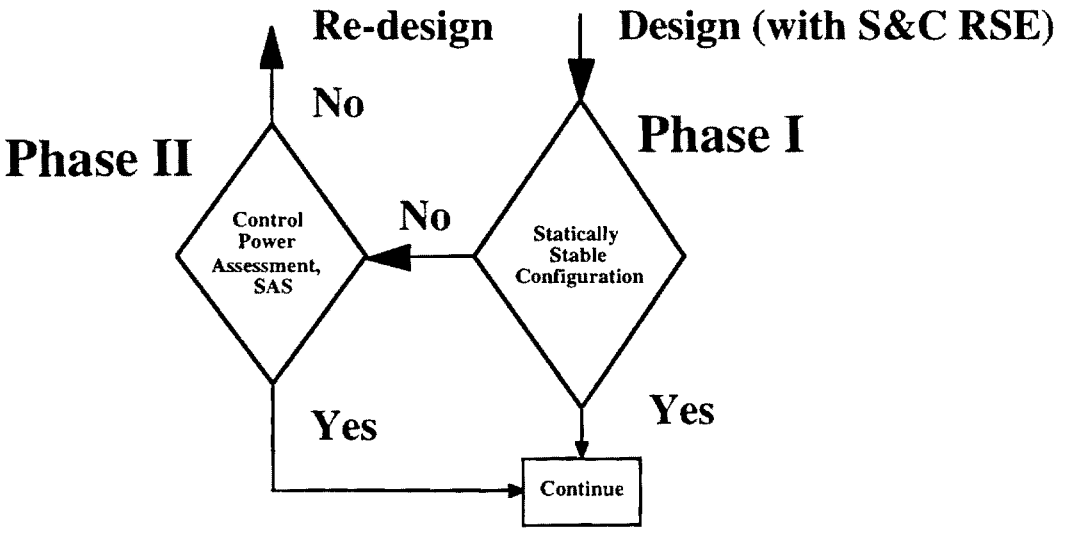

Figure 12: Stability Decision Logic

Figure 12 illustrates that determining the stability characteristics is the first step to be accomplished. If instabilities exist in any motion, a control authority assessment needs to be performed. If it is determined that RSS is feasible and a suitable SAS can be designed, the development can continue. In a simpler setting, static longitudinal stability (Cm_α) can be investigated as a constraint, understanding that any configuration chosen which violates this constraint would require a SAS. The development of this required SAS and the associated control design issues are not covered in this report.

With the main conclusions of SuperSonic Transport (SST) studies of the 70's/80's in hand, industry (mainly Boeing and Douglas) presently has undertaken the task of identifying requirements for the HSCT Flight Control System (FCS). One conclusion seems common; that the FCS for this airplane must be highly integrated (especially with regards to the propulsion system). As an example, the use of variable exhaust nozzles will be utilized for engine control and noise suppression. In light of the need for an integral control scheme, Boeing has stressed that MDO is critical, especially through a common database and integration of design and analysis tools.

The following, then, outlines probable requirements for the HSCT: In pitch, the FCS must provide augmentation for the unstable modes, provide enough pitch-up for nose wheel lift-off, supply sufficient longitudinal control for landing trim, and provide pitch limiting to avoid tail-strike at takeoff. The lateral-directional control of the FCS must be able to minimize dynamic response to engine out (both at takeoff or landing), augmentation at supersonic cruise for spiral and Dutch roll modes, and acceptable gust load alleviation. All of these need to be accomplished with small control surfaces and surface deflections to minimize drag[25, 26].

2.1.4.5 Noise Considerations

The literature concerning takeoff (and landing) noise for the HSCT has been quite universal in the conclusion that optimal takeoff procedures must be incorporated if the aircraft is to be an environmentally and economically viable project. One of the major lessons learned from the Concord is that by drastically reducing the number of available markets due to noise violations, the effectiveness of the aircraft as a profitable transport plummets. The Federal Aviation Administration (FAA) has stated its intention that any new supersonic transport must comply with current Federal Aviation Regulation (FAR) 36.

The FAA has established regulations governing the acceptable levels of aircraft noise around airports. Since sound waves are characterized by several different parameters (frequency, wavelength, tones, etc.), there are numerous ways to quantify noise intensity. Some of these measures are briefly described in Table 2.2. Note that many of the measures build on the more basic ones. The Effective Perceived Noise Level (EPNL), especially, is a good example of this. The important set of regulations laid out by the FAA are contained in FAR 36, which establishes EPNL (dB) as the measure of choice when certifying aircraft. As can be seen from Table 2.2, frequency, intensity, and tones are all accounted for in the EPNL making it a sensible measure.

Table 2.2: Noise Measures Summary

Abb.	*Name*	*Brief Description*
SPL	Sound Pressure Lev (in dB)	*SPL=10log(p1/po)^2;* where p1 = wave pressure, po = 20 micro Pa = 0 dB
PNL	Perceived Noise Level (in dB)	*PNL=40+33.22logN(k);* where N(k) = total perceived noiseness at time increment k. N(k)'s are computed from SPL, and weighted for frequencies
PNLT	Tone Corrected PNL (in dB)	PNLT is calculated through a procedure described in FAR 36, correcting PNL for tones (discrete frequency components)
EPNL	Effective Perceived Noise Level	$EPNL=10\log[(1/T)\int 10^{(PNLT/10)}\,dt]$; where T = 10 secs, t1 and t2 are the limits of the event interval. Units are dB

FAR 36 also specifies observer locations with respect to the runway to standardize the certification of aircraft (see Figure 13). Currently, the HSCT will be required to meet the same community noise levels as current large subsonic transport planes. However, an effort has been mounted to amend the regulations, not to change maximum EPNL levels, but to permit the use of currently banned advanced procedures for noise suppression such as digitally controlled flaps[37].

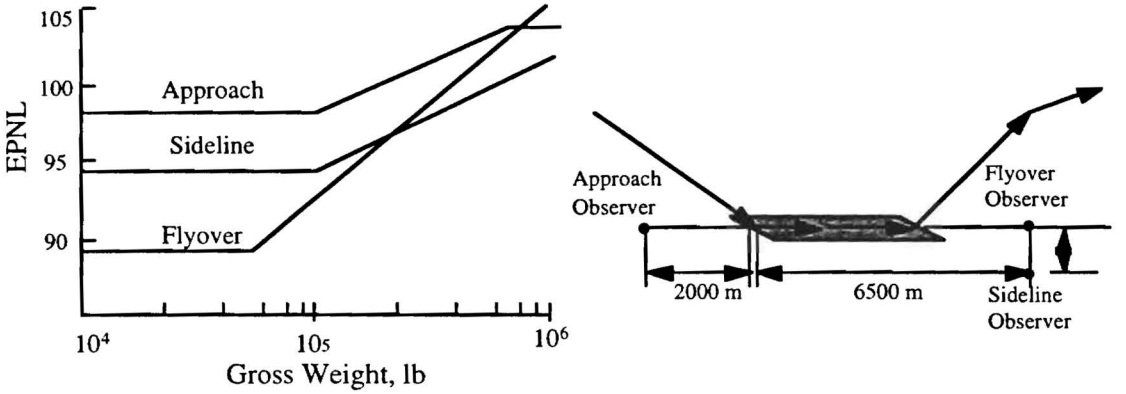

Figure 13: The FAR 36 EPNL Limits and Observer Locations

2.1.4.6 Manufacturing and Material Selection

Material selection often has a large impact on the design of a component. When selecting materials for components of an HSCT airframe and propulsion system, it is important to first consider their mechanical properties: strength-to-weight, stiffness-to-weight, ductility, hardness, elasticity, fatigue, and creep. These mechanical properties are then used as a guideline when considering the conditions under which the components will be expected to function. Next, the physical properties such as: density, specific heat, thermal expansion and conductivity, melting point, and electrical and magnetic properties are considered. The chart in Figure 14 was developed as an aid in the material selection process. The chemical properties can play a very important role in material selection for certain components of the propulsion system. Properties such as: oxidation, corrosion, general degradation of properties, toxicity and flammability are all important particularly considering the environment produced by the compression and combustion of gases which occur within an aircraft engine.

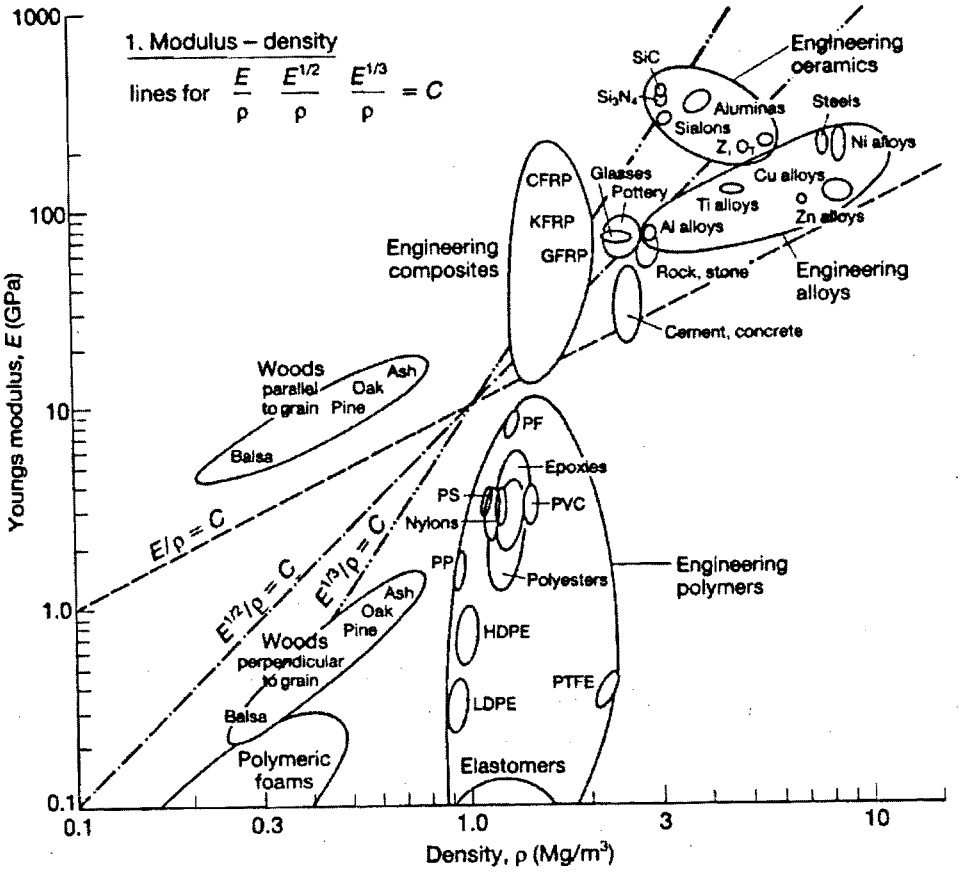

Figure 14: Ashby materials selection chart: Young's modulus vs. density Ref. (M. F. Ashby, Material Science and Technology volume 5, p. 521, 1989.)

All material properties must be considered during the selection phase as well as the manufacturing process selection. The properties of a material determine whether they can be cast formed, machined, welded, and heat treated with relative ease or whether some other more complex method must be used. The methods used to process materials to the desired shapes can adversely affect the product's final properties and service life. It becomes evident that material selection has an impact on product life cycle cost. The raw material cost, forming and manufacturing costs, as well as supportability and disposal costs are all functions of material selection.

The materials selection process is part of engineering design and therefore is a problem-solving process. This process can be divided into four steps:

1. Analyze the requirements of the materials. Determine the conditions of service and environment that the product must withstand. Translate these conditions into critical material properties.
2. Screen the candidate materials. Compare the needed properties with a large materials property data base to select several materials that look promising for the application.

3. Select the candidate materials. Analyze candidate materials in terms of product performance, cost, ease of fabrication, and availability of best material for the application.
4. Develop design data. Experimentally determine the key material properties for the selected material to obtain statistically reliable measures of the material's performance under the specific conditions expected to be encountered in service.

Step three has been the subject of various studies into the development of analytical methods for comparing and selecting the best available material in terms of cost and performance. Some of the common materials selection methods include: cost vs. performance indices, weighted property indices, value analysis, failure analysis, and benefit-cost analysis. The use of expert systems in the material selection process is also becoming more prominent in the design of complex systems[27].

Step four also deserves some extra attention due to the fact that the production of a HSCT airframe and propulsion system will require the utilization of new technologies in materials and manufacturing. The use of composites in the airframe and propulsion system will be necessary to realize the dramatic reduction in empty weight required for an economically viable HSCT. An example of some of the exotic materials which are being considered for a supersonic cruise engine are: titanium aluminides, ceramic matrix composites, high temperature intermetallics, and thermal protection coatings. The design data referred to in step four are the properties of the selected material in its fabricated state that must be known with sufficient confidence in order to permit the design and fabrication of a component that is to function with a specified reliability. The materials selection and evaluation process for a complex or advanced design are shown in Figure 15.

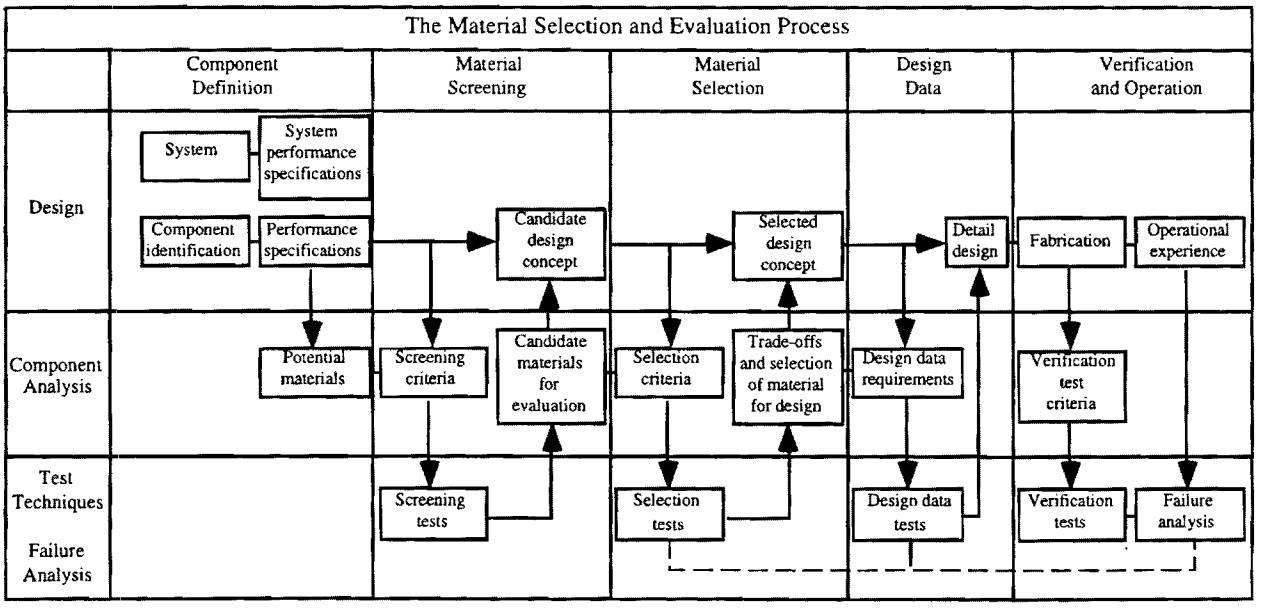

Figure 15: Materials Selection and Evaluation Process for a Complex Product

The material selection phase should be considered earlier in the design cycle during the conceptual phase of design. This action has several advantages over the previous convention of placing material selection near the end of the design cycle. At the conceptual phase of design, all of the options are open which allows for the broadest freedom in material selection and component design resulting in reduced cost and improved product performance.

Often there is more than one manufacturing method for producing the same part. Selection of the optimum process requires a comparison of the costs of manufacturing associated with each of the competing processes. These comparisons must include consideration of the material to be used, the cost of processing the material to a finished product, material utilization, the function of the finished product, and the effect of processing method on material properties. The primary parts of an airframe and propulsion system are generally produced by a variety of procedures including: several casting and forging processes, many machining operations, fabrication and assembly procedures, and finishing operations[27].

Casting procedures include the use of expendable and permanent molds. Forming and shaping procedures include the following processes: rolling, forging, extrusion, drawing, sheet forming, powder metallurgy, and molding. The machining procedures which will be employed include: turning, boring, drilling, milling, planing, shaping, broaching, grinding, ultrasonic machining, chemical, electrical, and electrochemical machining, and high-energy beam machining. The variety of joining methods include: welding, brazing, soldering, diffusion bonding, adhesive bonding, and mechanical joining. Finishing operations include: honing, lapping, polishing, burnishing, deburring, surface treating, coating, and plating[28].

As previously stated, there generally exists more than one manufacturing method for producing the same part. The selection of one process over another is made based on cost. The manufacturing cost associated with every method to be considered is a function of material costs, tooling costs, labor costs, fixed costs, availability, lead times, processing times and learning curve. The impact of each of these variables on manufacturing cost varies with method. The material costs variable is the cost of the material which will be used by the manufacturing technique under consideration during this phase. Material costs generally have a large impact on choice of manufacturing procedure. For example, if the cost of a material is high then a manufacturing method which produces the least waste will be most desirable. The tooling costs variable reflects the costs involved with utilities, equipment, operating supplies, and maintenance. Labor costs are concerned with the operating man-hours, fringe benefits, and the number of process steps. The fixed costs parameter includes depreciation, taxes, insurance, facilities or rent, and interest on investment. The learning curve variable represents the complexity of the manufacturing method

and the amount by which workers' level of skill increases. Learning curve indicates an improvement in the production method over time[27].

The utilization of technically advanced manufacturing methods will have as significant an impact on the economic viability of HSCT as technological breakthroughs in materials. New manufacturing methods will be necessary to: reduce the overall cost of the composite materials to be incorporated into the airframe and propulsion system, make it possible to fabricate the exotic materials needed for the engine core, and reduce the overall costs in manufacturing. Some of the methods which may contribute to these efforts include Microwave Chemical Vapor Infiltration (CVI), Flexible MMC Monotape processing, Virtual Prototyping & Manufacturing, and Rapid Prototyping[29].

2.2 Concept Modeling/Synthesis/Sizing (Step 2)

2.2.1 Sizing and Optimization Approach

Revisiting the IPPD flow of Figure 4, one sees the central role of vehicle sizing. Considering disciplines of the aircraft from the product side such as aerodynamics, structures, and propulsion, and the process side, such as manufacturing and supportability issues, the aircraft is sized via a computer simulation. The simulation tool incorporated for this study the FLight OPtimization System code (FLOPS), linked with the Aircraft Life Cycle Cost Analysis (ALCCA) module. This sizing process, in conjunction with a DOE, allows for the formulation of an response equation for the objective function, average yield per Revenue Passenger Mile ($/RPM). In order to validate this equation over the whole design space, the sizing procedure has to be unconstrained. Performance and environmental constraints are applied after sizing during optimization of the objective function. If economic viability is achieved, the program can be launched, if not, three possibilities are open to achieve this viability: increase of fare premium, yield management/reduce Return on Investment (ROI), or technology improvements (see Figure 2). An increase in fare premium, or a surcharge for flying supersonically, would move the target of economic viability closer to the achieved value by the economic uncertainty assessment. Yield management or a reduction in ROI for the airline or/and manufacturer will help to reduce the ticket price, shifting the distribution for $/RPM closer to the target of economic viability. The last option is to introduce new technologies to the program, if possible. If not so, the program can be terminated early in the conceptual/preliminary design phase without the manufacturer loosing money by building prototypes and testing of an aircraft that will never enter production. If improvements can be made for certain areas by infusion of new technologies, the sizing process has to account for these new changes and the process must be repeated again. These three possibilities are address later in section 2.

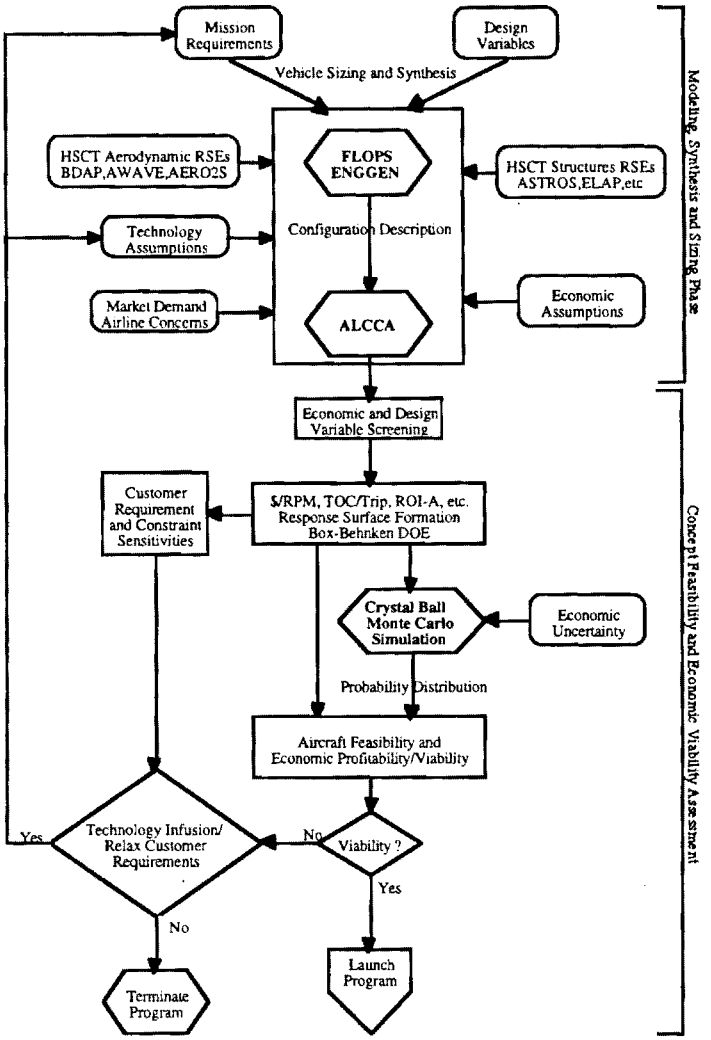

Figure 16: Methodology Implementation- Steps 2,3 Flow Diagram

The scope of Step 2 was to size the aircraft with improved aerodynamic and propulsion prediction procedures, generate equations for the objective function and constraints, and obtain a constrained solution that can be passed to the economic uncertainty assessment. Figure 17 below captures this scope with a box at the top of the flow chart. An improvement in accuracy of prediction of aerodynamics was achieved by replacing the drag polars in FLOPS with equations generated from BDAP, AWAVE, WingDes, and AERO2S. For the propulsion system, improved input files were utilized together with ENGGEN to enlarge the accuracy of the engine cycle prediction. Once the equations are installed in FLOPS, Figure 17 describes the final steps of the approach. Incorporating a DOE with 151 simulation runs for 11 variables from aerodynamics (x1, x3, x5, y1, xwing), propulsion (BPR, FPR, OPR, TIT), and size of the aircraft (T/W, S-wing), Response Surface Equations (RSE) for the objective function $/RPM and the constraints (V-app,

Cm_α, Flyover and Sideline EPNL, TOFL, and LFL) can be established. Utilizing the Solver in an Excel spread sheet, the objective function can be optimized, while the solution obtained has to meet all constraints. Hence, the solution found is the constrained point optimal configuration for an HSCT. Finally a confirmation run to validate results and obtain component weights is performed. These component weights together with the mission parameters describe the optimal configuration passed over to the economic uncertainty assessment.

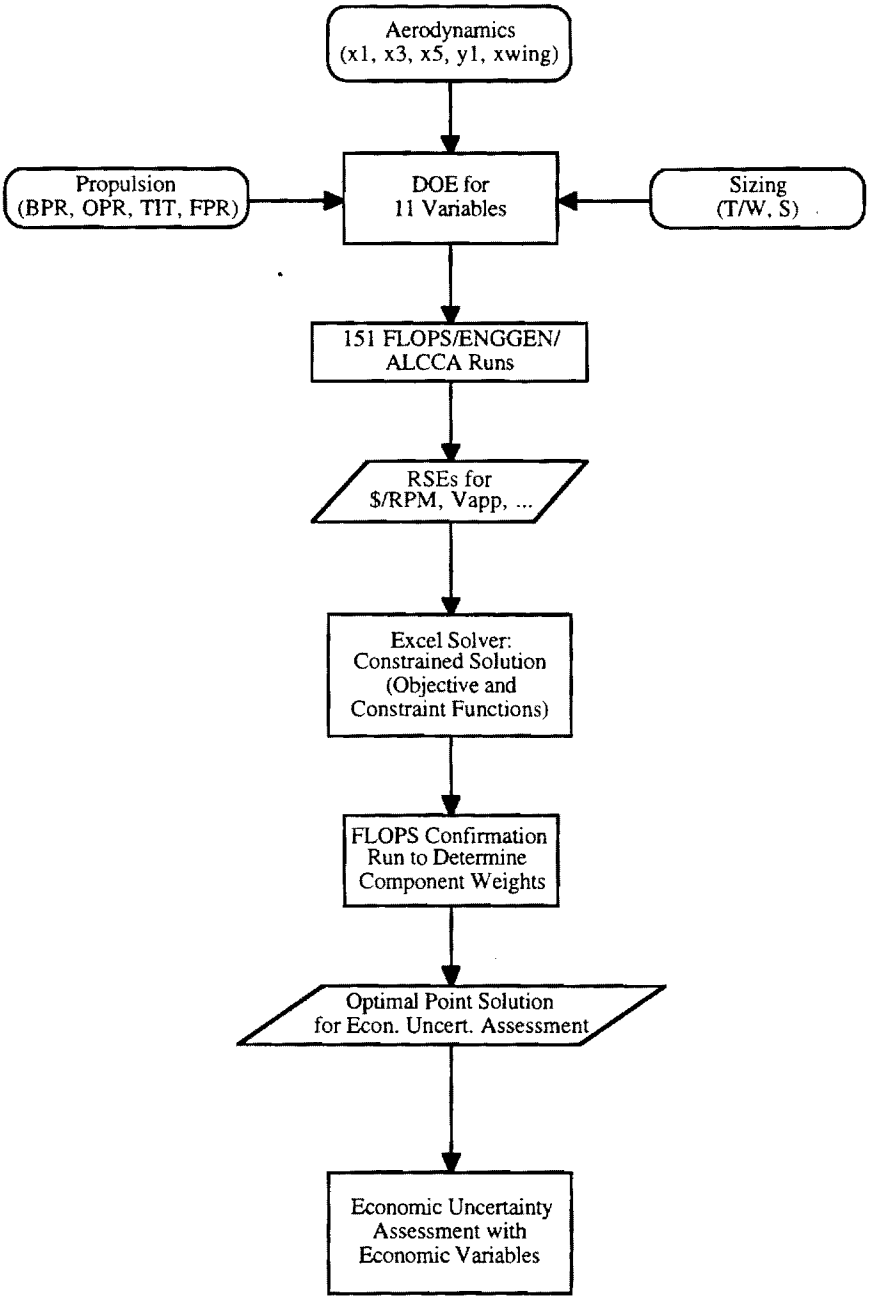

Figure 17: Steps 2 and 3: Design Optimization Approach

One final note on the synthesis/sizing which concerns nomenclature. There are two distinct Mach numbers which are involved during the design process. The *design Mach number* is that speed at which the aircraft is designed and sized for at a certain flight condition. This design Mach number determines the wing camber and twist, the material selection, and the inlet sizing / shaping. For our studies, the design Mach number was chosen to be the supersonic cruise speed (M=2.4). All other Mach numbers at which the aircraft flies are termed *operational Mach numbers*. There is an important consequence of this distinction, for the RSEs obtained for aerodynamics using a specific design Mach number will be valid then only for that design mach number. Thus, studies to determine the optimum cruise Mach number would require multiple collections of RSEs, one set for each configuration with differing design Mach number. Although this may sound like a prodigious amount of work, once a routine has been automated to generate the response equations, running this routine multiple times should be reasonable. Then, the problem could be seen as

min \$/RPM over all D_i

where D_i represents discrete configurations with differing design Mach numbers.

2.2.2 Aerodynamic Response Surface Equations

The goal of introducing RSE's is to replace the existing drag calculation in the synthesis code FLOPS by an RSE-based representation. FLOPS determines drag (in one of several ways, including table-lookup, internal calculation, polar equation) as a function of lift coefficient C_L and operational Mach number at each of numerous discrete points in the mission profile. To maintain this functional relationship, the following polar equation was used in considering the formation of RSEs.

$$C_D = C_{D_0} + k_1 * C_L + k_2 * C_L^2 \qquad (4.1)$$

RSE's for C_{D_0}, k_1 and k_2 were formed as a function of design variables and operational Mach number. Thus, the total drag for a given aircraft configuration was again a function of Mach number and C_L.

2.2.2.1 Design Variables

The design variables which were to make up the RSE's had to be the ones which have the most influence on the aerodynamic characteristics of the airplane and, perhaps most importantly, that the designer can control. This excludes, for example, fuselage length and diameter since these are given by the number of passengers to be carried. The design variables were determined by literature studies and several brainstorming sessions during the HSCT-Design Project in winter quarter 1995, as part of the course AE6351. A summary of all the design variables can be found in Figure 18.

Other Design Variables
for the Aerodynamic Screening

xwing
t/c at root
t/c at tip
Nacelle Scaling
Horizontal Tail Area
CL Design
Root Airfoil (loc. max. thickn.)
Tip Airfoil (loc. max. thickn.)
Nacelle X-location
Wing Reference Area

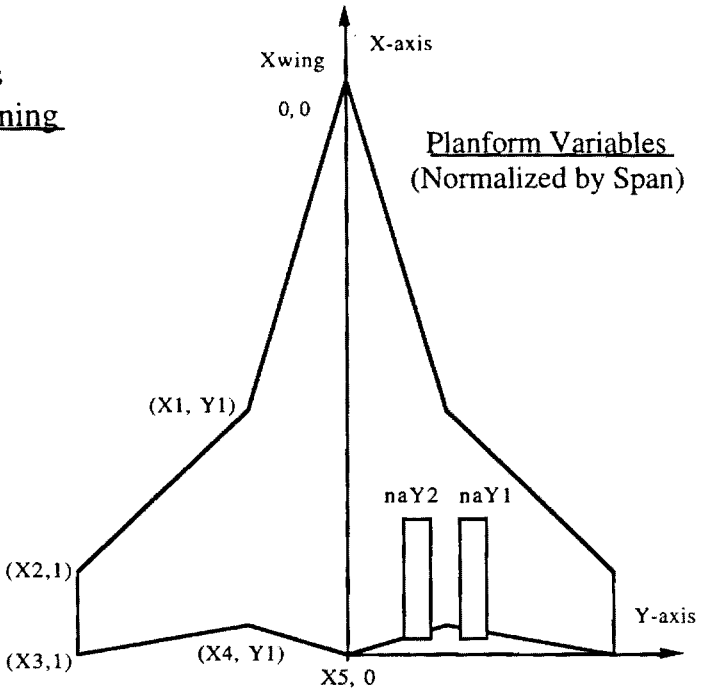

Figure 18: Aerodynamic Design Variable Selection

It should be noted that the parametric definition of the wing allows for the modeling of a variety of planforms, from pure arrow wings (delta wing) to double-delta types. A sampling of some of the shapes investigated is shown in Figure 19.

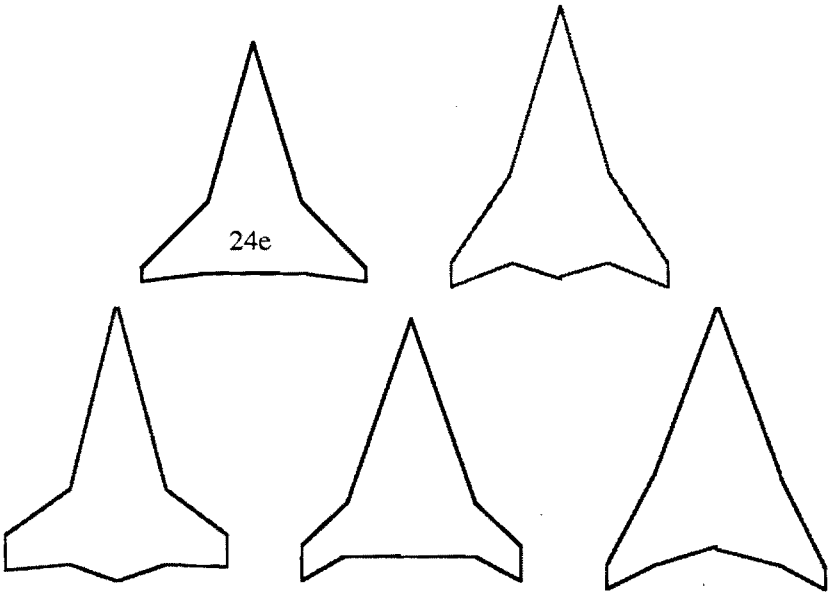

Figure 19: Planform Possibilities Studied

It is a crucial point to pick meaningful ranges for the design variables: On the one hand, the ranges should be somewhat large to include the greatest amount of configurations possible and increase

the chances that the true optimal configuration is captured. On the other hand, the range must not be chosen so large that a good fit for the RSE is not obtained. Additionally, there are physical restrictions which limit the choices, e.g. the wing at its aftmost location with longest root chord may not interfere with the horizontal tail. Finally, choosing appropriate design variable ranges depends on the experience of the design group with the particular type of aircraft being modeled. Table 2.3 shows a summary of all design variables with the chosen ranges.

Table 2.3: Aerodynamic Design Variable Ranges

Variable	Symbols	Lower Bound	Upper Bound
Kink X-loc.	X1	1.54	1.69
Tip loc. leading edge	X2	2.10	2.36
Tip loc. trailing edge	X3	2.40	2.58
Kink loc. trailing edge	X4	2.19	2.36
Kink Y-loc.	Y1	0.44	0.58
Root Chord	X5	2.19	2.50
Nacelle (1) Y-loc.	NAY1	0.25	0.35
Nacelle (2) Y-loc.	NAY2	0.45	0.55
Nacelle X-loc.	NAX	10.30	16.50
Wing Area	S	8500.00	9500.00
X-loc. of Wing	XWING	0.25	0.33
t/c Root	TCI	2.70	3.30
t/c Tip	TCO	2.30	2.80
Nacelle Scaling	NAC	1.00	1.20
Area of Hor. Tail	STAIL	400.00	750.00
CL Design	CLDES	0.08	0.12
Root Airfoil (loc. max. thickness)	IAF	0.50	0.60

Operational Mach number

Although it would be possible to make the RSE also a function of Mach number, it seemed to be more appropriate to generate RSE's for the coefficients of the drag equation (4.1) at discrete Mach numbers. This is mainly for two reasons:

1) The most important design variables to the RSE will be different for subsonic and supersonic flight regime. Additionally, none of the available analysis tools (described later in the report) is able to handle both sub- and supersonic Mach numbers.
2) It significantly reduces the number of experiments to be run.

Airfoils

Tools were not available to perform an airfoil optimization. Therefore, existing subsonic and supersonic airfoils were used. These airfoils were representative airfoils typical for use on a supersonic transport, where the outer portion of the wing requires a thin, sharp leading edge design while the inboard section, due to its high sweep angle, requires a subsonic shape. A scaling of the airfoil shape has been used to place the location of maximum thickness at the desired value without changing important characteristics of the original shape, such as nose radius.

Cl-design

CL-design is the lift coefficient required at the beginning of supersonic cruise. It is a variable that the designer has no control of and that is basically unknown until the weight of the aircraft is determined. Yet it has a significant impact on the design of the wing (as it is an input to the camber optimization code) and therefore, on aerodynamic performance. Thus, it was decided to carry this variable along and treat it as an important contributor to the response.

Horizontal Tail Area

This variable needs special treatment since the area of the horizontal tail actually depends on whether there is a horizontal tail at all. The approach was that for the screening cases the tail area was allowed to vary between 0 sq-ft (no tail) and the maximum value for a "with-tail" configuration (750 sq-ft). However, for the RSE's, a distinction between tail and no-tail configurations had to be made, i.e. for every flight condition both a tail and a no-tail RSE have been generated. For the no-tail cases, the tail area was naturally set to 0 sq-ft whereas it was varied between 400 sq-ft and 750 sq-ft for the tail cases.

2.2.2.2 Generating the Aerodynamic RSE's

The sheer amount of experiments that have to be carried out make an automated environment a necessity. The reader may easily appreciate this by looking at the following example: For the coefficient CD_0 at supersonic Mach numbers it turned out after the screening that 8 variables had significant influence on this response. The 5-level Central Composite Design requires 147 cases (i.e. different input files) to achieve a second order approximation to the response. Multiplying this by two gives 294 cases, and that means 294 for tail and no-tail RSE's respectively, for CD_0 only! Therefore, the task was undertaken to create an automated procedure for setting up, running, and formatting these numerous cases. The process now is automated to an extent that basically only one user interaction is necessary between receiving the DOE table from JMP (see Section 3.) and sending the table of results back to JMP, where the results are analyzed and the coefficients of the RSE are generated. A FORTRAN routine "SETUP_CASES" reads the DOE table, transforms the normalized settings of the design variables (-1,+1,etc) into actual values, and initializes a shell script (RUN_CASES). This shell script successively runs the cases, directly producing the result file for return to JMP. The flow chart of this process is shown in Figure 21. The user must supply all components of the baseline aircraft (except the wing) separately in craidon format, which is used by BDAP and AWAVE.

The main tool is the UNIX shell script "FL01", based on a script originally written by Peter Rohl, but vastly extended by Florian Bachmeier and Andreas Hahn of the ASDL. FL01 was still

subject to development and improvement during the time of this project. Some minor changes were necessary in order to tailor the shell for automatically running multiple cases with the chosen design variables (Table 2.3) as inputs and the drag parameters CD0, K1 and K2 as outputs. FL01 links together several aerodynamic design and analysis tools (see also Figure 20): FLOPS (V5.7), at this point, is used only as a pre-processor. Its main purpose is to output the wing planform in a format suitable for WINGDES and to give an estimate of the location of the Center of Gravity of the airplane. WINGDES generates an optimized twist and camber distribution for the wing at the design point (Cl-design, Mach number = 2.4). AWAVE performs area ruling of the fuselage at the design Mach number. AERO2S computes subsonic drag due to lift while BDAP computes zero-lift wavedrag, drag due to lift at supersonic Mach numbers, and skin friction drag for all Mach numbers.

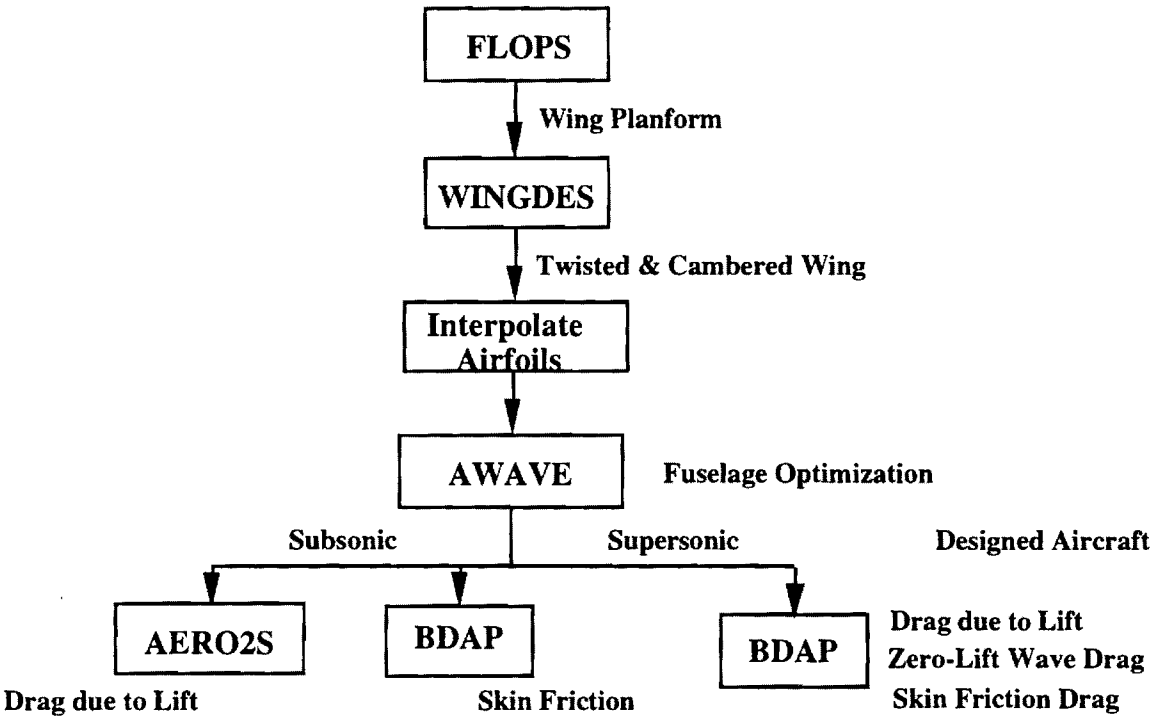

Figure 20: Flow Chart for FL01

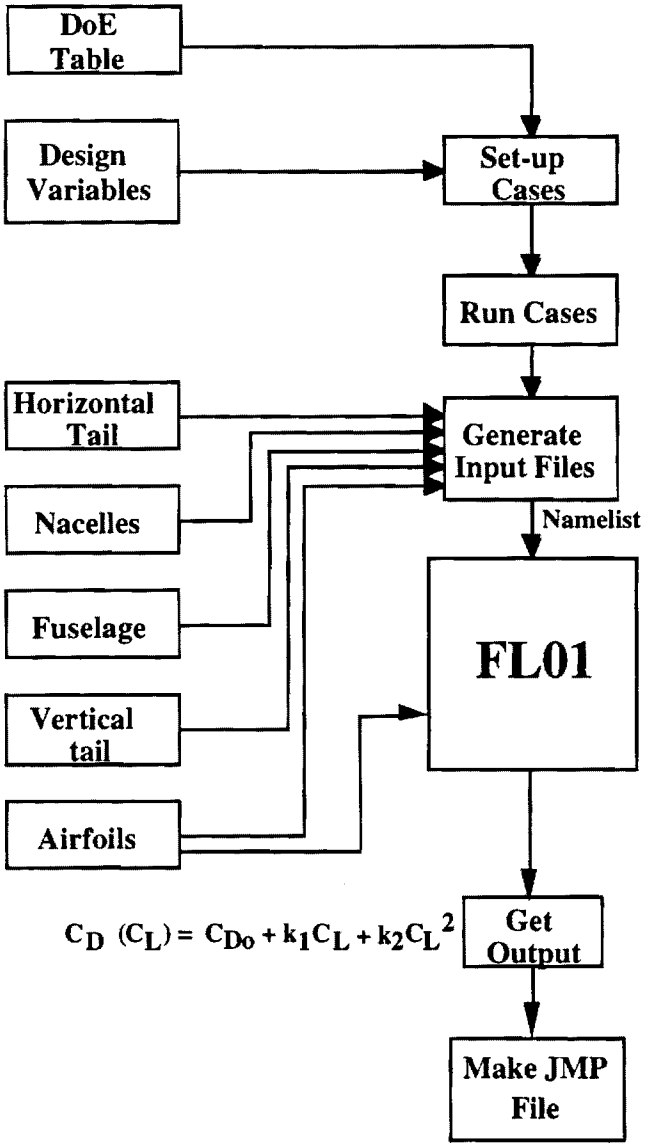

Figure 21: Flow Chart for Generation of Aerodynamic RSE's

Cases

The following steps must be executed to generate the aerodynamics RSE's.

- Setup a two level design of experiment as a variable screening test.
- Identify the most important parameters from the screening test.
- Set up the DOE for the selected design variables to obtain the RSE's for CDo, K1 and K2

The DOE tool JMP is only able to analyze up to 12 variables in generating the RSE coefficients. In order to find out which subset of design variables to choose from the original set to carry to the 5 level experiment, screening cases must be performed. These two-level

experiments are visually inspected via the aforementioned Pareto Chart, two of which appear next for the M=2.4 case as an example.

Summary of Fit

RSquare	0.931558
RSquare Adj	0.906265
Root Mean Square Error	0.007702
Mean of Response	0.600203
Observations (or Sum Wgts)	64

Analysis of Variance

Source	DF	Sum of Squares	Mean Square	F Ratio
Model	17	0.03714311	0.002185	36.8297
Error	46	0.00272891	0.000059	Prob>F
C Total	63	0.03987202		0.0000

Pareto Plot of Scaled Estimates

Term	Scaled Estimate
S-tail	-0.0157523
Y1	-0.0114986
X5	0.00898673
X1	0.00778688
X3	-0.0074093
S	-0.0020369
xwing	0.00125035
nal	0.00101272
X2	0.00096222
nay1	0.00077718
oaf	0.00069604
tco	-0.0005353
nay2	-0.0004162
iaf	0.00019885
X4	0.00011630
tci	-0.0000735
nax	-0.0000347

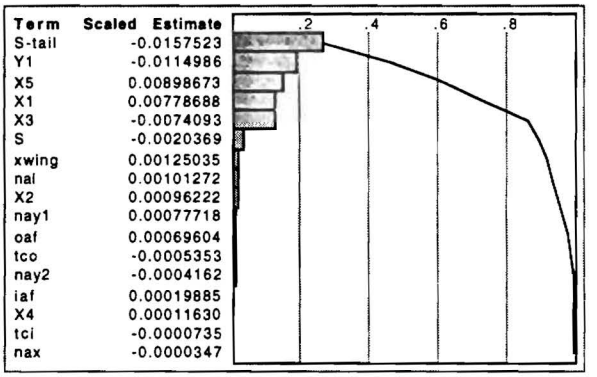

Figure 22: Screening of Aerodynamic Variables for k_2 at Mach 2.4

Summary of Fit

RSquare	0.837214

Pareto Plot of Scaled Estimates

Term	Scaled Estimate
nal	0.00029964
S	-0.0001615
S-tail	0.00013194
nay2	-0.0001070
xwing	0.00008539
tci	0.00007739
nay1	0.00007450
X5	0.00006732
Y1	0.00003904
X1	-0.0000382
tco	0.00003049
oaf	-0.0000234
nax	-0.0000228
X2	0.00001856
iaf	-0.0000039
X3	0.00000258
X4	0.00000038

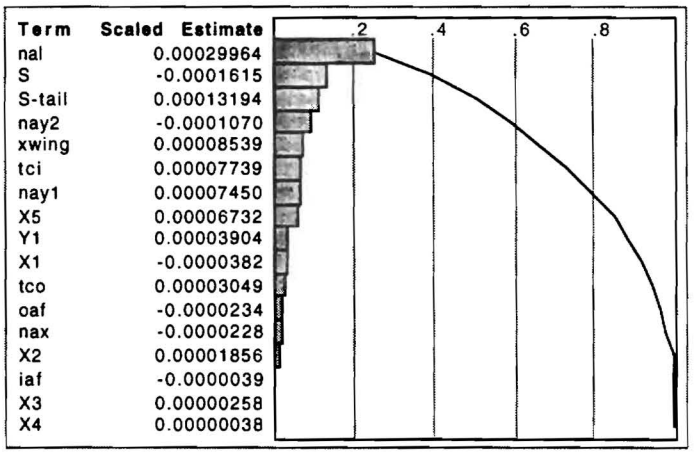

Figure 23: Screening of Aerodynamic Variables for CDo, Mach 2.4

Table 2.4 shows some sample screening results for both sub- and supersonic screening.

Table 2.4: Results of Screening Tests- The Important Variables

Sup k_2	Sub k_2	C_{Do} Sup	C_{Do} Sub
S_{tail}	y_1	S_{tail}	nal
y_1	x_1	S	y_1
x_1	x_2	tci	x_1
x_3	x_5	x_5	x_4
x_5	x-wing	x-wing	x-wing
$C_{Ldesign}$	$C_{Ldesign}$	$C_{Ldesign}$	$C_{Ldesign}$
		nay_1	
		nay_2	
		nal	

Some of the variables which turned out to be important would not have been recognized as such without the screening. For example, the area of the horizontal tail (Stail) is important for the drag due to lift at supersonic speeds. In this case, it is only due to the comparatively large range chosen for this parameter, since tail area, intuitively, should not contribute greatly to drag due to lift. Other variables, however, clearly proved their importance. For example the spanwise location of the kink (y1) was the most contributing parameter for lift induced drag in the subsonic flight regime. This is basically the only reason for having a kink at all: The outboard wing section with low sweep angle is the main producer of lift in subsonic flight whereas in supersonic conditions it only poses a drag penalty. The actual RSE runs have been performed with the most contributing parameters, as identified by the screening, varying leaving the others fixed at their nominal values.

2.2.2.3 Validation

There are several ways to validate the accuracy of the response surface equation. The first step always is to plot the obtained data. The Whole Model Test in Figure 24 is a plot of the actual response values for k2 over the predicted values, based on the second order model for the RSE. The straight line indicates a perfect fit, i.e. all predicted values are equal to the actual for the same levels of input variables. As illustrated in Figure 24, the model predicts the values for k2 quite well, since all data points are rather close to the straight line. This model fit corresponds to an R-

square value of 0.973728. The doted lines indicate the confidence interval for the model, showing a small range with no points falling outside of this range.

The Residual Plot on the right side of Figure 24 is an important verification for the assumption of normality for residuals or statistical error in the response. Hence, the residuals are plotted over predicted values for k2 based on the assumed model. A "cloud" of data points, indicating no particular pattern, proves the normality assumption for residuals. Hence, there is no reason to fear non-normality for the response k2, as Figure 24 illustrates.

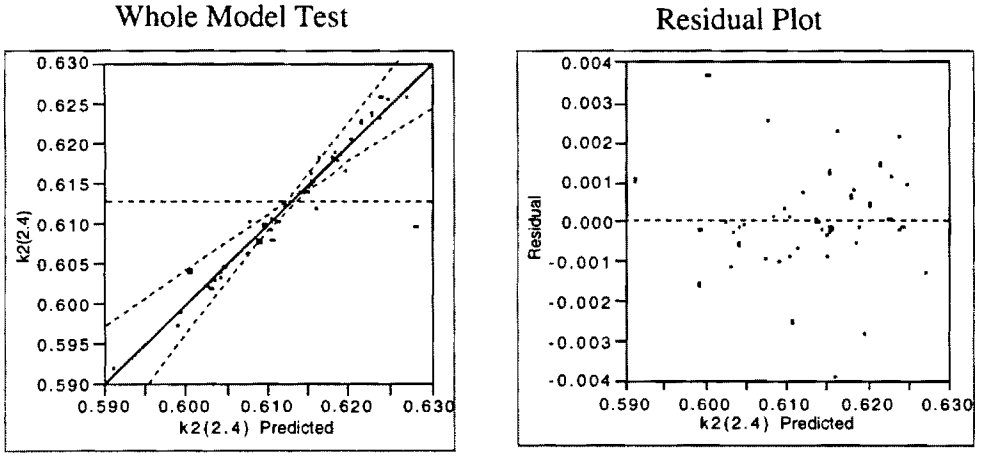

Figure 24: Whole Model Fit Test- A Validation

The left hand side plot is termed the Whole Model Test. It plots the actual values of a response (in this case k1). Figure 25 shows the output parameter estimates from JMP. These are the actual coefficients which, along with the design variables, make up the RSE of the form of Equation 3.1.

Parameter Estimates

Term	Estimate	Std Error	t Ratio	Prob>|t|
Intercept	-5.878813	5.372921	-1.09	0.2891
x1	2.3984876	2.573549	0.93	0.3644
x3	2.3956492	2.503083	0.96	0.3519
y1	-0.674068	1.963603	-0.34	0.7356
x5	1.1983904	1.05529	1.14	0.2719
S-Tail	-0.000415	0.000745	-0.56	0.5846
CLDes	8.6087716	6.640273	1.30	0.2121
x1*x1	-0.933080	0.661597	-1.41	0.1765
x3*x1	0.4738990	0.484103	0.98	0.3413
x3*x3	-0.701553	0.459443	-1.53	0.1452
y1*x1	2.240618	0.622419	3.60	0.0022
y1*x3	-1.013835	0.518682	-1.95	0.0673
y1*y1	-1.678383	0.759487	-2.21	0.0411
x5*x1	-0.696132	0.281092	-2.48	0.0241
x5*x3	0.3819572	0.234244	1.63	0.1214
x5*y1	0.5088605	0.301170	1.69	0.1094
x5*x5	-0.257235	0.154901	-1.66	0.1151
S-Tail*x1	0.0003073	0.000249	1.23	0.2339
S-Tail*x3	0.0000541	0.000207	0.26	0.7975
S-Tail*y1	-0.000355	0.000267	-1.33	0.2008
S-Tail*x5	0.0000482	0.000120	0.40	0.6940
S-Tail*S-Tail	-1.814e-7	1.215e-7	-1.49	0.1538
CLDes*x1	-1.891504	2.178464	-0.87	0.3973
CLDes*x3	-1.331705	1.815387	-0.73	0.4732
CLDes*y1	1.7865949	2.334069	0.77	0.4545
CLDes*x5	-0.481944	1.054096	-0.46	0.6533
CLDes*S-Tail	0.0002250	0.000934	0.24	0.8124
CLDes*CLDes	-11.20019	9.303713	-1.20	0.2451

Figure 25: Response Surface Equation for k2 at M=2.4

2.2.2.4 Issues involving tools used

A majority of the problems encountered during the aerodynamic analysis were most often due to the tools in use.

WINGDES, in conjunction with AERO2S, has proven to be the biggest trouble maker. Both codes are very sensitive to the number of wing stations, i.e. the number of spanwise stations at which airfoils are specified. The converged camber distribution computed by WINGDES varies greatly with the number of wing stations. For values of about less than 15, excessive camber may be produced for certain configurations that can even reach the order of the diameter of the fuselage. Defining a higher number of wing stations would be desirable, but unfortunately AERO2S can handle only up to 20 and for this number, the computation time was exorbitant. For example, it took more than 48 hours on six RS6000 workstations to produce the RSE's for the subsonic drag coefficients CD0, k1 and k2.

Particulars of the aerodynamic model

All the results obtained are for a non-trimmed aircraft, which implies that trim drag was neglected. AERO2S and WINGDES only have inputs for the wing itself, thus neglecting any lift contribution coming from the fuselage. This additional lift reaches significant values, especially for low subsonic Mach numbers up to approximately 0.5. It would also be necessary to generate take-off and landing drag polars for different flap settings and for each configuration. Since this step would again involve the computationally intensive AERO2S it was omitted because of time constraints. A sample take-off polar was generated with all design variables set to their nominal values and for 5deg deflection of the leading edge flaps and 15 degree deflection of the trailing edge flaps.

2.2.3 Propulsion Design Variable Selection

A 2-level screening was performed (similar to the aerodynamic screening described above) to determine the key parameters from the propulsion discipline. In the case of the engine cycle, the design variables were somewhat clear, though their choice was confirmed by the screening analysis. Those cycle variables selected were: Overall, Fan, and Bypass Pressure Ratios, and the Turbine Inlet Temperature. After determining the most important design variables, an engine cycle optimization for a given mission was performed through FLOPS in order to find a starting point value for all the control factors. The results are presented in Table 2.5 below.

Table 2.5: Initial Optimum Values for Cycle Design Variables

OPR	18.731
FPR	3.281
BPR	0.436
TIT	3206.8
TTR	1.036

The thrust to weight ratio (T/W) was given a range based on experience for this type of vehicle. Although a vehicle sizing variable, the thrust to weight ratio determines the thrust required from the engine and is also directly influenced by the engine cycle design. The percent cooling changed as a function of TIT. An equation based on a statistical regression was used to relate the cooling fraction to the TIT. Thus, % cooling became implicitly related to TIT and was dropped as a control factor. However, it is important to understand the implications of adopting a cooling scheme in order to lower the TIT to manageable levels[35]. The actual blade cooling was assumed to be carried out through either convective, transpiration, film, or impingement cooling[36]. Figure 26 shows the conventional cooling method used.

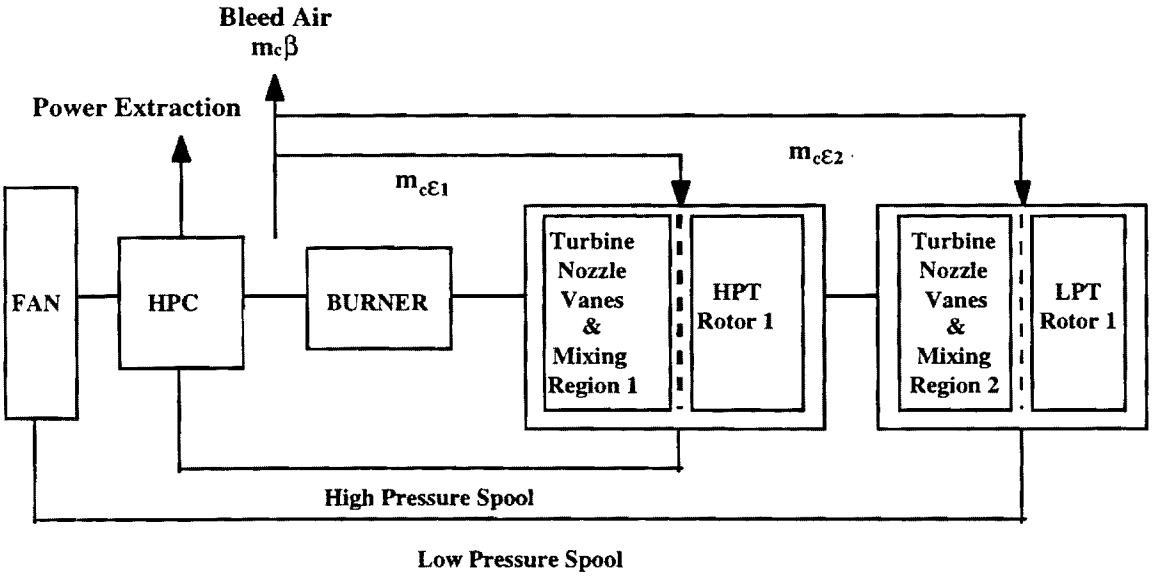

Figure 26: Turbine Blade Cooling Scheme

The cooling cycle is started by extracting a fraction of the compressor bleed flow and ducting it to two stations, one before the high pressure turbine and the other before the low

pressure turbine. The fraction of the air mass flow (ε_1) needed to cool down the high pressure turbine's first stage is a function of TIT and can be obtained by using the following equation:

$$\varepsilon_1 = (TIT - 2400\ ^oR)/16000 \tag{4.2}$$

The remaining part of the cooling, "bled" flow is ducted directly to the low pressure turbine's first stage nozzle guide vanes. As before, the fraction of the flow needed for cooling depends on the TIT. Likewise, this relation is captured in an equation. However, the equation accounts for the cooling that has already taken place as the flow traveled through the high pressure turbine. From experience, it is assumed that the flow is cooled down close to 860 ^oF (400^oR) as it goes through the high pressure turbine. Thus, the fraction of air mass flow (ε_2) needed to cool down the low pressure turbine's first stage is calculated as follows:

$$\varepsilon_2 = (TIT - 400\ ^oR - 2400\ ^oR)/16000 \tag{4.3}$$

Figure 27 shows the effect of cooling on engine sizing. As the TIT rises, a greater fraction of the flow has to be bled in order to provide for the necessary turbine vane or blade cooling. The more bleed, the bigger the engine and the greater the drag and weight penalties. This is the "pitfall" of turbine blade cooling[35].

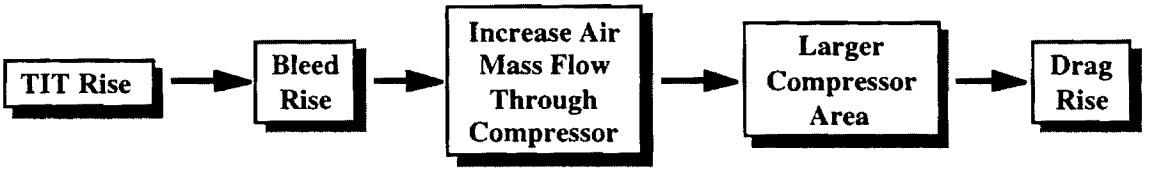

Figure 27: Turbine Cooling Drawbacks

The propulsion system optimization did not require the generation of RSE's due to the fact that FLOPS contains a sub-program called ENGGEN which can generate engine decks and optimize for the input cycle. Figure 28 shows the experimental set-up used for the engine optimization in this study.

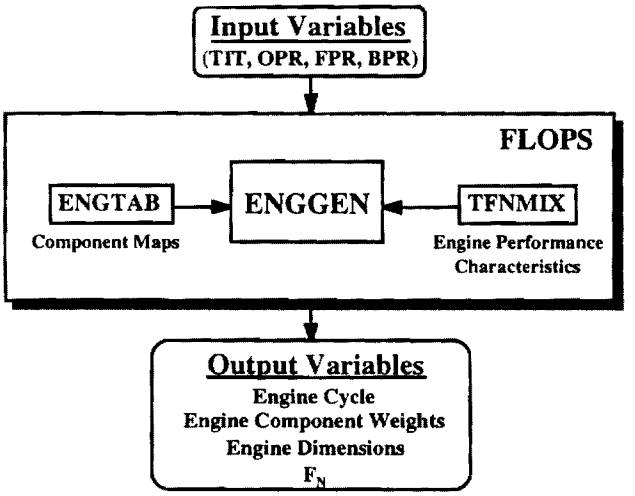

Figure 28: Experimental Set-Up for Engine Cycle Analysis

The cycle, as mentioned, is generated via a modified version (ENGGEN) of the engine sizing code QNEPP. Therefore, ENGGEN provides FLOPS with a satisfactory engine cycle analysis capability and a fully operational ability to optimize an engine for the selected cycle variables. The engine design sub-program relies on external files to generate the appropriate engine deck. The external file ENGTAB contains the compressor and turbine maps used to size the engine cycle components according to the thrust requirements. Component maps are data tables expressed in graphical form that describe the off-design performance of the compressor or turbine analyzed. In essence, these maps predict the performance of the engine cycle at different flight conditions. The other external file, TFNMIX is used by ENGGEN as a data manager. TFNMIX contains control laws, correct component map addresses, engine cycle constraints, and engine configuration. Furthermore, the cooling fraction for the required TIT must be input in this file. The master control shell (aero-propulsion integration) must correct the cooling fraction every time the TIT is changed.

Table 2.6 below shows the ranges for the design variables used in the combined aerodynamics/propulsion experiment.

Table 2.6: Ranges for the Engine Design Variables

Design Variable	Minimum	Most Likely	Maximum
T/W	0.23	0.32	0.35
OPR	17	19	21
FPR	2.89 (2)	3.45 (3)	4.99 (3)
BPR	0.35	0.4	0.45
TIT	2800	3025	3260
TTR	1.00	1.04	1.07

The fan pressure ratios take into account the number of fan stages in order to account correctly for the manufacturing feasibility of the design (i.e. a fan with 2.5 stages would be impossible to manufacture).

Thus, once the correct aerodynamic Response Surface Equations are in place and a correct mission is encoded in FLOPS, the engine cycle variables can also be included into the analysis in order to achieve an optimum aero-propulsion $/RPM value.

2.2.4 A New FLOPS-ALCCA Tool

2.2.4.1 Implementation

FLOPS (FLight OPtimization System) is the code selected to perform the vehicle sizing portion of the overall methodology. FLOPS was developed and is maintained by NASA Langley Research Center as a multidisciplinary design tool to assist the user in his/her conceptual and preliminary design process. FLOPS contains nine modules involved in aircraft systems synthesis: weights, aerodynamics, engine cycle analysis, propulsion data scaling and interpolation, mission performance, takeoff and landing, noise footprint, cost analysis, and program control.

An upgraded capability was recently added to FLOPS by ASDL by incorporating a second, more accurate cost analysis module called ALCCA (Aircraft Life Cycle Cost Analysis). ALCCA was developed by NASA Ames Research Center and was chosen to be integrated with FLOPS because it contains a more accurate aircraft cost model in comparison to the current FLOPS cost capability. In general, the integrated FLOPS/ALCCA code works the same as before, taking the weight breakdown of the aircraft and the associated mission parameters, along with the revenue required (or more appropriately "desired") by both the aircraft manufacturer and the airline, to calculate the average yield per Revenue Passenger Mile ($/RPM).

In addition to upgrading the FLOPS cost estimation routine, the previously discussed aerodynamic RSE's were included internally in order to improve the program's aerodynamic prediction capabilities. The current internal aerodynamic computation method and scaling technique in FLOPS was developed by A. Warner Robins. It uses regression equations based on current aircraft configurations to estimate subsonic and supersonic drag. This model is based on historical data for existing aircraft and can accurately predict aerodynamic properties for conventional aircraft geometry's. Since an aircraft similar to the HSCT does not currently exist, a model based on existing aircraft will result in poor predictions for unconventional configurations, such as that of the HSCT. Therefore, the internal drag estimation routine was considered inadequate for this study on an HSCT, and another more accurate method of calculating drag was pursued.

The developers of FLOPS foresaw this deficiency, so they offered an option to use an external program to generate the aerodynamic deck. However, this attempt to provide better drag polars has some major drawbacks. First, the user must develop an interface to get the aerodynamic tables generated from an external code to be compatible with FLOPS. The second drawback, which is much more sever, is that the resulting aerodynamic deck can only be used for a single configuration. This mean that every time the aerodynamic (planform) configuration is changed, the tables must be re-generated using the external aerodynamic codes. In an optimization study, a sizing code is used to alter the aircraft configuration, and many iterations are usually required before the optimum solution is found. Therefore, the use of external codes for lift and drag estimation basically forces the user to link two massive, complicated programs together, which is a very time consuming and computationally inefficient process.

The use of RSM overcomes the limitations of using a single aerodynamics deck for each corresponding configuration and of linking large programs. The RSM gives the user the ability to optimize a configuration without regenerating aerodynamic decks (for each iteration) by representing the output of the aerodynamic programs with an RSE. The RSE's can then be integrated into an existing sizing code such as FLOPS. Once FLOPS has a set of RSEs internal to it, it then becomes a simple exercise to evaluate the equation, often if required, to find the new aerodynamic properties as Mach, altitude, CL, area, etc. vary. In effect, the RSE has captured the essence of a complex aerodynamic analysis in a single equation which can be used as an internal module in FLOPS. This utilization of RSM in this setting is depicted below in Figure 29.

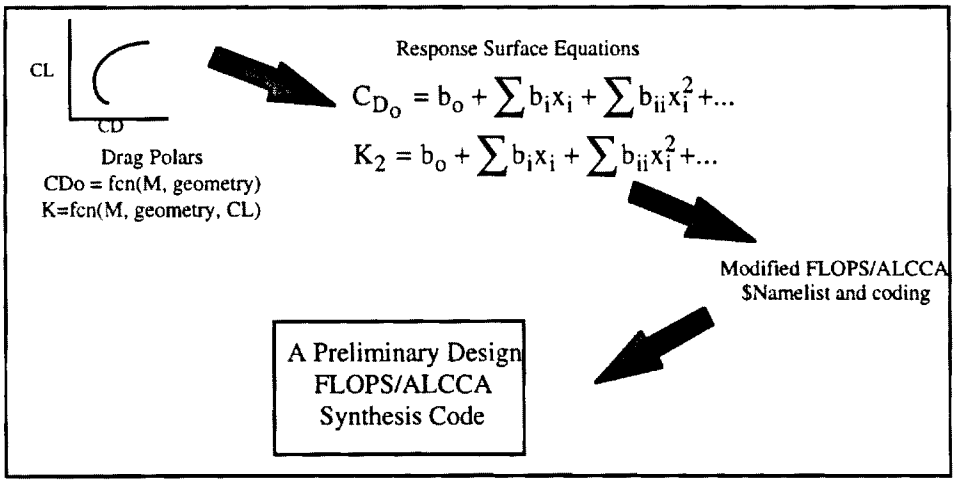

Figure 29: Generating Response Model Equations

With the implementation of a "variable" aerodynamic deck, altering the design variables and recalculating the aerodynamic properties internally are now possible. However, care must be taken to make sure that the valid ranges of the RSE's are not exceeded.

Recall that the coefficient of drag (C_D) for an aircraft is typically represented by a parabolic equation which is given by Equation 4.1, in which CDo, K1 and K2 are constants that are dependent on the wing configuration as well as on the altitude and the design Mach number of the vehicle. Each of these constants must be represented by a RSE for both subsonic and supersonic cases. Thus, a set ("set" meaning several equations spanning the operational Mach number range) of six RSE's are needed to completely describe the aerodynamic properties of an individual.

The FLOPS/RSE integration process has been structured for the use of multiple aerodynamic RSE's. This means that the process can be applied for a large number of aerodynamic design variables at a variety of Mach numbers. RSE's can be generated for HSCT configurations with an increased number of design variables and an increased range for each variable. The application of the internal aerodynamic RSE subroutine is not limited to an HSCT configuration. A different configuration can be accommodated without requiring any changes to the FLOPS source code. This is possible because the program inputs are independent of the of the variable names. Only the variable values and boundary values are necessary for the inputs. But, the order of the variable values must match that for which the RSE has been generated, and the corresponding coefficient tables must also follow the same format.

Additional inputs required by the new FLOPS/RSE program are:

i) The series of Mach numbers used in the aerodynamic code simulations to generate the RSE coefficients.

ii) The number of key design variables in the equations.

iii) A table for each RSE which carries the RSE coefficient tables. The tables are set up in a matrix form of Mach numbers across and design variable and design variable coupling going down. Each value in the matrix corresponds to a RSE coefficient calculated for that particular Mach number and design variable.

iv) The actual values of the design variables. They must be in the order of the RSE designated by JMP.

v) The upper and lower bounds of the design variables.

FLOPS reads in the designated aerodynamics data through an existing namelist and computes the RSE's in a modified aerodynamics subroutine. All other subroutines in FLOPS have been relatively unchanged. When computing drag, FLOPS first determines a required C_L and Mach number based on the mission profile and the initial guess of the gross weight. The C_L and Mach number enter the drag subroutine and are used as inputs for C_D calculations. The Mach number desired by FLOPS entering the subroutine is used to determine which set of upper and lower RSE coefficients tables to be selected and utilized to calculate the RSE's (C_{Do}, K1, K2). The

upper and lower bound RSE's result in two C_D calculations using Equation 4.1. These two C_D values determine the needed C_D through linearly interpolation.

Since the aerodynamic properties can be vastly different between the subsonic, transonic, and supersonic flight regimes, dividing the RSE's into three groups corresponding to each flight regime was necessary. The subsonic and supersonic calculations are performed by linear interpolation, as previously described, but the low subsonic and transonic regimes required additional information.

The transonic segment involves the interpolation between the largest subsonic Mach number and the lowest supersonic Mach number provided in the input. It is apparent that that a linear interpolation between the two transonic Mach number values does not model the transonic regime properly, but the aerodynamics codes used in the study were unable to model the transonic regime accurately due to their limitations. A CFD code would be required to provide an accurate model of the transonic regime. In future uses of the RSE subroutine, the Mach numbers specified in the input can be used in the transonic region with smaller increments between the transonic Mach numbers, but only with codes capable of modeling the transonic regime.

After reviewing the resulting L/D's of the low subsonic Mach numbers, it was discovered that the C_D's generated by the RSE's were high for Mach numbers between 0.3 and 0.5. Further review provided evidence that the aerodynamics code used to develop the subsonic RSE's did not model the lift due to the fuselage but did model the fuselage skin friction effect. The effect was an over-estimation of the C_D at high C_L's, such as during landing and take-off. In order to address this problem, a correction factor was developed through a linear regression which can be applied to the K_2 RSE's. The correction factor multiplied by K_2 created a closer approximation of the behavior of the analyzed configurations during low subsonic climb segments. In the future, the correction factor can be switched off by defining a default value of one. For a more accurate calculation of the subsonic, transonic and supersonic aerodynamics data for an HSCT, it is recommended that CFD codes be implemented as the aerodynamics codes used to generate the RSE's because they offer the most accurate simulation capability.

Overall, the implementation of the RSE's in FLOPS has proven that RSE's can be used as disciplinary models, in this case in the form of a parabolic equation. Future use of RSM for synthesis codes could involve the implementation of RSE's in structural analyses in order to calculate component weights. With this new tool in hand, attention now turns towards using it to obtain a point-design optimum configuration. This optimization is the precursor to the economic viability assessment.

2.2.5 Constrained Optimization

2.2.5.1 The Optimization Approach

The final activity for this sizing/synthesis step is the determination of an optimized solution in the presence of performance and noise constraints. In order to find an optimal configuration for the HSCT, an objective function and relevant design parameters have to be established first. The objective function (to be minimized) for this study was selected to be the average yield per Revenue Passenger Mile ($/RPM, i.e. the effective ticket price per mile). The design parameters are chosen from the sets used previously for aerodynamics and propulsion analysis and are the fundamental variables seen at the top level of the Funnel Chart of Figure 4. This combination of aerodynamic and propulsion design parameters brings to fruition the "aero-propulsion integration" aspect of this research. The hope is that a more desirable result will be achieved via simultaneous optimization for both disciplines. While the design variables at this stage are "technical" in nature, the $/RPM objective function allows one to investigate directly the influence of traditional design variables on economic performance, perhaps a more relevant measure for the airline/passenger.

With the aerodynamic RSEs incorporated into FLOPS, one should be able to use the optimizer within FLOPS to vary design parameters (e.g. planform and cycle variables) to minimize $/RPM. However, the optimizer within FLOPS is unable to vary the parametric aerodynamic variables (x1, x2, y1, . . .) within its optimization routine, since it was designed to accept only a small subset of the total number of inputs for use in optimization. So the alternative plan of creating a RSE for the needed response from FLOPS ($/RPM) was formulated. In this way, FLOPS could be run without using its internal optimizer, with the optimization taking place externally once the $/RPM equation (and constraint equations) were formed. The process of constructing response surface equations has already been described above and in Appendix A, so a detailed description of forming the $/RPM RSE will not be done. However, the results for it are presented in Section 2.2.5.3 below.

Since a response consisting of *more* than eleven variables for one equation generally yields statistically inconclusive results[30, 31], the eleven most significant variables to the response are chosen to be the design variables for this optimization process. Those identified were x1, x3, x5, y1, xwing, BPR, FPR, OPR, TIT, S-wing, and T/W (refer to Figure 18 and Table 2.6). In order to make the response equation valid over the whole design spaced spanned by the design variables, it has to be obtained unconstrained. Thus, all constraints implied by the simulation model (except obvious ones, such as fuel balance and fuel volume) or the problem itself (e.g. noise, approach speed, etc.) have to be inoperative. By generating equations for the constraints in parallel to the objective function, a constrained optimization can be accomplished by optimizing the $/RPM

response while requiring that the value of the constraint equations at those variable settings satisfy the limits.

2.2.5.2 Generation of Experiments

After determining the number of variables for the $/RPM RSE, a DOE for the generation of simulation results had to be selected. Since eleven is a relatively large number of variables for a DOE, the Central Composite Design (CCD) was selected to generate the minimum number of data points required to produce a quadratic estimation equation. Use of the CCD with eleven variables requires 151 simulation runs if an additional center point is added and the cube design has resolution V. According to Ref. 30, the design must have an α-value of 3.3636 for 128 cube design points (Resolution V, 11 variables) to be rotatable. Due to its size, no resulting table for this design is displayed at this point. Instead, Table 2.7 depicts the design variables and their ranges, equivalent to the range spanned by the star points of the CCD. Note that all variables used for this equation are either aerodynamic or propulsion variables. Incorporation of RSEs into the simulation process capturing the effect of structures, manufacturing, or economics was not part of this project. Background on the CCD and associated definitions are contained in Appendix A.

Table 2.7: Design Variables for the Aero-Propulsion Optimization

Aero / Propulsion Variables	Lower Bound	Upper Bound
X1	1.54	1.62
X3	2.48	2.58
Y1	.50	.58
Root Chord	2.19	2.35
Surface Area	8500 sq ft	9500 sq ft
X-wing loc.	.25	.29
Thrust / Weight Ratio	.28	.32
TIT	3000	3250
OPR	19	21
FPR	3.5	4.5
BPR	.35	.45

Using the CCD for the variables and their design ranges depicted in Table 2.7, 151 simulation runs are carried out to provide the necessary data points for a linear regression. Through the regression approach, a quadratic equation is established using least square estimators

for the parameters. This analysis is carried out with a commercial statistics package called JMP[37], which provides a visual way of presenting the obtained results.

2.2.5.3 Results for $/RPM RSE

Figure 30 displays two statistics and their validation. The "Summary of Fit" lists some characterizations of the least square estimation such as the RSquare (or RSquare Adjusted) value, which indicates the quality of fit of the data points to the estimated line. Since a value of 1 denotes a 100% fit with all data points lying exactly on the regression line, the displayed value of 0.981485 (0.961956) indicates a very good fit for the $/RPM. The Root Mean Square Error (RSME) is the standard deviation around the mean of the response, both listed in the Summary of Fit. The low RMSE value of 0.000956 for a mean of 0.152887 also attests to a very good fit of the regression line to the data points. Finally, the number of Observations closes the list with the number of data points entered into the program and used for the statistical analysis.

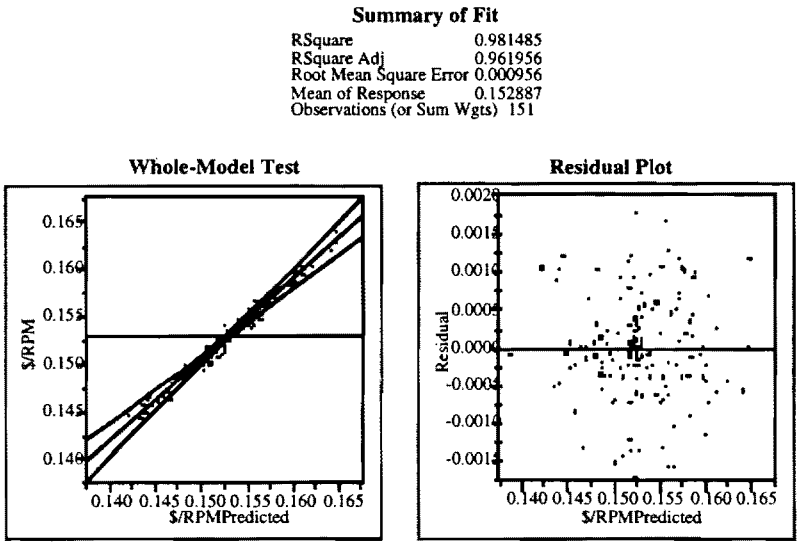

Figure 30: Summary of Fit and Analysis Validation

The Whole Model Test plots data of actual $/RPM values against the values predicted with the equation, for the same set of inputs. For a perfect fit, all points would lie on a straight line indicating that the predicted outcome is exactly the same as actually computed by the simulation routine. The Whole Model Test also displays a 95 % prediction interval, denoting that of all predicted outcomes, 95 % of the data points will fall between these two lines. The statistical analysis used here is heavily based on the assumption of normally distributed data. This assumption can be verified with the Residual Plot. It plots the residuals (difference of predicted and actual value) of the response ($/RPM) against the predicted values. If this plot shows a pattern or a non-scattered behavior of the residuals, the normality assumption can usually not be justified.

For this analysis, the plot shows a distinct scatter without any pattern, therefore validating the assumption of normality.

The main result of this statistical analysis is now presented in Figure 31. It displays the sensitivities of the objective function ($/RPM) and the constraints (GW, Vapp, TOFL, SLNoise, FONoise, and LFL) with respect to the design variables (T/W, Sref, x-wing, x1, y1, x3, x5, OPR, TIT, FPR, and BPR). These sensitivities indicate the behavior of the response variables with a change in the design variable setting. The statistical analysis tool used here (JMP) allows the user to change a design variable setting and see a real-time update of the response variables, giving the designer a feel for an the behavior of the design space. As a result of this present sensitivity analysis, it can be seen that only the effect of T/W on noise is highly significant, with the effect of root chord (x5) on $/RPM and the effect of wing area on approach speed being important to a lesser extent.

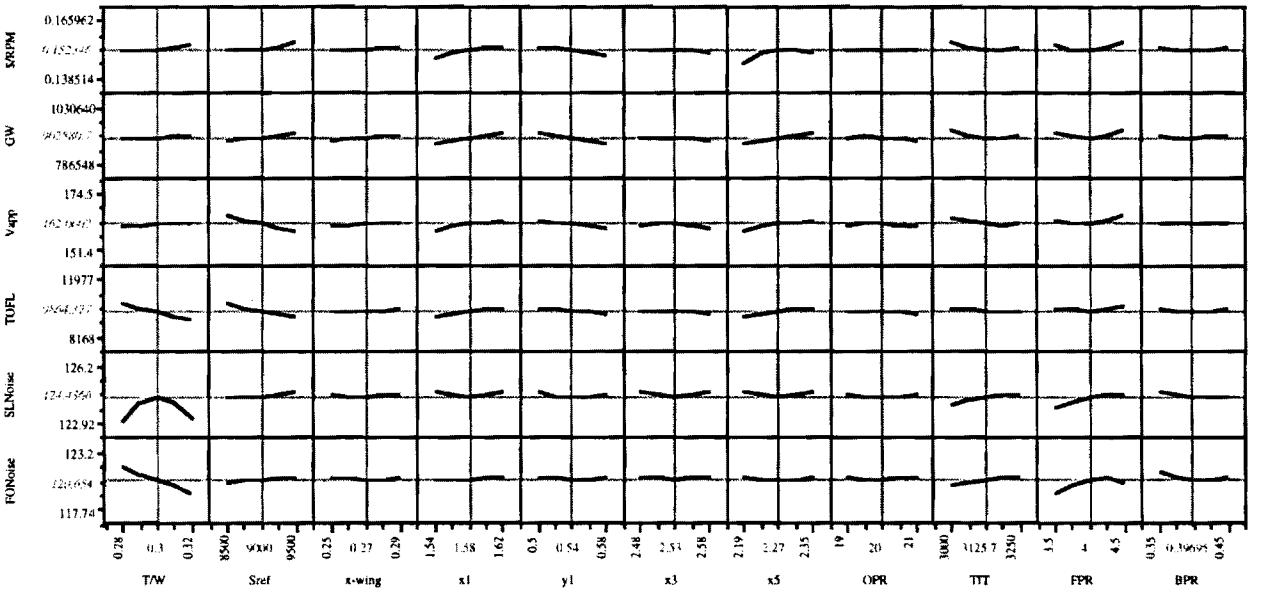

Figure 31: Response Surface Equation Sensitivities

2.2.6 Noise and Performance Constraints

For this study, the internal noise prediction capability in FLOPS was used to generate EPNL values at the FAR 36 observers for each case in the DOE. The noise module in FLOPS is based mainly on the ANOPP Noise prediction method developed at NASA Langley[37]. Jet mixing noise, which results from the intrusion of hot jet exhaust into the relatively stationary atmosphere, is the main noise source considered by ANOPP. However, fan, airframe, and turbine noise source are also taken into account. A response surface equation was formed for EPNL levels at the flyover and sideline observers and fed as a constraint to the optimizer. The form of these constraints appears below.

$$\text{Flyover EPNL} = f(\text{T/W}, \text{S}, \text{x1}, \ldots, \text{OPR}, \text{FPR}, \ldots)$$
$$\text{Sideline EPNL} = f(\text{T/W}, \text{S}, \text{x1}, \ldots, \text{OPR}, \text{FPR}, \ldots)$$

Eventually, the "other" noise restriction needs to be addressed in the methodology; that is the community noise issue. This constraint is investigated in terms of the so-called noise footprints, as it represents an integrated effect over time and area. Community noise is approached with the objective of minimizing the footprint area above a certain EPNL level. Unfortunately, methods employed for meeting both the FAR 36 observer and community noise constraints often conflict with each other.

Other constraints to be tracked for this problem include the approach speed (Vapp), the take-off field length (TOFL), and the landing field length (LFL). Vapp is a strong function of the wing area and is usually around 1.3 times the stall speed on approach. Vapp becomes an active constraint when the aircraft has too much energy for a safe landing. The TOFL and LFL constraints (currently at 11,000 feet) are a direct result of requiring the HSCT to operate from existing runways at major airports.

2.2.7 Optimized Configuration

Since the quadratic RSE capturing $/RPM has been formed through the aerodynamic / propulsion experiment, it is possible to utilize an efficient tool such as the EXCEL optimizer (again recalling the impossibility of using the internal FLOPS optimization routine). This procedure avoids the need for multiple simulation runs that are very time consuming. The optimization also guarantees the satisfaction of the constraints by using constraint RSEs which constantly update constraint values (with changing design variables). Thus, using the EXCEL optimizer allows for the capability to execute the optimization using aerodynamic and propulsion variables simultaneously for the objective function ($/RPM). Since the EXCEL optimizer is in a spread sheet format, the RSEs can be converted into sheets calculating the objective function and constraints with changing design variable values. The EXCEL Solver now has the option of restricting the values of distinguished cells. Hence, a range for the design variables can be specified to correspond with the ranges for which the various RSEs are valid. Further, the cells containing the constraint equations can be restricted to a certain value. While the Solver changes the cell values of the design variables, it tries to simultaneously minimize the value for $/RPM (i.e. the cell containing the objective function) while not exceeding the specified constraint values (i.e. the specified value of the cell containing the constraint equations). The obtained minimum value is therefore a constrained solution for this optimization problem. Together with the sensitivity

analysis from chapter 2.2.5.3, the designer has a fairly complete understanding of the behavior of the objective function.

The optimization results with the equations obtained for this study are summarized in Table 2.8 and Table 2.9. Table 2.8 contains the optimal setting of the design variables while Table 2.9 lists the minimal value for $/RPM and the values for the constraints generated by the RSEs as well as the results of a verification run of FLOPS. The bottom row displays the difference of these two values indicating a percentage error for the Response Surface Equation as measured against "reality" (an actual FLOPS analysis).

Table 2.8: Constrained Optimization for Minimum $/RPM

x1	y1	x3	x5	Sref	x-wing	T/W	OPR	TIT	FPR	BPR
1.54	0.58	2.58	2.19	8,500	0.28	0.28	21.00	3,148.44	4.50	0.45

Table 2.9: Constrained Optimization Results

	$/RPM	GW	V_{app}	TOFL	LFL	FONoise	SLNoise
RSE	0.14059	804,552	157.45	10,080	10,107	121.87	124.78
FLOPS	0.14347	831,323	160.0	10,165	10,271	121.48	124.31
% Error	-2.00	-3.22	-1.59	-0.83	-1.59	+0.33	+0.38

Note that for this optimization the noise constraints for the actual HSCT (see Figure 13) were not applied since noise suppression techniques were not modeled in the synthesis code. Hence, the noise constraints are not active during this scheme, though they are carried through to the end to demonstrate the capability to do so. The optimum aerodynamic design variable settings from Table 2.8 yield a wing planform illustrated in Figure 32. The figure on the right displays the location of the variables and their nominal values. It can be seen from the overlay plot (left) that the baseline had a lager span but a smaller sweep in the outer part of the wing than the optimized planform. This may indicate that, for the given split mission percentage (~ 15% subsonic, 85% supersonic), the optimal planform prefers less outboard panel sweep. Note that the optimal planform had a root chord (variable x5) significantly smaller than the baseline. This concurs nicely with Figure 31, which shows that as x5 is reduced, $/RPM is reduced.

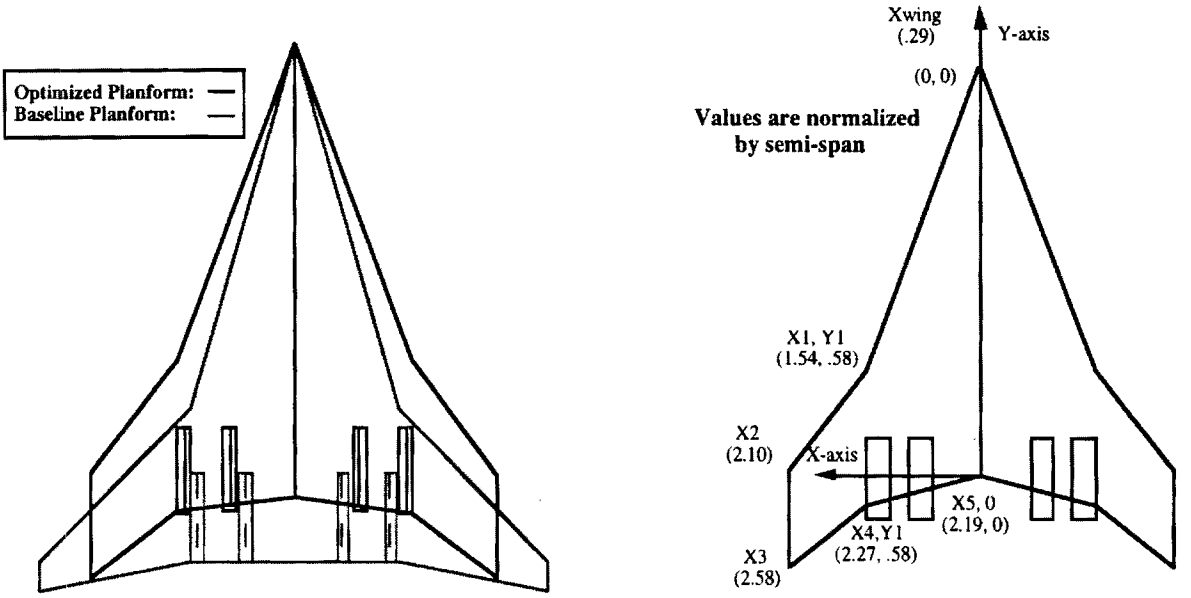

Figure 32: Optimal Design Planform Comparison

2.2.8 Lessons Learned

The correct application of Response Surface Methodology is dependent on several fundamental facts. These are outlined below.

- Polynomials often do not extrapolate well; thus, the equations are not valid for design variable settings outside of the ranges originally chosen.
- Not all phenomena will be well fit by polynomials. If this is the case, a new form of the response must be modeled (e.g. exponential, logarithmic).
- Don't expect more resolution than the provided by the simulation code used

The low speed aerodynamic analysis was found to be quite difficult to handle and seems to require further research in order to arrive at the best model possible (if good wind tunnel data is not available). Most likely, higher fidelity tools are required to accurately predict this flight regime even at the early preliminary design level.

In looking at the funnel chart depicted in Figure 4, it seems clear that ideally, one would like to generate a response surface equation for the $/RPM based on the system metrics, such as expressed below.

$$\$/\text{RPM} = f(\text{T/W}, \text{S}, \text{L/D}_{\text{cruise}}, \text{L/D}_{\text{TO}}, \text{SFC}, \ldots)$$

This would not only reduce the number of parameters to be varied in the RSE generation, it also would make sense from a designer's point of view in that he would likely have an idea of what are the achievable ranges for the system level metrics. However, this approach cannot currently be employed since it would necessarily require the selection of ranges for these metrics. And therein lies the problem. There is not a unique choice of design variables which corresponds to a specific L/D, lets say. This lack of uniqueness would lead to a variety of possible responses for a given

L/D. Additional research is required in order to determine if there is any way to deal with this issue.

2.3 Economic Viability Evaluation (Step 3)

Now that Step 2 is complete, Step 3 begins with the goal of taking the feasible, optimized vehicle and subjecting it to an economic evaluation to determine whether the concept is economically viable. As introduced earlier, in order to determine the $/RPM value, a code accounting for manufacturing and airline business practices must be introduced and linked to the actual synthesis code. The authors have found that ALCCA[10,11], the Aircraft Life Cycle Cost Analysis program, is the most suitable code to estimate the economic aspects. The code is actually comprised of a series of individual subroutines or programs capable of predicting aircraft acquisition costs, Return on Investment (ROI) for both airline and manufacturer, cash flows, etc. This series of programs was incorporated in NASA Ames' ACSYNT (Aircraft Synthesis) program and has been maintained as an integral part of this code. ASDL has been using ALCCA, under permission of Ames' SAB, for internal economic studies, educational purposes, and for support of on-going research. Hence, this code was linked to FLOPS by members of ASDL.

2.3.1 Economic Uncertainty Methodology

Figure 33 repeats Figure 16, though now the emphasis is on the bottom portion which depicts the procedure to address the economic variability due to uncertainty for a generalized HSCT configuration. For the vehicle sizing and synthesis, the FLight OPtimization System code (FLOPS)[39] is used to translate mission requirements, design variables, and constraints at a certain technology level into an aircraft configuration. The geometric, weight, and propulsion characteristics of this vehicle are then passed on to the Aircraft Life Cycle Cost Analysis (ALCCA)[40] module to complete the economic assessment.

Through the application of a Design of Experiments (DOE) approach, a quadratic regression analysis is used to form an RSE representing the ($/RPM) as a function of the most significant economic variables based on calculations performed by ALCCA. Next, economic uncertainty is introduced into the model, and a Monte Carlo Simulation is performed with the aid of a software package called Crystal Ball[4]. Crystal Ball randomly generates numbers for these variables based on user-defined probability distributions and computes a probability distribution for the response. . Without the aid of the RSE approach, the task of conducting a Monte Carlo simulation would be computationally demanding (and in many cases impractical) when one considers that this Monte Carlo simulation would have to be wrapped around an actual computer program. This distribution of $/RPM is based on a feasible design. However, the design must be economically viable as well as feasible, and if a Monte Carlo simulation indicates an economically

non-viable solution, areas of possible technology improvement (and their associated risk) have to be identified to make the design both feasible and economically viable. This takes us to Steps 4 and beyond of the overall process.

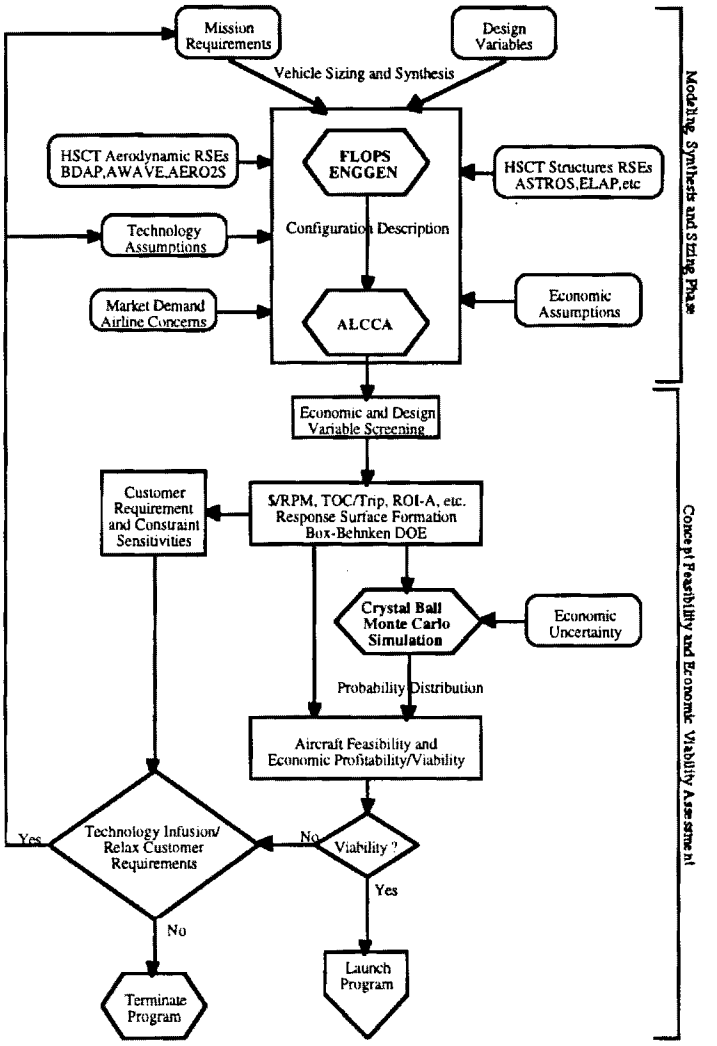

Figure 33: Methodology Implementation- Steps 2,3 Flow Diagram

2.3.2 Identification of Critical Design Variables

The first step in an economic uncertainty assessment is the identification of all pertinent cost parameters. Figure 34 depicts the considerations addressed by ALCCA. The Ishikawa or "fishbone" diagram displayed in this figure presents the various design and cost variables which affect the chosen overall criterion, $/RPM.

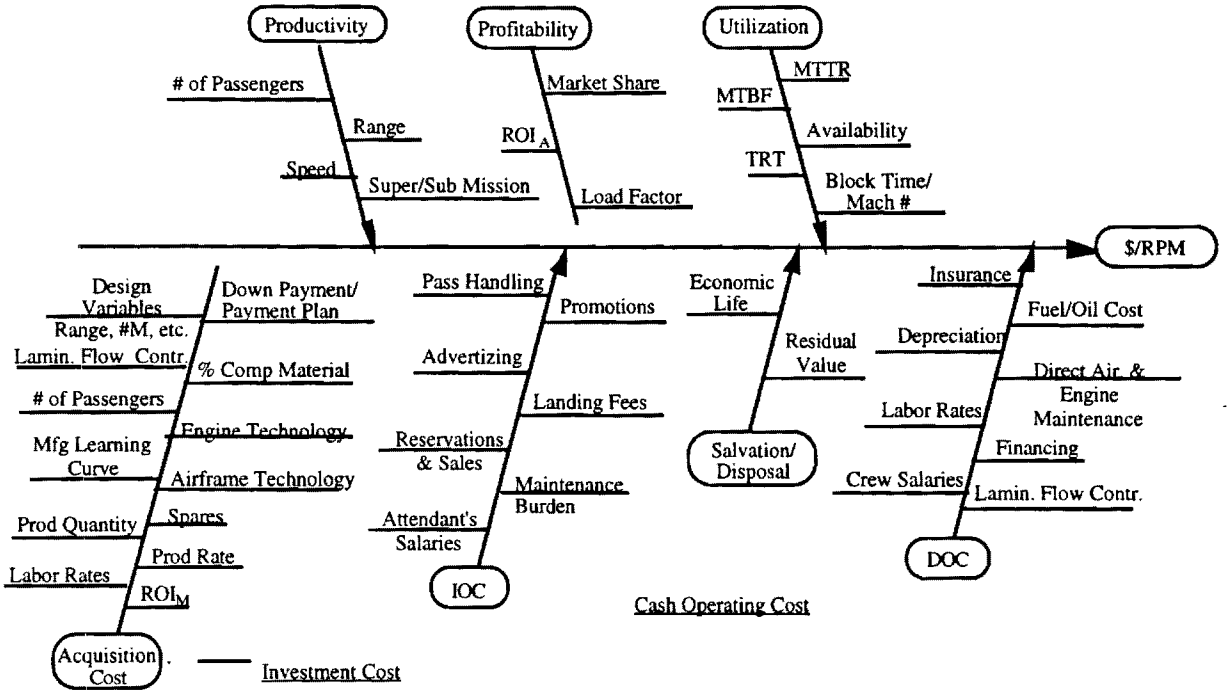

Figure 34 : Ishikawa Diagram: Cost Parameter Organization

This diagram takes an airline point of view; all of the economic variables above the horizontal vector leading to $/RPM refer to airline revenue, while all entries below that vector correspond to expenditures.

From this breakdown, 16 variables were identified as pertinent. Ranges for each were selected. The remaining variables were set to their default values in ALCCA or they were based on results from recent market studies. In general, since the range, the Mach number at optimum altitude, and the number of engines were fixed for the configuration studied, the number of passengers and use of composites were the only remaining sizing or synthesis variables allowed to vary in FLOPS. Of course, the aircraft would have to be resized if the number of passengers changes. Table 2.10 presents the ranges for the 16 most important variables selected in terms of their extreme settings and a most likely value. These values were input into FLOPS and ALCCA in accordance with the DOE table for the screening or the Box-Behnken format for the RSE (see Appendix A for explanations). This way, each row in the DOE table, for example, yielded one ALCCA output, i.e. $/RPM and acquisition cost, based on the input variables and their assigned levels in that row.

Table 2.10: Economic Input Variables and their Settings

Variable	minimum	most likely	maximum
ROI - Airline	5 %	10 %	15 %
ROI - Manufacturer	10 %	15 %	20 %
Production Quantity	300	548	798
Labor Rate	90 %	100 %*	110 %
Number of Passengers	280	300	320
Ground Time	0.5 hours	1.0 hours	1.5 hours
Utilization	4500 hours/year	5000 hours/year	5500 hours/year
Use of Composites	No	N/A	Yes
Engine Technology Factor	2	3	4
Load Factor	55 %	65 %	75 %
Learning Curve	75 %	80 %	85 %
Fuel Cost, $/lb	.09	.13	.17
Reservation & Sales	90 %	100 %*	110 %
Maintenance	90 %	100 %*	110 %
Insurance	0.5 % of acq. cost	0.75 % of acq. cost	1.0 % of acq. cost
Airframe Technology Factor	Cost Today	N/A	Cost of Aluminum

* 100% refers to present day levels

The definition of some of the variables in Table 2.10 is not intuitively obvious and needs further explanation. First of all, they all are uncontrollable parameters for the designers, thus bringing uncertainty to the evaluation. The uncertainty associated with engine acquisition cost, for example, is accounted for by the engine technology factor. The engine technology factor is an adjustment factor affecting engine cost, which accounts for the unpredictability of engine development cost. Experience has shown that the engine purchase cost is about two to four times more than originally predicted. Therefore, the maximum and minimum levels were set according to the values obtained from an for economic uncertainty assessment. Similarly, the Airframe Technology Factor captures the variability of the cost to manufacture airframe components made of composite materials. The lower level of this factor corresponds to present levels of manufacturing cost for composites, while the higher level refers to the optimistic expectation of reducing the production cost to that of aluminum. Obviously, this factor will only apply if composites are actually used on the aircraft.

The use of composite materials itself is treated only at two levels: no use at all or maximum use of composites for the wing, fuselage, and empennage structure. The Labor Rates, Reservation

& Sales (accounting for all premiums paid to travel agents, etc.), and Maintenance expenses were varied by 10% in either direction from their default or most likely values. The insurance rate was also varied to account for the risk associated with the use of new technologies and engines, which will increase the value of the aircraft in comparison to proven, existing wide-body transports.

2.3.3 Screening and Response Surface Equation Evaluation

The next step of the economic viability determination is the development of an equation for the metric response in terms of economic variables using the RSM. As discussed in Appendix A, a 3-level DOE for 16 variables requires too many runs to obtain an equation in a reasonable amount of time. Therefore, a screening test was conducted using a 2-level DOE linear model in order to identify which seven of the sixteen variables make the greatest contribution to the response. After obtaining the $/RPM and the acquisition cost for all level combinations displayed in the DOE table, an ANOVA (Analysis of Variance) for the main model effects is performed to obtain each contribution. A Pareto plot, Figure 35, displays these contributions, employing a bar chart for their relative influence, while the solid curve represents the cumulative contribution to the response. Figure 35 also depicts a Summary of Fit for the $/RPM and Acquisition Cost equations. Since the "experiments" performed are computer simulations, fit error is only due to lack of model fit or model error, i.e. curvature and correlation of parameters not accounted for in the model.

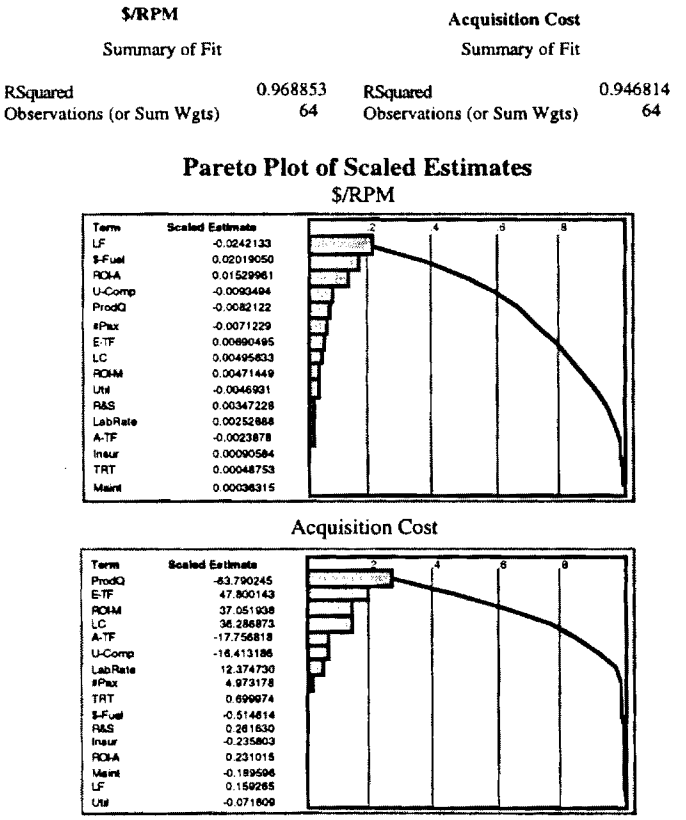

Figure 35: Screening of Main Effects for $/RPM and Acquisition Cost

Figure 36 shows a model test for the $/RPM response. The data plot on the left shows the response values predicted by the regression model (solid) superimposed on actual values from each run (points). The right graph reveals a plot of the residuals over the predicted response values. From the right graph, a typical model non-additivity can be seen, indicated by large negative residual values for mid-values of the response and large positive residual values for small and large prediction values. Accordingly, the left graph indicates a true parabolic lapse of the data, while the model is trying to fit a straight line. This phenomenon is explained numerically by the fact that the R^2 values are smaller

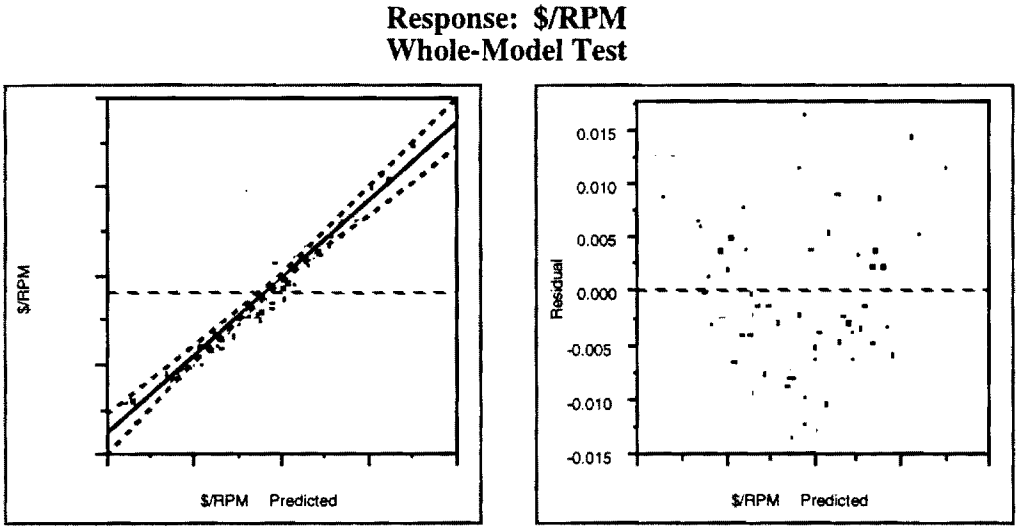

Figure 36: Screening Model (Main Effects only) Test

than one. Once again, a perfect model fit would yield an R^2 value of one, since no statistical error occurs.

Using the Pareto chart in Figure 36, the seven highest contributing variables to the response $/RPM are identified as: the Load Factor, Cost of Fuel, Production Quantity, Engine Technology Factor, Learning Curve, ROI-Manufacturer, and Utilization. These independent variables were next used to form the RSE for the $/RPM. As Figure 36 indicates, these variables constitute 90 to 95 % of the response. The remainder of the variables in Figure 36 are insignificant to the response and are set at a fixed value. The configuration from the point design optimization (Figure 32) makes sense to be used here for the RSM, since the number of passengers was fixed to 300. No synthesis or sizing was needed for this particular set of variables. Hence, FLOPS was not part of the RSM at this stage, while ALCCA simply used the fixed configuration. All other variables not addressed in the RSE were set to their default or most likely values.

Table 2.11 : Independent RSE and Fixed RSM Variables

Independent Variable	minimum	most likely	maximum
Load Factor	55 %	65 %	75 %
Fuel Cost	.09	.13	.17
Production Quantity	300	548	798
Engine Technology Factor	2	3	4
Learning Curve	75 %	80 %	85 %
ROI - Manufacturer	10 %	15 %	20 %
Utilization	4,500 hours/year	5,000 hours/year	5,500 hours/year

Fixed Variable		Value	
ROI - Airline		5% and 10%	
Number of Passengers		300	
Use of Composites		Yes	
Ground Time		1.0 hours	
Labor Rate		100 %	
Reservation & Sales		100 %	
Maintenance		100 %	
Insurance		0.75 % of acq. cost	
Airframe Technology Factor		Cost Today	

Table 2.11 summarizes the independent RSE variables and their values. It also lists the remaining variables that were fixed during the RSE development. Furthermore, separate RSEs at two discrete levels were developed for ROI_A of 5% and 10% so that the general trend of $/RPM with respect to ROI_A could be observed.

Figure 37 displays the RSM outcome for Airline-ROI of 5 and 10 %, based on an ANOVA for parameters of a quadratic model with second order interactions. This figure illustrates the relationship of each variable to the responses. The Cost of Fuel, for example, has approximately a linear influence, as indicated by the equivalent plot in Figure 37. On the other hand, the Load Factor, Production Quantity, and the Learning Curve show a weak quadratic response, which is reflected in Figure 37 as curvature. The linearity in the response is due to the small investigation intervals of the variables, hardly indicating a practical significance for the quadratic slope.

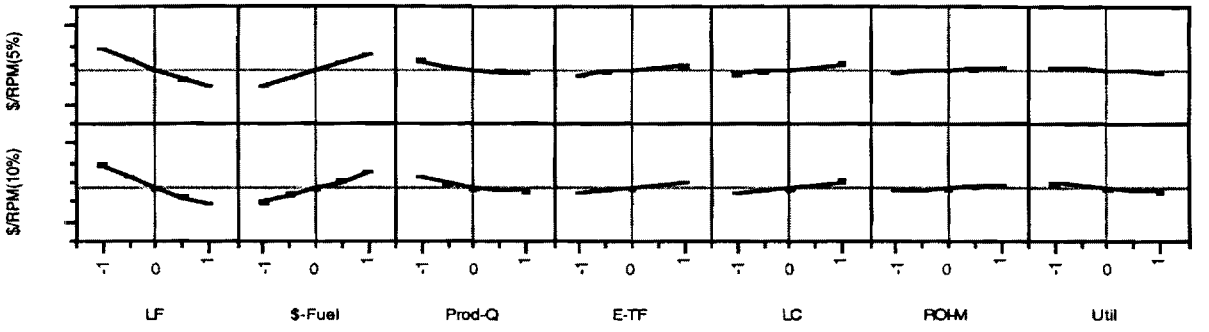

Figure 37: Prediction Profiles of the RSM for 5% and 10% ROI for the Airline

The prediction profiles in Figure 37 illustrate the key variables on the interval from -1 to 1. These numbers are just the indicators for the levels at which the variables are examined. In fact, all simulation runs were performed using the actual values for each input variable. A model test similar to the one performed for the screening test was also repeated for this three level RSE. As Figure 38 illustrates, the new model yields an almost perfect fit.

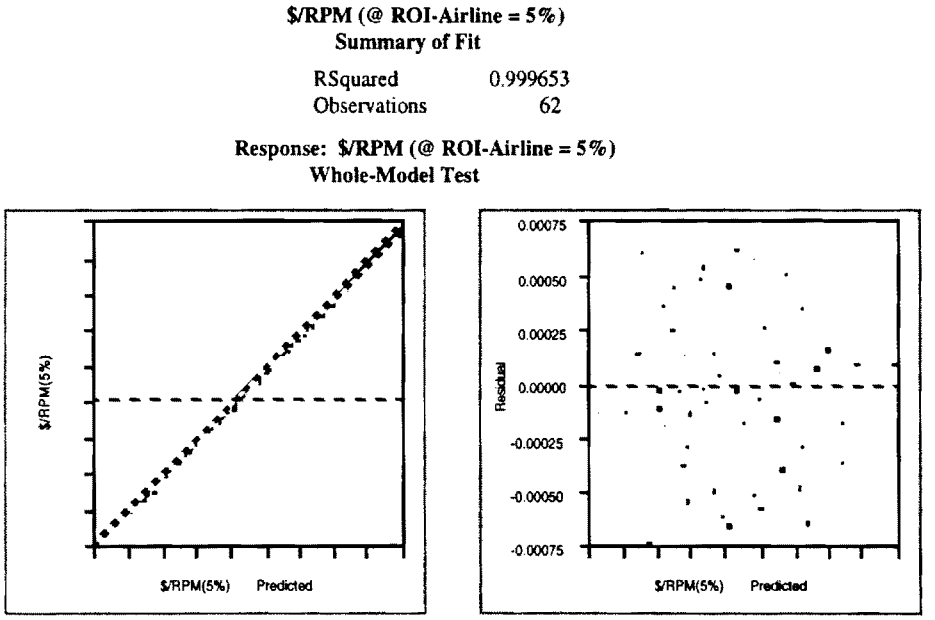

Figure 38: Response Surface Analysis Model Testing

Because the R^2 value is very close to one, and both graphs show a very good fit for the additive model, with no distinguishable pattern in the residual plot, it can be assumed no higher order interactions are statistically significant to the response $/RPM.

Table 2.12 displays the coefficients obtained for the $/RPM response surface equation. The columns presented correspond to the coefficient notation used in equation A.1, i.e. b_i, b_{ii}, etc.

Also shown are the actual independent design variable names and the corresponding coefficient value as obtained from the regression analysis. The value for the intercept has been erased for proprietary reasons. The actual equation can now be obtained by the summation of the intercept and all parameter estimates multiplied by their according variable.

Table 2.12: Response Surface Equation Coefficients

RSE Coeff.	Term	Estimate	RSE Coeff.	Term	Estimate
b_o	Intercept	---------	b_{51}	LC*LF	-0.000749
b_1	LF	-0.020684	b_{52}	LC*$-Fuel	-0.000005
b_2	$-Fuel	0.0178773	b_{53}	LC*Prod-Q	-0.000279
b_3	Prod-Q	-0.006609	b_{54}	LC*E-TF	-0.000004
b_4	E-TF	0.0048334	b_{55}	LC*LC	0.0011328
b_5	LC	0.0052615	b_{61}	ROI_M*LF	-0.000555
b_6	ROI_M	0.0030223	b_{62}	ROI_M*$-Fuel	0.0000116
b_7	Util	-0.003478	b_{63}	ROI_M*Prod-Q	-0.000625
b_{11}	LF*LF	0.0031372	b_{64}	ROI_M*E-TF	0.000082
b_{21}	$-Fuel	-0.002799	b_{65}	ROI_M*LC	0.0000466
b_{22}	$-Fuel	-0.000073	b_{66}	ROI_M*ROI_M	-0.000003
b_{31}	Prod-Q*LF	0.0010476	b_{71}	Util*LF	0.0005534
b_{32}	Prod-Q*$-Fuel	0.0000019	b_{72}	Util*$-Fuel	0.0000171
b_{33}	Prod-Q*Prod-Q	0.0034157	b_{73}	Util*Prod-Q	0.0005631
b_{41}	E-TF*LF	-0.000774	b_{74}	Util*E-TF	-0.000363
b_{42}	E-TF*$-Fuel	-0.000012	b_{75}	Util*LC	-0.000423
b_{43}	E-TF*Prod-Q	0.0000395	b_{76}	Util*ROI_M	-0.000246
b_{44}	E-TF*E-TF	0.0000027	b_{77}	Util*Util	0.0003300

2.3.4 Viability Assessment

Using the $/RPM RSE determined above, an uncertainty assessment was performed. Since the Monte Carlo Simulation is basically a random number generator, ranges for the variables used in the response surface equation had to be identified. Each of these variables was assigned a probability distribution over the range addressed for the RSM. In principle, these distributions could be of any variety, including common ones such as normal, beta, or triangular. For this study, as illustrated in Figure 39, all variables except for the Engine Technology Factor were

assigned a triangular distribution with the mean at the interval midpoint. The triangular distribution was chosen since very little knowledge was available about the probability of achieving certain values. Therefore, the triangular distribution was treated as a kind of first guess, knowing that the interval midpoint is the most likely and the range endpoint are very unlikely to be achieved. For the Engine Technology Factor, no real most likely point could be identified. Hence, a uniform distribution was assumed over the entire range.

After assigning these probability functions to the economic variables, the random number generator in Crystal Ball generated values for the independent variables according to their individual probability functions. It then used those values to compute the $/RPM value through the response surface equation. This procedure was repeated 10,000 times to obtain the probability distribution sown in Figure 40. This figure also provides a simulation, once again, summary and characteristics of the density function. For proprietary reasons, the mean, median, mode, and the range statistics are not shown in this publicly available report.

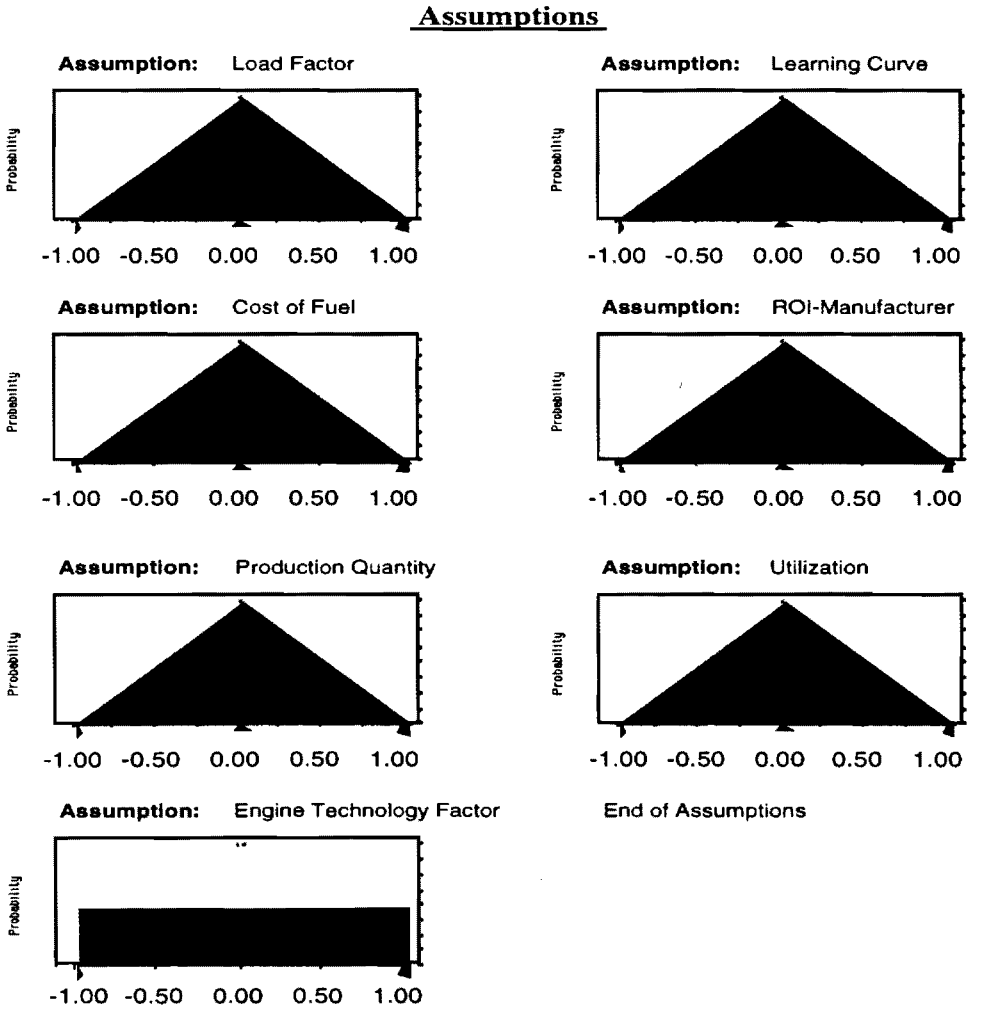

Figure 39: Assumed Probability Distributions for Selected Economic Variables

As visible as Figure 40 is for shifting the mean and reducing the variance, Figure 41 illustrates the decision supportability of this methodology even better. The cumulative probability distribution visually displays the probability of achieving a certain value of $/RPM. This figure can be used by decision makers as a means of assessing the economic viability of a feasible aircraft design. This can be achieved by determining the $/RPM value which corresponds to the probability/confidence target set by the management. If the probability distribution of $/RPM relative to the target is as shown in Figure 41, with an 85% probability of success, the program may be selected to be launched. If, on the other hand, the probability distribution not acceptable, a means of shifting the distribution towards the viable region must be found. This can be accomplished through a number of avenues, and this is explored next in Step 4 of the methodology.

Crystal Ball® Simulation

Forecast: 5% ROI-A

Summary: Certainty Level is 100.00% based on Entire Range
Certainty Range is from -∞ to ∞
After 10,000 Trials, the Std. Error of the Mean is 0.00

Statistics:	Display Range	Entire Range
Trials	10,000	10,000
Percent of Other	100.00	100.00
Mean	—	—
Median	—	—
Mode	—	—
Standard Deviation	0.01	0.01
Variance	0.00	0.00
Skewness	0.05	0.05
Kurtosis	2.81	2.81
Coeff. of Variability	3.86	3.86
Range Width	0.05	0.04
Range Minimum	—	—
Range Maximum	—	—
Mean Std. Error	0.00	0.00

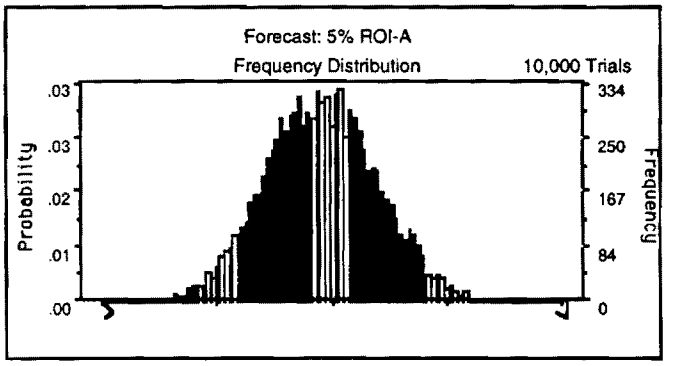

Figure 40: Economic Uncertainty (Frequency Distribution) for $/RPM

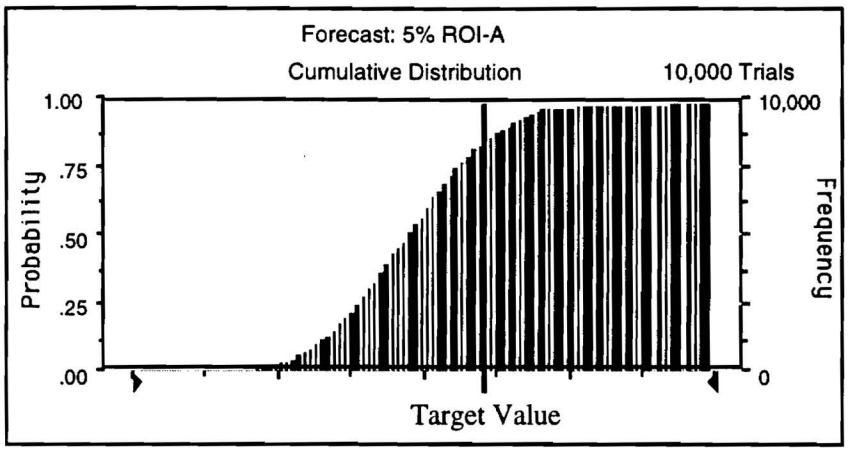

Figure 41 : Cumulative Function of Risk Assessment for $/RPM

2.4 Identification of Means to Improve the Economic Viability (Step 4)

If the previous investigation determines that the resulting $/RPM distribution corresponds to a feasible but not necessarily economically viable, means must be identified to shift the distribution from the feasible but economically non-viable region into the feasible *and* economically viable region as displayed in Figure 42.

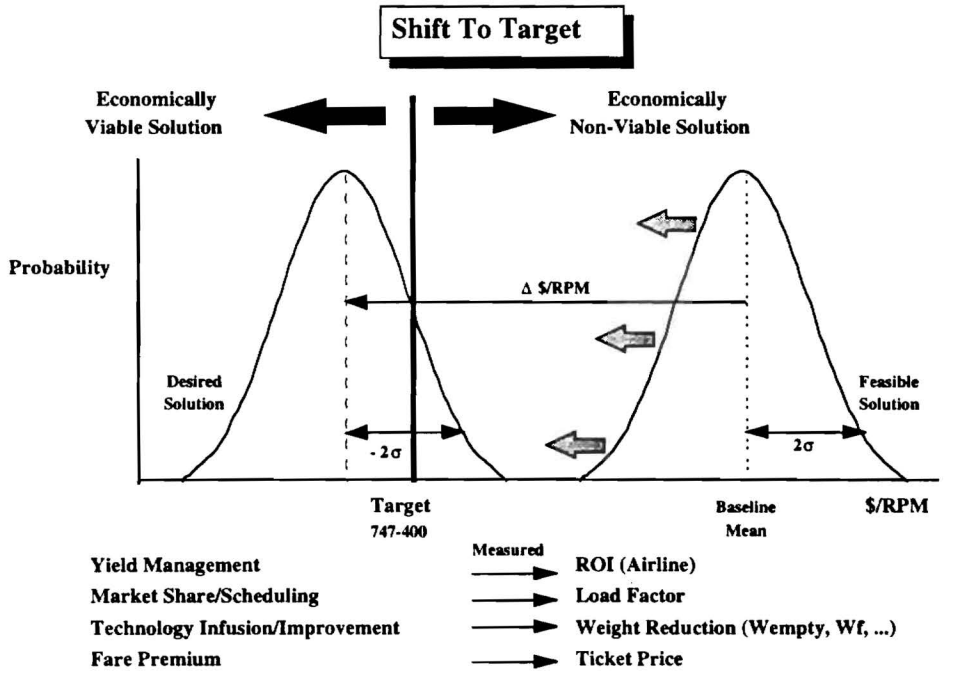

Figure 42: Possible Actions for the Transition of a Feasible Design Into the Economically Viable Solution Design Space - "Shifting the Target"

This can be accomplished by a combination of four means. Viability can be achieved through the introduction of a fare premium (to reflect the benefits associated with travel time reduction), yield management, market share/scheduling, or technology improvements (which may simply be viewed as weight reduction). All four methods seek to affect the economic viability of an HSCT in different fashions. However, it might be necessary to use a combination of these methods, if none by themselves can improve the prospects to a point where production can be initiated. Of all these choices, the engineer can only control the design improvement aspects. Through the infusion of a new technology, the designer can produce a system that is more fuel efficient, more reliable, more efficient from a producibility point of view, etc.

Figure 43 shows the effect of each means of improving the economic viability, based on the results from the economic viability analysis of Section 2.3. The figure also quantifies the relative importance of technology benefits with respect to all other means which are outside the engineer's control. For this study it has been assumed that improvement through new technology is synonymous to a vehicle gross weight reduction. Therefore, for a 10% reduction in weight Figure 43 indicates that the $/RPM distribution will be shifted to target by 23%, 10% increase in Fare Premium results in 38.7% shift, and so on.

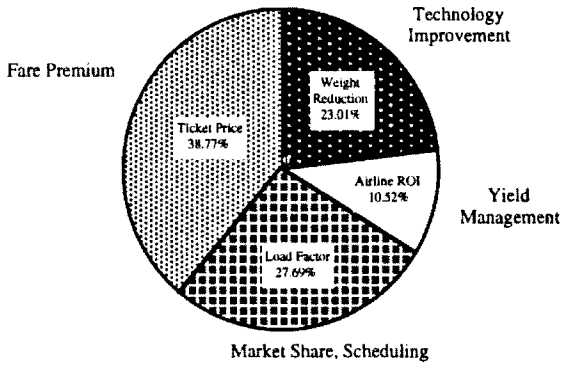

Figure 43: Means of Improving the Economic Viability of an HSCT (% shift of $/RPM Distribution for a 10% Change in each Option)

Referring back to Figure 42, one can compute a required %-reduction in $/RPM in order to shift the probability distribution into the economically viable region. Figures 44 to 46 depict the effect that yield management, market share, and technology improvement have on shifting the mean to target for various fixed ticket surcharges. The line graph on these charts is read from the *right y-axis* as the % reduction in $/RPM that is required to produce an economically viable aircraft. As seen with the increase in fare premium, the % required reduction in $/RPM is decreasing. This is due to the fact that the target value in Figure 46 is being shifted to the right.

Therefore, the probability distribution does not have to be shifted as far to the left with the increased surcharge on the ticket fare. The bar charts depicted are with respect to the *left y-axis* values. For example, if a 10% fare premium was introduced, from Figure 46, it can be seen that for the aircraft to be economically viable, the weight of the aircraft would need to be decreased by 42% with respect to the baseline configuration. Assuming that the economic requirements can not be relaxed, the designer has to find a way of reducing the vehicle gross weight by 10-63% depending on the ticket fare premium.

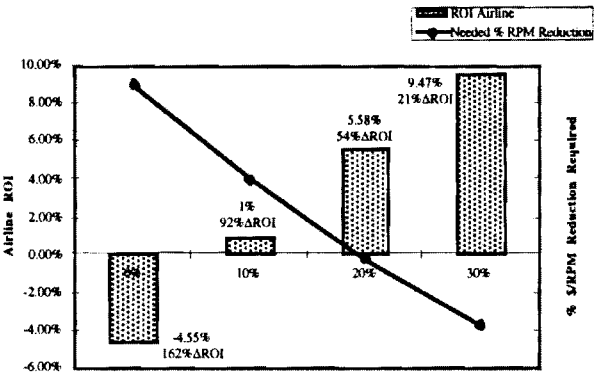

Figure 44: Yield Management Effect on Shifting Probability Distribution to Target

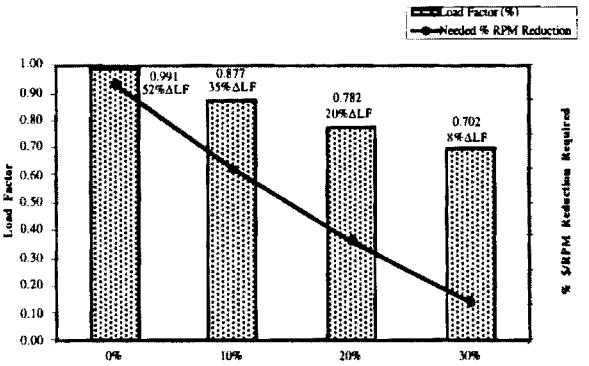

Figure 45: Market Share Effect on Shifting Probability Distribution to Target

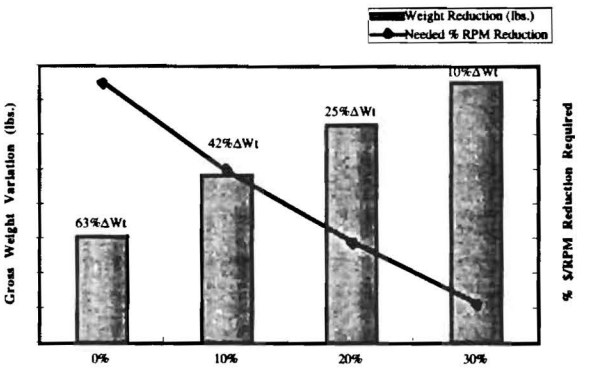

Figure 46: Technology Improvement Effect on Shifting Probability Distribution to Target

If new technologies must be identified, risk must also be assigned to each of these areas. Once the technologies and their associated risks have been identified, the entire scheme must be repeated hoping to yield an economically viable solution. This risk assessment is described next in Step 5.

2.5 Technology Benefit Assessment (Step 5)

The study performed at the previous step helped identify the need for new technologies. But it also raises questions, such as:

- Is any technology critical to success of the project? At what price ?
- What is the benefit (and later risk) associated with it ?
- Are there any alternatives ?
- What is the state of development ?
- Can this technology be demonstrated/incorporated by date needed ?

In general, the need for technology infusion falls under either one of the following two categories:

A) Technology infusion associated with feasibility, performance criteria, violation of constraints.

This implies the introduction of a technological advance/breakthrough to satisfy design requirements. This in turn translates to an increase in developmental cost that has to be quantified. An increase in risk associated with this technology which may lead to schedule or cost overruns, and the possibility of program cancellation.

B) Technology infusion associated with economic viability.

If the baseline cannot achieve economic viability, new technologies may be introduced. This can imply a possible reduction in acquisition cost through advances in material usage or

manufacturing process. Or a reduction in supportability or Life Cycle Cost through increased reliability. This of course will translate to added RDT&E expenses and possibly an increased acquisition cost.

For both categories the following questions have to be answered next:

i) Can existing technology lead to a successful product, measured by the selected overall evaluation metric?

ii) Can the program benefit from the infusion of "state-of-the- art" technology ?

iii) Are there any alternatives ? Which one of these alternatives may benefit the program most without taking any unrealistic risk?

Since advances in technology are needed to make this program successful, all critical technologies that could benefit for the program must be identified before improvements can be made. This objective can be best achieved through a decomposition technique called the relevance or objective tree[12]. A relevance tree is a method which enables the totality of the contributing technologies of a complex product (that possesses a number of functions, systems, sub-systems, and components) to be explored in a systematic manner. This method can be used as both a forecasting and a planning tool. Such a tree illustrates that the fulfillment of the objective depends upon the accomplishment of substantial advances either from new technologies or significant progress in existing technologies. Relevance trees are used[12]:

- To establish whether a specified goal or objective is feasible.
- To identify alternative methods for satisfying requirements at each level of the tree hierarchy.
- To decide performance objectives for each of the constituent parts.
- To focus attention on the need for radical new technological solutions if the overall objective is to be attained.
- To highlight where detailed forecasts for the constituent technologies are necessary when the achievement of a specified performance level within a given time scale is critical for success[12].

An example of a top level relevance tree is presented in Figure 47. It displays a relevance tree structure which was constructed for the overall objective of reduction in $/RPM. This overall objective can be decomposed into an economic objective, reduction in acquisition cost, and an equivalent design objective improvement through weight reduction. Ranges of possible values must be assigned to the design variables depicted in level 10, as seen in Figure 47. Within these ranges, optimal settings have to be found that minimize the gross weight of the aircraft, which in turn minimizes the acquisition cost, which reduces the OEC, $/RPM. If no optimum can be found within the design ranges, areas where new technology infusion might occur must be identified, and the optimization analysis must be repeated.

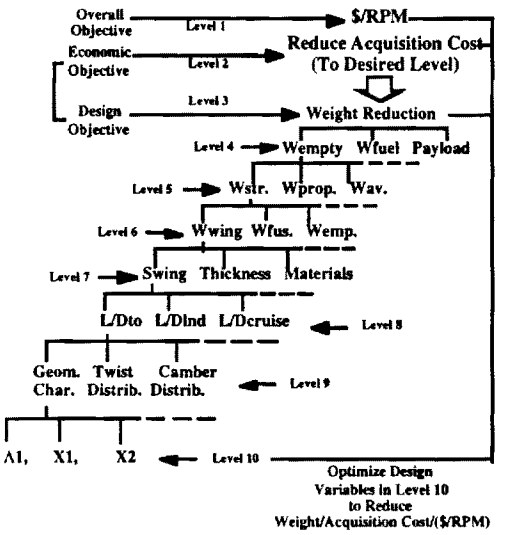

Figure 47: Acquisition Cost Relevance Tree

For instance, Laminar Flow Control (LFC) is one technique that can be used to increase the L/D ratio of the aircraft during the supersonic cruise segment to provide better aerodynamic characteristics. The proposed methodology would evaluate the values of the level 10 design variables for this technology that yield the optimum evaluation criterion. If the LFC cannot provide a viable solution by itself, benefits from other technologies infusions must be considered, The process is then repeated until a satisfactory solution is found. If none of the proposed options works, the decision maker might consider terminating the project before more money is spend on it. If on the other hand, one or a combination of new technologies are viewed as prime candidates for incorporation due to their benefit contributions, a risk analysis has to be performed to determine the risk penalty associated with it. If the risk and corresponding RDT&E cost are acceptable, the program can be launched. In general, the decision on use of a new critical technology will always depend on its maturity and the funding resources available. To investigate the quantification of risk, we go to Step 6.

2.6 Technology Risk Assessment (Step 6)

Traditionally, risk is encountered every time there is a technological advancement or an engineering development. Risk may also be associated with scheduling, reliability, producibility, or cost estimating uncertainty. The Risk Assessment methodology proposed in this research effort separates risk into two categories: risk through cost estimating uncertainty and schedule/ technological risk. Although here the cost estimating risk is assumed to be independent of schedule/technical risk, the cost prediction does remain dependent on the schedule and technical assumptions. The risk analysis assessment performed on any project or technology evaluated is

comprised of three distinct phases: risk identification, risk determination, and risk control or mitigation. These stages of risk management are defined next.

2.6.1 Risk Identification

Risk identification is the process of determining which areas are most likely to affect the project. This process relies on historical information, formalized risk checklists (Table 2.13), and the collective knowledge and experience of the project personnel. Schedule/Technical risk is defined as the risk associated with evolving a new design to provide a greater level of performance or the same level of performance with the consideration of some new constraints, within a designated schedule.

Table 2.13 may be viewed as a standardized risk identification chart. It contains six different technology/ schedule categories which may be encountered and assigns ten readiness or risk levels for each of the different categories, such as technology advancement, engineering development, reliability, producibility, alternate item, and schedule. Schedule and the various technical risk categories are treated together because they are interrelated and it is often very difficult to separate them. Sources contributing to schedule/technical risk are testing requirements, integration considerations, requirement changes, schedule aggressiveness, technological maturity, and system complexities. Similarly, the risk in cost estimation translates to the confidence of accurately predicting the cost of the project. Table 2.14 lists these categories.

Table 2.13: Technology/Schedule Risk Categories and Scores[12]

Categories	Risk			0=Low, 5=Med.,	10=High
	0	1-2	3-5	6-8	9-10
Technology Advancements	Completed (State of the art)	Minimum advancement required	Modest advancement required	Significant advancement required	New technology
Engineering Development	Completed (Fully tested)	Prototype	HW/SW development	Detailed design	Concept defined
Reliability	Historically high for same item	Historically high on similar items	Known modest problems	Known serious problems	Uncertain
Producibility	Production & yield shown on same item	Production & yield shown on similar items	Production & yield feasible	Production feasible & serious yield problems	No known production experience
Alternate Item	Exists or availability of other items not important	Exists or availability of other items somewhat important	Potential alternative under development	Potential alternative in design	Alternative does not exist & is required
Schedule	Easily achievable	Achievable	Somewhat challenging	Challenging	Very challenging

Table 2.14: Cost Estimation Uncertainty Scores

	0 - Extremely Confident	1 - Very Confident	2 - Confident	3 - Fairly Confident	4 - Slightly Confident
Cost	Historically known for same item Off-the-shelf item Well defined price	Prediction Extrapolation Historically estimated for similar items	Estimated based on proven method Scope/definition of system is adequate Data are within CER Ranges	Estimated based on unproved method but certain assumptions Data outside CER limits	Major uncertainties exist Analyst unfamiliar with the cost model Estimating data sources not documented

Cost estimating risk is defined as uncertainty in a cost estimate due to limitations of the methodology employed. Some examples of uncertainty sources are: historical data (i.e., normalization or applicability of data), scope of program definition, degree of applicability and standard error of available CERs, extrapolation from data, and differences in "expert opinion." The cost estimating distribution is additionally based on uncertainty associated with any input parameter that was used to develop the point estimate. These can include: first unit costs, learning curves, cost-to-cost factors, complexity factors, etc.

2.6.2 Risk Determination

Risk Determination is the process of quantifying and evaluating the probability of risk occurrence and risk impact. In fact, risk is usually quantified in terms of potential cost or schedule impacts. Methods for performing risk determination include:

i) Traditional approaches that assign risks based on the experience of similar projects
ii) Monte-Carlo simulation techniques, which predict a possible range of outcomes for the task
iii) Analytical methods that use mathematical probability to assess and combine the effects of individual risk events into an overall measure of risk
iv) A discrete event approach that uses decision trees, and influence diagrams to analyze risk.

In this study, the risk determination is achieved by directly assigning confidence levels to projects/technologies depending on their readiness or risk. Table 2.15 lists ten readiness descriptions and their corresponding risk level, readiness level, and confidence. According to this chart, risk is a probability distribution which reflects confidence. Each risk or readiness (the two are complimentary to each other) category maps to a specific point on this probability distribution. These confidence values are typical but by no means unique. In fact, they will vary from organization to organization and are dependent on such things as program starting date, budget restrictions, etc.

Table 2.15: Technology Readiness and Confidence Levels

Risk Levels	Readiness Levels	Readiness Description	Confidence
0	9	Actual system flight proven on operational flight	100%
1	8	Actual system completed and flight qualified through test and demonstration	95%
2	7	System prototype demonstrated in flight	90%
3	6	System model or prototype demonstrated in a relevant environment	80%
4	5	Component validation in a relevant environment	65%
5	4	Component validation in laboratory environment	45%
6	3	Analytical and experimental proof of concept	30%
7	2	Technology concept formulated	12%
8	1	Basic principles observed and reported	5%
9	0	No concept formulation or only basic ideas	0%

2.6.3 Risk Control

Risk Control is the process for defining avoidance and/or mitigation procedures for minimizing downside risk. The primary approaches to risk control include:

i) Risk avoidance that typically involves canceling a project or changing a technology
ii) Risk reduction that involves identifying alternative approaches that with less loss potential or conducting a more sophisticated engineering analysis
iii) Risk transfer that relocates risk to another party, (i.e., to another contractor who is better trained or equipped to handle a specific scope of work)
iv) Contingency funding that establishes a budget to cover costs that may result from incomplete design, unforeseen and unpredictable conditions, or uncertainties.

Risk control in the proposed methodology is achieved through the inception of the risk-to-benefit-ratio. The concept, as depicted in Figure 48, is relatively simple. A risky endeavor is to be undertaken if and only if, adequate product improvement (benefit with respect to the objective) is associated with it. Inspection of Figure 48 indicates that for marginal benefit improvements the decision maker does not have much incentive to take risk. On the other hand, technological breakthroughs that can offer a significant improvement (i.e. greater 10%) are more appealing for risk taking. Clearly, the lower the value of this ratio, the better.

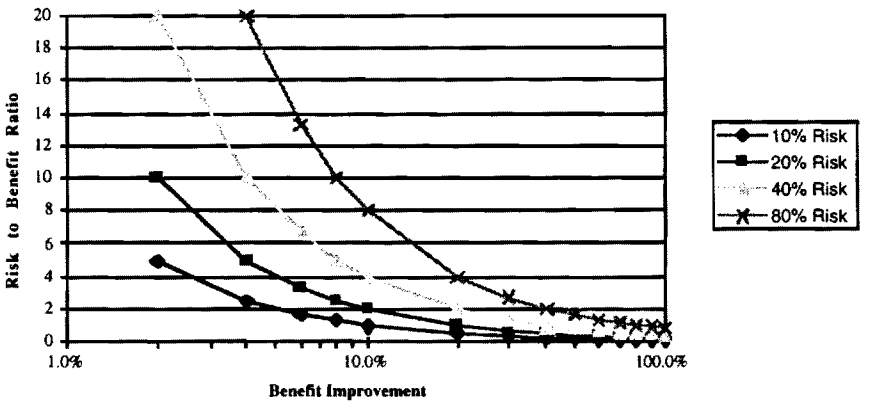

Figure 48: Risk to Benefit Ratio as a means of Risk Control

2.7 Decision Making and Resource Allocation (Step 7)

The various viable options must next be evaluated from a scheduling and/or a resource allocation view point. The decision making process may be assisted by a minimization of the risk-to-benefit-ratio between the various options. Benefit may also be adjusted to account for the increase in development cost. Projects or just technologies that exhibit the lowest risk-to-benefit-ratio may be given first priority over riskier alternatives yielding a higher benefit. Once the most appealing projects/technologies are selected, the evaluator must verify that these projects can be completed by the scheduled date. That can be achieved through an activity network diagram, which can easily illustrate and identify all bottlenecks and tasks that need to be performed either parallel or consecutively. Subsequently, a resource allocation must be carried out to identify if adequate manpower is available to complete all tasks within the allocated budget and schedule. Since this is a stochastic sequence of events, probability distributions for each step or path can be assigned or computed.

The following example illustrates how the decision making process can be altered once risk and budget constraints are taken into consideration. According to this hypothetical example (Figure 49), the $/RPM for an HSCT is to be optimized. It was determined that improvement could be achieved through either one of four different means: aerodynamics, propulsion, structures, and manufacturing. Furthermore, their relative importance or contribution to the response is identified. In this case any improvement associated with the propulsion system will yield the most benefit (50%). Each of the means depicted has one or more projects associated with it which could yield an improvement to the overall objective. The increase in yield from each action with respect to the baseline is listed in Table 2.16 for each project. Each project is also associated with a specific uncertainty of achieving the targeted yield increase. This is expressed in

the form of readiness for each project (see Table 2.13). This readiness can be quantified once it is translated into confidence in that project using the probability distribution from Table 2.15. Finally the last column lists the cost that is anticipated with each project.

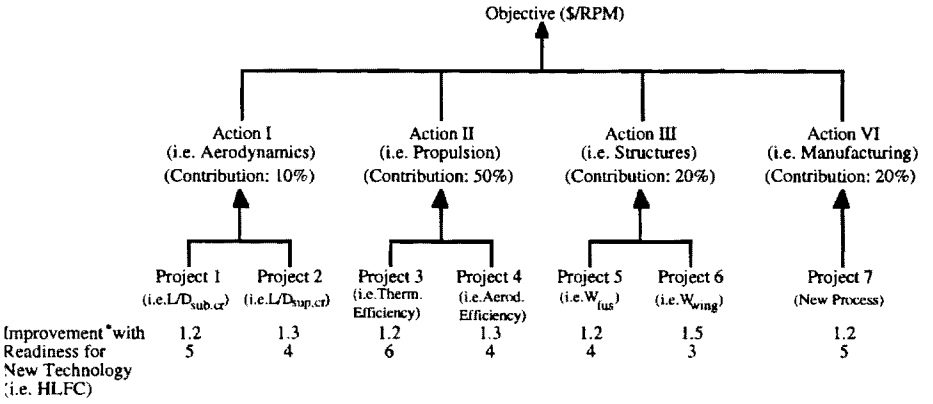

Figure 49: Hypothetical Relevance Tree Structure

Table 2.16: Projects to Increase Objective Yield

Project #	Benefit in μ	Readiness	Confidence	Cost in K$
1	1.2	5	65%	350
2	1.3	4	45%	550
3	1.2	6	80%	300
4	1.3	4	45%	600
5	1.2	4	45%	400
6	1.5	3	30%	800
7	1.2	5	65%	350

The example presented here has the purpose of illustrating the process of determining the Worth of Investment. Obviously, this value is highly dependent on the selection of projects, their readiness, and their associated cost, which have been chosen arbitrarily for demonstration purposes. The example is also meant to demonstrate that the project (or combination of projects) with the highest benefit (yield in objective) is not necessarily the most profitable one. The example has to satisfy a budget constraint of $1,000,000 and a required minimum benefit of 10% of the original objective outcome. Since there is not enough funding, according to the budget, to fund all seven projects, the decision maker must decide which one(s) he or she ought to fund.

Every possible project combination which does not exceed the budget limit was examined. These feasible projects are presented in the first column of Table 2.17. For each project, the overall objective benefit, the associated risk, and the risk-to-benefit-ratio was estimated.

Table 2.17: Resource Allocation Exercise for a List of Feasible Projects

Feasible Projects	Risk/Benefit	Objective Improvement	Actual Investment ($K)	Actual Worth of Investment ($K)	Normalized Worth of Investment ($K)
1-2	1.80	1.05	900	500.00	555.5
2-3	1.19	1.13	850	714.00	840.3
1-3-7	1.28	1.16	1000	781.20	701.2
1-4	1.82	1.17	950	522.00	549.4
3-4	1.50	1.25	900	600.00	666.6
4-5	2.03	1.19	1000	493.50	492.6
3-5	1.50	1.14	700	467.00	666.6
2-5	2.36	1.07	950	403.00	423.7
6	1.40	1.10	800	570.00	714.3
4-7	1.80	1.19	950	523.00	555.5
5-7	2.25	1.08	750	333.33	444.4
5-1	2.42	1.06	750	310.30	413.2

Inspection of Table 2.17 indicates that if risk taking was not a consideration, projects 3-4 should be funded, since they provide a 25% improvement. Once risk is considered, the decision maker may bypass that option and select option 2-3 for it provides reasonable improvement (13%) at a reduced risk-to-benefit-ratio of 1.19 versus 1.50.

During the resource allocation phase of the development, the effect of risk may be included in the decision making process through Worth of Investment. Worth of Investment combines the effect of the risk-to-benefit-ratio with the budget spent on the project. Hence the objective is to minimize the risk-to-benefit-ratio or maximize the Worth of Investment which is defined as investment divided by the risk-to-benefit-ratio. By evaluating and comparing the actual Worth of Investment for all projects or their combinations, the optimal project (combination) with the highest actual Worth of Investment value can be determined. Table 2.17 also includes the figures for the actual Worth of Investment and the normalized Worth of Investment, which is defined as the actual Worth normalized by the total budget. Review of this column indicates that projects 2-3 has a normalized Worth of Investment of $840.3 K versus $666.6 K for projects 3-4. A simple way of interpreting these figures may be to consider that if risk was not present a $ 1 M investment will have the same buying power. On the other hand, with the presence of risk the investment made is worth less, because resources will have to be allocated to mitigate risk.

2.8 Project/Overall Program Tracking (Step 8)

Provided that a critical technology development effort is going to be pursued, the program manager will have to conduct a series of periodic evaluations to determine if the program is on schedule (see Figure 50). In order to avoid delays and cost overruns, the program will have to undergo evaluation at constant intervals and remedies will have to be proposed if that happens. This process can be assisted through the identification of critical paths, show stoppers or potential problems ahead of time and carefully plan around them. Keeping in mind that when a program execution is compressed in time, risk increases significantly with more manpower required to get back to schedule and no room for further delays.

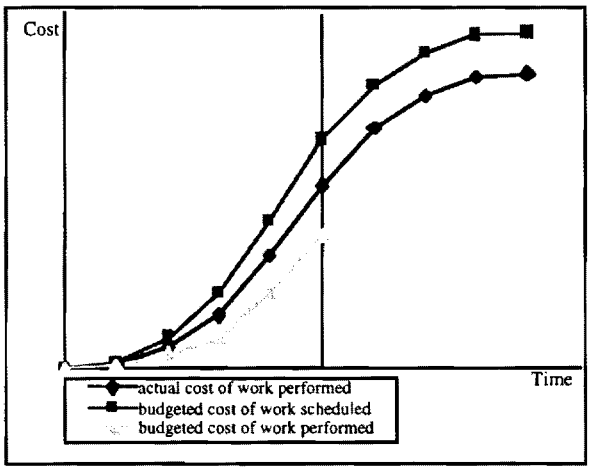

Figure 50: Program Cost/Schedule Tracking

3. Conclusions

A robust aircraft design simulation methodology has been developed under this Grant and has been described in this report. The methodology employs Concurrent Engineering practices and is set up within an IPPD framework. Furthermore, it focuses on design for affordability and the means of achieving economic viability. This procedure has been applied on a hypothetical High Speed Civil Transport configuration, where a detailed optimization in the presence of design and environmental constraints was conducted. After an economic viability study was performed, it was determined that this concept may benefit greatly from the infusion of new technologies. Given this incentive, a means for the identification and evaluation of new technologies from both a benefit and risk point of view has been proposed. Finally, the procedure on how to assess and select the most suitable technologies was illustrated through an example.

The overall objective in the *Concept Formulation and Synthesis/Sizing* portion of the study was the integration of aerodynamic and propulsion analyses and the investigation of their combined effects on the design of an HSCT. Under this task, the use of Response Surface Methodology (RSM) was a central part of the solution approach. RSM was successfully used to generate Response Model Equations representing vehicle drag as a function of geometry and flight condition parameters. These equations were subsequently integrated into the sizing program FLOPS, replacing prediction methods in the code. This transformation of the sizing code into a more powerful preliminary design tool enabled an innovative aerodynamic / propulsion integration and optimization to take place. Preliminary conclusions illustrated the apparent successful application of RSM in generating response model equations for drag prediction. These equations have been validated against the original simulation data and appear to provide a good fit.

A five level, eleven (11) factor Design of Experiment was executed using this new tool. Included in the 11 factors were critical aerodynamic, propulsion, and sizing design variables. The result of the experiment was a response equation for the overall system objective, the $ / Revenue Passenger Mile ($/RPM), representing the response for and setting of the 11 factors composing the design space. This RSE was then used to obtain the optimal setting of the design variables which minimized the $/RPM in the presence of constraints such as field length, noise, and approach speed. The resulting settings represent a "optimal point design" solution, as it represents a deterministic design since uncertainties such as economic variance or technology risk were not addressed.

The next step in the process is to perform an economic uncertainty assessment to determine the variability of the $/RPM objective to uncertainty factors (i.e. noise factors). The newly developed ASDL approach was implemented for the economic uncertainty assessment of the HSCT configuration, resulting in a probability distribution for the overall evaluation criterion, the average yield per revenue passenger mile. An assessment as to the proximity of this distribution to the target value (in this case the 747-400) led to a series of recommended solutions in order to shift this distribution closer to the target.

The conclusion reached from the assessment was that, although the production of an HSCT is currently feasible, it could lead to unsatisfactory economic results without the infusion of new technology. The HSCT, more than any other program, lends itself to the use of new technologies which could lower the overall life cycle cost of the vehicle and make it competitive. If the infusion of new technology is not sufficient to make the aircraft economically viable, the planners could also influence the outcome by increasing fare premiums or through yield management by reducing their expected return on investment. Either way, a series of trade-off studies must be conducted before one can answer with confidence whether this concept will be successful. These trade-off issues can be examined through a risk / benefit approach, such as the one developed for this current

research. The resulting risk-to-benefit ratio is a metric which provides insight into the potential usefulness of new technologies in making concepts economically viable.

References

[1] Kusiak, A., *"Concurrent Engineering"*, John Wiley & Sons, Inc., 1993.

[2] Henderson, M., HSCT Project Manager, The Boeing Commercial Aircraft Group, *High Speed Civil Transport Program Review*, Seattle, WA.

[3] Mavris, D., Brewer, J., and Schrage, D., *Economic Risk Analysis for a High Speed Civil Transport*, Presented at the 16th Annual Conference of the International Society of Parametric Analysts, Boston, MA, May 1994.

[4] *High Speed Civil Transport Study*, Boeing Commercial Airplanes, New Airplanes Development, NASA CR4233, 1989.

[5] Mavris, D., Bandte, O., and Schrage, D., *Economic Uncertainty Assessment of an HSCT Using a Combined Design of Experiments/Monte Carlo Simulation Approach*, Presented at the 17th Annual Conference of the International Society of Parametric Analysts, San Diego, CA, June, 1995.

[6] Roy, R., *Taguchi Method*, Van Nostrand Reinhold, New York, NY, 1990

[7] McCullers, L.A., *Flight Optimization System*, User's Guide, Version 5.41, NASA Langley Research Center, December 1993.

[8] ACSYNT, Aircraft Synthesis Program, User's Guide, Version 3.0, NASA Ames Research Center, January, 1995

[9] Box, G.E.P., Draper, N.R., *Empirical Model-Building and Response Surfaces*, John Wiley & Sons, Inc., New York, NY, 1987.

[10] Galloway, T.L., and Mavris, D.N., *Aircraft Life Cycle Cost Analysis (ALCCA) Program*, NASA Ames Research Center, September 1993.

[11] Bobick, J.C., Braun, R.L., and Denny, R.E., "Documentation of the Analysis of the Benefits and Costs of Aeronautical Research and Technology Models". Technical Report submitted by SRI International to NASA Ames Research Center, Contract No. NAS2-10026, July 1979.

[12] Twiss, B.C., *Forecasting for Technologists and Engineers*, Peter Peregrinus Ltd., London, United Kingdom, 1992.

[13] Hoy, K.L. and Hudak, D.G., *Advances in Quantifying Schedule/Technical Risk*, The Analytical Sciences Corporation, The 28th DoD Cost Analysis Symposium, Xerox Document University, Leesburg, VA.

[14] Schrage, D.P., Aerospace Systems Design I, Class Notes, 1995.

[15] Unal, Resit, "Parametric Modeling Using Saturated Experimental Designs", 16th Annual Conference of the ISPA, Boston, MA, May 1994.

[16] Brassard, M., The Memory Jogger Plus+, GOAL/QPC, Methuen, MA, 1989.

[17] Swan, W. "Design Evolution of the Boeing 2707-300 Supersonic Transport". Boeing Commercial Airplane Company, No Date Available.

[18] Butter, D. J., "Recent Progress on Development and Understanding of High Lift Systems," AGARD Report, British Aerospace, 1982.

[19] Treager, Irwin E. Aircraft Gas Turbine Engine Technology, Glencoe Division of McGrawHill, New York, 1979.

[20] Seidel, J., W. Haller, J. Berton. "Comparison of Turbine Bypass and Mixed Flow Turbo-fan Engines for a Flight Speed Civil Transport." AIAA-91-3132, September 23-25, 1991.

[21] Smith, M. G., George A. Champagne. "P&W Propulsion Systems Studies Results/Status." Advanced Engine Program Status, Pratt & Whitney, May 1991.

[22] McNeil, W., Robert W. Suderth, "Development of Longitudinal Handling Qualities for Large Advanced Supersonic Aircraft," Performed under NASA contract NAS2-7966. March 1975.

[23] Berry, D. T., Donald L. Mallick and Glenn B. Gilyard, "Handling Qualities Aspect of NASA YF-12 Flight Experience," NASA Dryden Flight Research Center.

[24] Gerald Miller, "An Active Flexible Wing Multi-Disciplinary Design Optimization Method", Rockwell International, AIAA-94-4412-CP. 1994.

[25] Ray, J.K. et al. "High-Speed Civil Transport Flight and Propulsion Control Technological Issues,". Boeing Company. NASA-CR-186015. March 1992.

[26] McCarty, C.A. et al. "Design and Analysis Issues of Integrated Control Systems for High-Speed Civil Transport,". Douglass Aircraft Company. NASA-CR-186022. May 1992.

[27] Dieter, George E., Engineering Design A Materials and Processing Approach. McGraw-Hill Publishing, New York, 1991.

[28] Treager, Irwin E. Aircraft Gas Turbine Engine Technology, Glencoe Division of McGrawHill, New York, 1979.

[29] Kalpakjian, Serope, Manufacturing Processes for Engineering Materials. Second Edition, Addidon-Wesley Publishing Company, New York, 1991.

[30] Box, G.E.P., Draper, N.R.; Empirical Model-Building and Response Surfaces; John Wiley & Sons, Inc.; New York; 1987.

[31] Box, G.E.P., Hunter, W.G., Hunter, J.S.; Statistics for Experimenters; John Wiley & Sons, Inc.; New York; 1978

[32] SAS Institute Inc.; JMP, Computer Program and Users Manual; Cary; 1994

[33] Montgomery, D.C.; Design and Analysis of Experiments; John Wiley & Sons, Inc.; New York; 1991.

[34] Mavris, D. N., Bandte, O., Schrage D.P., "Economic Uncertainty Assessment of an HSCT using a Combined Design of Experiments / Monte Carlo Approach," 17th Annual Conference of the ISPA, San Diego, CA, May 1995.

[35] Mattingly, Jack D., et. al., Aircraft Engine Design. AIAA, 1987.

[36] Treager, Irwin E. Aircraft Gas Turbine Engine Technology, Glencoe Division of McGrawHill, New York, 1979.

[37] SAS Institute Inc., *JMP*, Computer Program User's Manual, Cary, NC, 1994.

[38] Olson, E.D. "Advanced Takeoff Procedures for High-Speed Civil Transport Community Noise Reduction,". NASA Langley Research Center. 1992.

[39] McCullers, L.A., *Flight Optimization System, Computer Program and Users Guide*, Version 5.7, NASA Langley Research Center, Hampton, VA, December 1994.

[40] Galloway, T.L. and Mavris, D.N., *Aircraft Life Cycle Cost Analysis (ALCCA) Program*, NASA Ames RC, Moffett Field, CA, September 1993.

[41] SAS Institute Inc., *JMP, Computer Program and Users Manual*, Cary, NC, 1994.

[42] Decisioneering, Inc., *Crystal Ball, Computer Program and Users Guide*, Denver, CO, 1993.

[43] Box, G.E.P., Draper, N.R., *Empirical Model-Building and Response Surfaces*, John Wiley & Sons, Inc., New York, NY, 1987.

[44] Box, G.E.P., Hunter, W.G., Hunter, J.S., *Statistics for Experimenters*, John Wiley & Sons, Inc., New York, NY, 1978.

APPENDIX

A. Design of Experiments (DOE) and the Response Surface Method (RSM)

Understanding the characteristics of the design space and behavior of the proposed designs as efficiently as possible is as important to the designer as finding the numerical optimum. This is particularly true for complex aerospace system designs that require multidisciplinary analyses, a large investment of computing resources, and numerous parameter trade studies. Although automated iterative optimization programs are useful in that they are readily applied to engineering design in general, their drawbacks include an inability to exploit domain knowledge and high sensitivity to the manner which a problem is formulated. In addition, due to the iterative character of the optimization procedure, a lot of analyses are merely intermediate steps in the iteration process and are lost when the optimization run is finished.

The Response Surface Methodology (RSM) comprises a group of statistical techniques for empirical model building and exploitation. By careful design and analysis of experiments, it seeks to relate a response, or output variable, to the levels of a number of predictors, or input variables. In most cases, the behavior of a measured or computed response is governed by certain laws which can be approximated by a deterministic relationship between the response and a set of design variables; thus, it should be possible to determine the best conditions (levels) of the factors to optimize a desired output[8]. Unfortunately, many times the relationship between response and predictors is either too complex to determine or unknown, and an empirical approach is necessary to determine the behavior. The strategy employed in such an approach is the basis of the RSM. In this current application, a second degree model of the selected responses in k-variables is assumed to exist. A notional example of a second order model is displayed in Figure A1 for two variables **x1** and **x2**.

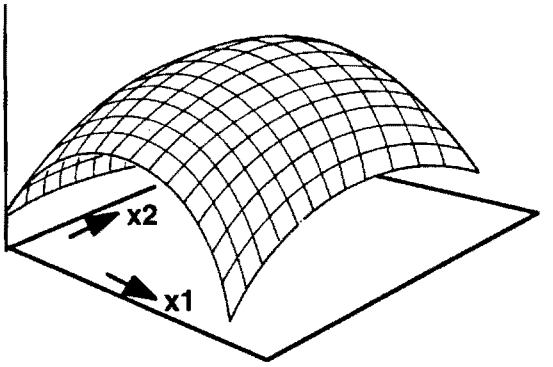

Figure A1: Second Order Response Surface Model

The second degree RSE takes the form of:

$$R = b_0 + \sum_{i=1}^{k} b_i x_i + \sum_{i=1}^{k} b_{ii} x_i^2 + \sum \sum_{i<j}^{k} b_{ij} x_i x_j \qquad (A.1)$$

where, b_i are regression coefficients for the first degree terms, b_{ii} are coefficients for the pure quadratic terms, b_{ij} are coefficients for the cross-product terms (second order interactions), and b_o is the intercept term. To facilitate the discussion to follow, the components of equation (A.1) are further defined. The x_i terms are the "main effects", the x_i^2 terms are the "quadratic effects", and the $x_i x_j$ are the "second-order interaction terms".

Once this equation is constructed from the sample data through a least squares technique, it can be used in lieu of more sophisticated, time consuming computations to predict and/or optimize the response R. If one is optimizing on R, the "optimal" settings for the design variables are identified (through any number of techniques) and a confirmation case is run using the actual simulation code to verify the results. Since the RSE is in essence a regression curve, a series of experimental or computer simulation runs must be performed to obtain a set of data for regression. One organized way of obtaining these data is the aforementioned DOE, which is used to determine a table of input variables and combinations of their levels yielding a response value (but also encompasses other procedures, like Analysis of Variance). There are many types of DOEs. Table A.1 displays a simple full factorial example for three variables at two levels, a minimum and a maximum (sometimes also described as "-1" and "+1" points). The response can be any of a variety of metrics (such as thrust, drag, pitching moment, weight, cost, etc.), while the design variables(or control factors) define the design space. For the approach in this report, the factors become input variables to the analysis code, while the response is generally the desired output of the program.

Table A.1: Design of Experiment Example for a two-level, 2^3 Factorial Design[9]

	Factors			
Run	1	2	3	**Response**
1	-	-	-	y_1
2	+	-	-	y_2
3	-	+	-	y_3
4	+	+	-	y_4
5	-	-	+	y_5
6	+	-	+	y_6
7	-	+	+	y_7
8	+	+	+	y_8

A statistical analysis can be performed using Analysis of Variance (ANOVA) with t-Tests in estimating the model parameters for the RSE. The same DOE approach can be used for variables at three levels, requiring more runs to obtain the same information. On the other hand,

evaluation of all possible combinations of variables at two or three levels increases the number of cases that need to be tested exponentially, and thus is not practical. In fact, testing these variables at three levels, their two extremes and a center point, would take a total of 531,441 cases for a 3^{12} factorial design. Table A.2 illustrates that one way of decreasing the number of experiments or simulation runs required is to reduce the number of variables. But as Table A.2 also displays, a 3^7 full factorial design requires 2,187 runs, which is still considered impractical for experiments or computer simulations. Hence, fractional factorial and second order model designs (of which the Central Composite is an example) are proposed as a more plausible means to perform experiments. Table A.2 provides three examples.

Table A.2: Number of Cases Required for Different DOEs[9]

DOE	7 Variables	12 Variables	Equation
3-level, Full Factorial	2,187	531,441	3^n
Central Composite	143	4,121	2^n+2n+1
Box Behnken	62	2,187	-
D-Optimal Design	36	91	$(n+1)(n+2)/2$

Fractional factorial DOEs use less information to come up with results similar to full factorial designs. This is accomplished by reducing the model to only account for parameters of interest. Therefore, fractional factorial designs often neglect third or higher order interactions for an analysis (see RSE in Equation (A.1)), accounting only for main and quadratic effects and second order interactions. Thus, the model used in this report neglects third and higher order interactions and a tradeoff exists in fractional factorial designs. The number of experiments or simulations (often referred to as "cases") rises as the increasing degree to which interaction and/or high order effects are desired to be estimated. Practically, since generally only a fraction of the full factorial design number of cases can be run, high order effects and interactions are not estimable. They are said to be confounded, or indistinguishable, from each other in terms of their effect on the response. This aspect of fractional factorial designs is described by the *resolution*. Resolution III implies that main effects are confounded with second order interactions. Thus, one must assume these interactions to be zero in order to estimate the main effects. Resolution IV indicates that all main effects are estimable, though second order interactions are confounded with other such interactions. Resolution V or greater means that both main effects and second order interactions are estimable (though for Resolution V designs, third order interactions would be confounded with

second order effects, hence must be zero)[10]. The example presented in Section 2.2 of the report will employ a Resolution V design for the generation of RSEs. Another possibility for reducing the number of cases is to give up the ability of accounting for replicates. Replicates are normally used to provide for the calculation of experimental error (as opposed to model fit error). Since we assume that our computer simulations are "exact" or repeatable, replicates are not needed for this application of DOE.

As a general approach, a first DOE is performed in order to reduce the number of variables by identifying the contribution to the response of each variable considered. This exercise, termed a screening test, uses a two level fractional DOE for testing a linear model, thus estimating the main effects of the design variables on the response. It allows for an investigation of a high number of variables to gain a first understanding of the problem and the design space. A visual way to see the results of this screening is through a Pareto Chart[11], displayed in Figure A3. It identifies in a bar chart the most significant contributors to the response based on the linear equation generated from the DOE data. A line of cumulative contribution indicates which variables contribute how much. By defining the percentage of contribution desired, the number of variables needed to be carried along can be determined from the array of variables in the Pareto Chart. Usually, 7 to 8 variables are selected from the Pareto Chart to be carried over to the next step of generating the RSE.

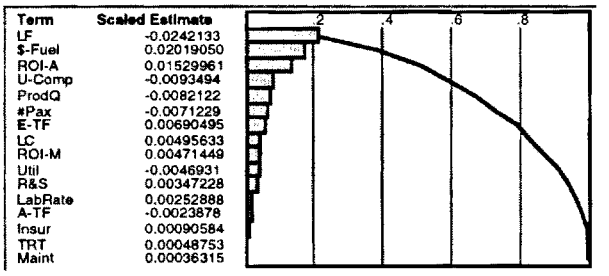

Figure A2: Example Pareto Plot - Effect of Design Variables on the Response

Figure A4 illustrates for a simple two variable case the two steps of this approach and the different shapes of the response function. The two level, linear model of **y** as a function of $\mathbf{x}_1$ and $\mathbf{x}_2$ represents the screening test. Here it is seen that response **y** is not highly dependent on $\mathbf{x}_1$. With this information, the actual generation of an RSE takes place only with $\mathbf{x}_2$ but in a quadratic model setting. By reducing the number of variables considered, the order of effects estimable in the RSE is increased. The payoff, of course, is for cases for numerous variables. Unfortunately, the process can be depicted visually only for the simple two variable case.

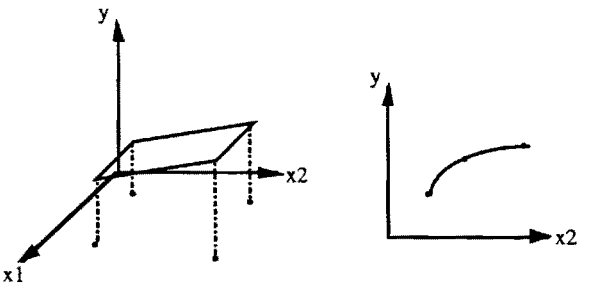

Figure A3: Two Steps Towards Response Surface Equations

After identifying the variables to be carried through to an RSE, a particular type of DOE must be selected. For the purposes of aerodynamic modeling portion of this study, the Central Composite Design (CCD), Figure A5, was selected to form the RSE. For the formation of the economic RSE, a Box-Behnken DOE was used. The particular CCD chosen is a five level composite design formed by combining a two level full or fractional factorial design with a set of axial or star and center points as described in References 8 and 12. It is an economical design in terms of the number of runs required, as Figure A5 illustrates by displaying a design for three variables as a cube with star and center points. The distance between axial points describes the extents of the design space. The points on the corners of the cube, on the axis, and in the center of the cube are additionally examined points as identified by the DOE scheme of levels for each variable. The center provides multiple replicates, for estimating experimental error, which is assumed non-existent for simulation-based analysis. Hence, just one replicate is required.

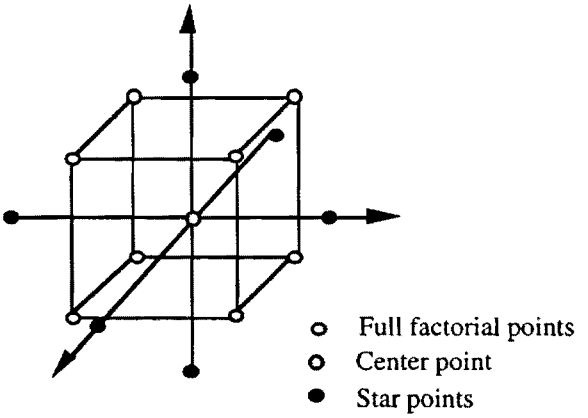

Figure A4: Central Composite Design Illustration for Three Variables

Finally, with the Central Composite Design in hand, an RSE can be obtained by using Equation (A.1) as a model for regression on the generated data. Unlike for true experiments, a statistical environment without any error can be assumed, so that all deviations from the predicted values are true measures of a model fit. A lack of fit parameter for the model expresses how good

the model represents the true response. A small lack of fit parameter usually indicates existing higher order interactions not accounted for in the model. Depending on the level of this lack of fit, a new design with a transformed model to account for these interactions should be used.

For the economic ($/RPM RSE) analysis, the Box-Behnken Design was used. The Box-Behnken Design is a three level composite design formed by combining a two-level factorial with an incomplete block design as described in Reference 43. This design is computationally efficient as shown by the number of runs required. Figure A6 illustrates the combinations needed for an example case, depicted as a cube, in which three variables are considered with one variable on each axis. The cube identifies the design space which is defined by the ranges selected for each variable. The points on the edges and in the middle of the cube represent cases that need to be tested. The middle points in particular provide replicates, giving a means for evaluating for experimental error. It should be noted that the obtained RSE will only be valid within the region defined by the selected design variable ranges. If an outcome outside these ranges is desired, then the process must be repeated and a new RSE must be formed. Use of the RSE outside the ranges selected is not recommended since polynomials do not extrapolate well.

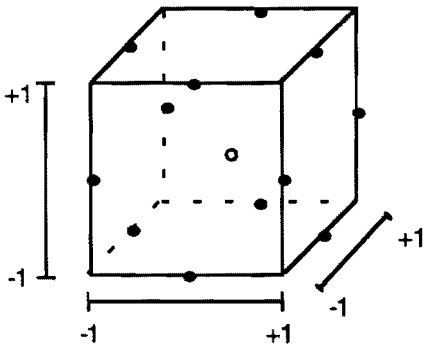

Figure A5: Box-Behnken Design Illustration for Three Variables

EXCEL Optimizer

For the optimization procedure, the Microsoft Excel tool Solver was utilized. The Solver gives a user the ability to specify a destination cell in his spread sheet that is to be optimized. This cell usually contains an equation, dependent on a set of specified cells. By running the Solver, this set of independent cells is varied within specified boundaries until a solution for the destination cell is found. This solution can be a minimum, maximum, or specified value for the objective cell. The optimizing procedure is based on a steepest ascent approach. Additionally, the Solver solution provides the actual settings for the variable cells used to obtain the objective extremal.

The format of the spreadsheet also allows for a constrained optimization. This enables the user to obtain unconstrained equations from, say, a synthesis program, and constrain the solution

during optimization. This is achieved by implementing equations for constraints into the spreadsheet that are dependent on the same cells varied for the destination cell. By limiting the values for the constraint cells, the Solver will change the variable cells only within those limits. Hence, the solution obtained is constrained by the specified values for the constraints. This method has been employed for this study using the equations obtained for the objective ($/RPM) as well as numerous constraints.